

**DEVELOPMENT OF $\text{Mg}(\text{NO}_3)_2 \cdot 6\text{H}_2\text{O}$ PHASE CHANGE MATERIAL
BASED SOLAR THERMAL ENERGY STORAGE SYSTEM
FOR COMMUNITY SOLAR COOKING
APPLICATION**



**A Dissertation submitted to Graduate School of Naresuan University
in Partial Fulfillment of the Requirements
for the Doctor of Philosophy Degree in Renewable Energy
June 2018
Copyright by Naresuan University**


Thesis entitled “Development of $\text{Mg}(\text{NO}_3)_2 \cdot 6\text{H}_2\text{O}$ phase change material based solar thermal energy storage system for community solar cooking application”


by Miss Santhi Rekha Santhimurthy


has been approved by the Graduate School as partial fulfillment of the requirements for the Doctor of Philosophy Program in Renewable Energy of Naresuan University

Oral Defense Committee

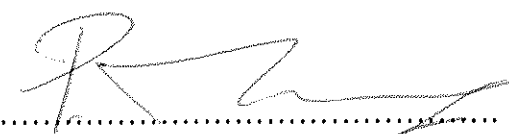

..... Chair
(Associate Professor Santi Wangnipparnto, Ph.D.)


..... Advisor
(Sukruedee Sukchai, Ph.D.)


..... Internal Examiner
(Assistant Professor Chatchai Sirisamphanwong, Ph.D.)


..... Internal Examiner
(Pisit Maneechot, Ph.D.)

Approved


.....
(Associate Professor Paisarn Muneesawang, Ph.D.)

Dean of the Graduate School

18 JAN 2018

ACKNOWLEDGEMENT

I would like to express my sincere gratitude to my advisor Dr. Sukruedee Sukchai for the continuous support of throughout my Ph. D study and related research, for her patience, motivation and immense knowledge. Her guidance helped me in all the time of research and writing of this dissertation and to complete my Ph. D successfully.

I also would like to express my sincere thanks to Dr. Yodthong Mensin and Mr. Wikarn Wansungnern for their constant support and help to conduct my research with all the needful equipment. I would like to extend my sincere thanks to my fellow students for sharing their knowledge, constant motivation and the moral support in the duration my dissertation.

I sincerely thank the staff of Central Science Lab Center, Naresuan University for helping me in the analysis of the dissertation. I would like to extend my sincere thanks to all the staff members of School of Renewable Energy Technology (SERT) for their constant support, help and motivation throughout my study period to complete the dissertation in time.

I would like to express my Sincere thanks to the administration of Naresun University for giving me a wonderful opportunity to do my doctoral studies in the university by providing fellowship throughout my dissertation period.

Finally, I thank my parents for their unconditional love, support, moral guidance in all stages of my studies. The in-time completion of the dissertation could not be possible without their great understanding and support towards my career.

Santhi Rekha Santhi Murthy

Title	DEVELOPMENT OF $\text{Mg}(\text{NO}_3)_2 \cdot 6\text{H}_2\text{O}$ PHASE CHANGE MATERIAL BASED SOLAR THERMAL ENERGY STORAGE SYSTEM FOR COMMUNITY SOLAR COOKING APPLICATION
Author	Santhi Rekha Santhi Murthy
Advisor	Sukruedee Sukchai, Ph.D.
Academic paper	Thesis Ph.D. in Renewable Energy (International Program)
Keywords	Solar cooking technology, Thermal energy storage, Latent heat energy storage, Phase Change Materials

ABSTRACT

The purpose of this dissertation was to design and develop $\text{Mg}(\text{NO}_3)_2 \cdot 6\text{H}_2\text{O}$ phase change material based solar thermal energy storage system for community solar cooking application. The present dissertation is conducted in five task which are development of PCM storage system, design of solar cooking system, incorporating PCM storage with solar cooking system, performance evaluation of the developed system and economic and emission analysis of the system.

A parabolic antenna dish of 1.495 m diameter and 0.268 m height and 0.520 m of focal length was developed as a solar concentrator by fixing the pieces high reflective mirror on the surface. A hollow concentric cylindrical shape stainless steel receiver was designed for the cooking purpose and which was placed at the focal point of the concentrator. 28 stainless steel cylindrical tubes were welded on the surface of the receiver to fill $\text{Mg}(\text{NO}_3)_2 \cdot 6\text{H}_2\text{O}$ inside the tubes to use as the storage system. $\text{Mg}(\text{NO}_3)_2 \cdot 6\text{H}_2\text{O}$ was selected as PCM from different selection criteria of the PCMs. 1000 thermal cycles were performed to analyze the performance of $\text{Mg}(\text{NO}_3)_2 \cdot 6\text{H}_2\text{O}$. In 1000 thermal cycles the weight and time taken for solidification were more in solidification cycle than that of melting cycle. After 1000 thermal cycles, from the DSC analysis, variations in melting point temperature and latent heat of fusion were analyzed. The $\text{Mg}(\text{NO}_3)_2 \cdot 6\text{H}_2\text{O}$ sample has 78.71 % of latent heat of fusion from the initial sample after 1000 thermal cycles. From the corrosion analysis of $\text{Mg}(\text{NO}_3)_2 \cdot 6\text{H}_2\text{O}$ on container material and SEM analysis, it was concluded that the stainless steel has the less corrosive

effect due to $\text{Mg}(\text{NO}_3)_2 \cdot 6\text{H}_2\text{O}$ and that material was selected to design the PCM tubes and receiver of the solar cooking system.

From the results of performance analysis, the parabolic solar cooker parameters heat loss factor ($F'U_L$), optical efficiency factor ($F'\eta_o$), cooking power (P) and the standard cooking power (P_s) were calculated for three sets of collected data. 0.51 and 0.22 are the optical efficiency factors of the solar cooker with all the layers the receiver was filled with water and receiver layers were filled with the corresponding materials respectively. 165.10 W and 210.76 W were the cooking powers of the solar cooker with load conditions with and without receiver is placed in the insulation box respectively. The optical efficiency factor of the solar cooker with PCM receiver is 2 times more than that receiver without PCM. The three stage heat storage capacity of the selected PCM for this proposed solar cooking system helps to sustain the more amount of heat inside the cooking stuff layer. The efficiency of the solar cooker is more in the case of PCM incorporation which is about 40.00%.

From the results of economic analysis of the solar cooker compared with LPG cooking system. The saved money per year by using the developed solar cooker over LPG cooking system is about 455.04 \$ and 408.96 \$ in India and Thailand respectively. The payback period of the solar cooking system is 1.1 years and 1.22 years in India and Thailand respectively. From the emission analysis it was concluded that The reduced amount of CO_2 emission per year by using the developed PCM solar cooker is about 725 kg.

LIST OF CONTENTS

Chapter		Page
I	INTRODUCTION	1
	Thermal energy storage	9
	Rationale / statement of the problem	15
	Purpose of the study	16
	Scope of the study	17
	Significance of the study	17
	.	
II	LITERATURE REVIEW	19
	Introduction.....	19
	Review of related articles	22
III	RESEARCH METHODOLOGY	30
	Development of PCM storage system.....	30
	Design of solar cooking System	42
	Incorporating the storage system with solar cooking system...	51
	Performance evaluation the developed system	52
	Economic and emission analysis of the system.....	63
IV	RESLUTS AND DISCUSSION	66
	Design parameters of solar cooking system.....	66
	PCM analysis	67
	Experimental data analysis.....	76
	Real time application analysis.....	96
	Thermal imager analysis.....	102
	Economic and emission analysis.....	106

LIST OF CONTENTS (CONT.)

Chapter	Page
V CONCLUSION AND RECOMMENDATIONS.....	109
Conclusion	109
Recommendation	110
REFERNCECS	112
APPENDIX	118
BIOGRAPHY	144



LIST OF TABLES

Table	Page
1 Distribution of primary fuel use for cooking in India, NFHS-3, 2005.....	3
2 Advantages and disadvantages of different PCMs	14
3 Examples of salts that have been investigated as PCMs.....	15
4 Description and specification of the four main CSP technologies.....	20
5 Performance data of various concentrating solar power (CSP) technologies.....	21
6 Properties of inorganic phase change materials	34
7 Different applications of PCMs.....	35
8 Parameters of solar concentrator and receiver	66
9 Variation in weight and time for $Mg(NO_3)_2 \cdot 6H_2O$ thermal cycling process.....	68
10 Results of DSC thermograms	74
11 Parameters of solar cooking system.....	93
12 Different parameters to cook same food material in a day	100
13 Different parameters to cook different food material in a day.....	101
14 Different parameters for frying application	101
15 Price details of different components	106
16 Economic analysis parameters	108
17 Temperature profile of receiver	124
18 Temperature profile of PCM in PCM tubes	125
19 Specific heat capacity of different food materials	129

LIST OF FIGURES

Figure	Page
1 Renewable power capacity since 2001 to 2014 throughout the world.....	1
2 Consumption charts of resources in rural and urban areas.....	2
3 Percentage distribution of primary energy sources used for cooking in rural and urban areas.....	4
4 Annual deaths due to different causes	4
5 Annual deaths due to diseases caused by indoor air pollution.....	5
6 Direct or panel type solar cookers	6
7 Schematic view of solar box cooker	7
8 Schematic view of advanced type solar cooker.....	7
9 Classification of thermal energy storage systems.....	10
10 Sensible and latent heat storage	11
11 Schematic change of temperature during melting and solidification cycles	12
12 Classification of latent heat storage materials	13
13 Daily residential load characteristics throughout the week.....	20
14 Combination of storage and hybridization in solar plant.....	22
15 Flow chart of complete research methodology	31
16 Flowchart of development of storage system.....	33
17 Thermal energy storage design considerations at each level.....	35
18 $Mg(NO_3)_2 \cdot 6H_2O$ (a) Sample at 0 th cycle (b) Weight measurement of the sample.....	38
19 $Mg(NO_3)_2 \cdot 6H_2O$ (a) Melting cycle (b) Solidification cycle.....	38
20 Schematic view of interior view of DSC.....	39
21 (a) DSC (b) DSC loaded with $Mg(NO_3)_2 \cdot 6H_2O$ sample.....	40
22 Schematic graph of a DSC thermogram.....	41
23 (a) Image of SEM (b) Container materials inside $Mg(NO_3)_2 \cdot 6H_2O$	42

LIST OF FIGURES (CONT.)

Figure	Page
24 Construction of solar concentrator	43
25 Geometrical representation of design parameters of solar concentrator.....	45
26 Schematic view of (a) Cooking pot layers (b) Cooking pot with PCM tubes.....	46
27 Heat transfer network of PCM solar cooker	47
28 Modified heat transfer network	48
29 Schematic view of (a) cylinder (b) concentric cylinder.....	50
30 Manual tracking system with (a) Vertical arm (b) horizontal arm...	51
31 Design of the receiver (a) front view (b) top view.....	52
32 Schematic diagram of heat balance network for first stage	55
33 Schematic diagram of heat balance network for second stage.....	55
34 Schematic diagram of heat balance network for third stage	56
35 Schematic diagram of heat balance network for fourth stage.....	57
36 Various positions of the thermocouples placed in receiver and solar concentrator	59
37 The complete design of developed PCM solar cooking system.....	67
38 Variation in weight of PCM.....	68
39 Variation in time taken for melting and solidification of PCM.....	69
40 DSC thermogram of $\text{Mg}(\text{NO}_3)_2 \cdot 6\text{H}_2\text{O}$ sample at 0 th cycle.....	70
41 DSC thermogram of $\text{Mg}(\text{NO}_3)_2 \cdot 6\text{H}_2\text{O}$ sample after 100 th cycle.....	70
42 DSC thermogram of $\text{Mg}(\text{NO}_3)_2 \cdot 6\text{H}_2\text{O}$ sample after 200 th cycle.....	71
43 DSC thermogram of $\text{Mg}(\text{NO}_3)_2 \cdot 6\text{H}_2\text{O}$ sample after 400 th cycle.....	71
44 DSC thermogram of $\text{Mg}(\text{NO}_3)_2 \cdot 6\text{H}_2\text{O}$ sample after 600 th cycle.....	73
45 DSC thermogram of $\text{Mg}(\text{NO}_3)_2 \cdot 6\text{H}_2\text{O}$ sample after 800 th cycle.....	73
46 DSC thermogram of $\text{Mg}(\text{NO}_3)_2 \cdot 6\text{H}_2\text{O}$ sample after 1000 th cycle.....	74
47 SEM images of zeroth cycle (a) Stainless steel (b) Aluminum.....	75
48 SEM images of 500 th cycle (a) Stainless steel (b) Aluminum.....	75

LIST OF FIGURES (CONT.)

Figure	Page
49 SEM images of 1000 th cycle (a) Stainless steel (b) Aluminum.....	76
50 Temperature profile of the solar cooking system with empty receiver.....	77
51 Temperature profile of the system with water inside the HTF layer and PCM.....	77
52 Temperature profile of the system with palm oil in HTF layer and water inside PCM tubes.....	78
53 Temperature profile of the system with water, oil and PCM respective layers of the receiver.....	79
54 Heating curve of the system with no load conditions in the first set.....	80
55 Cooling curve of the system with no load conditions in the first set.....	80
56 Heating curve of the system with load conditions in the first set.....	81
57 Cooling curve of the system with load conditions in the first set.....	81
58 Temperature profile of the system with no load conditions in second set	82
59 Temperature profile of the PCM with no load conditions in second set.....	83
60 Temperature profile of the system with no load conditions in second set by placing receiver inside insulation box.....	83
61 Temperature profile of the PCM with no load conditions in second set by placing receiver inside insulation box.....	84
62 Temperature profile of the system with load conditions in second set.....	85

LIST OF FIGURES (CONT.)

Figure	Page
63 Temperature profile of the PCM with load conditions in second set.....	86
64 Temperature profile of the system with load conditions in second set by placing receiver inside insulation box.....	86
65 Temperature profile of the PCM with load conditions in second set by placing receiver inside insulation box.....	87
66 Comparison of second set no load heating curves with and without insulation box.....	88
67 Comparison of second set load heating curves with and without insulation box.....	88
68 Comparison of second set no load cooling curves with and without insulation box.....	89
69 Comparison second set of load cooling curves with and without insulation box.....	90
70 Temperature profile of continuous no load test	91
71 Temperature profile of continuous load test.....	91
72 Thermal energy of the receiver in different layers.....	94
73 Total amount of heat stored in the receiver	95
74 Efficiencies of the system in different cases	96
75 Temperature profile for day 1 boiling	96
76 Temperature profile for day 2 boiling	97
77 Temperature profile for day 3 boiling.....	97
78 Temperature profile for frying	97
79 Some of the cooked food materials in PCM solar cooker	102
80 Thermal image of the receiver in the morning (a) bottom view (b) top view	103
81 Thermal image of the receiver in the afternoon (a) bottom view (b) top view	103

LIST OF FIGURES (CONT.)

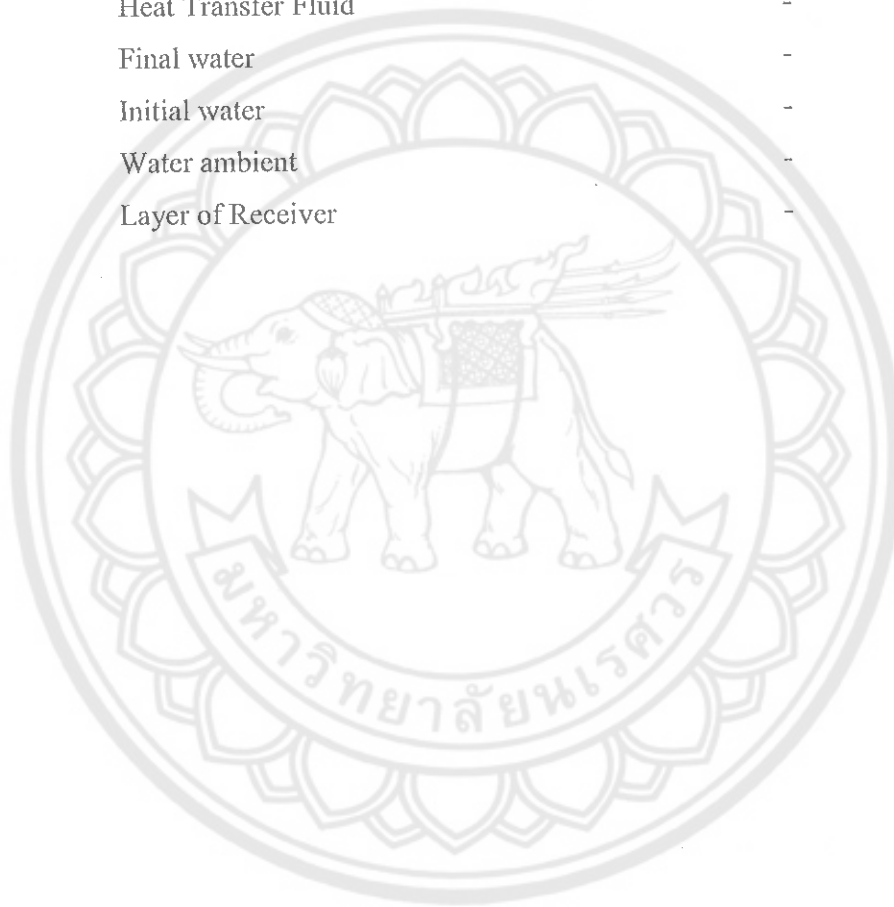
Figure	Page
82 Thermal image of the receiver in the evening (a) bottom view (b) top view	105
83 Thermal image of (a) receiver inside insulation box (b) total system.....	105
84 Thermal image of (a) receiver inside insulation box (b) safety operation	106
85 Instruments	119
86 Instruments	120
87 Comparison of set 3 no load heating curves with and without insulation box	126
88 Comparison of set 3 load heating curves with and without insulation box	126
89 Comparison of set 3 no load cooling curves with and without insulation box.....	137
90 Comparison of set 3 load cooling curves with and without insulation box.....	127
91 Slope curve for U_L calculation	127
92 Temperature profile for day 4 boiling	129
93 Temperature profile for day 5 boiling	130
94 3D thermal image of the receiver bottom view	131
95 3D thermal image of the receiver top view	131
96 3D thermal image of the complete system.....	132
97 3D thermal image of the receiver inside the insulation box.....	132
98 Variation in wind speed for continuous no-load test.....	133
99 Variation in wind speed for continuous load test.....	133

LIST OF NOMENCLATURE

Symbol	Description	Units
Latin Symbols		
D	Diameter of parabolic dish	m
h	Height of parabolic dish	m
f	Focal length of parabolic dish	m
C	Concentration ratio	-
P	Maximum radius of parabolic dish	m
A_s	Surface area of the dish	m ²
A_a	Aperture area of the dish	m ²
r_i	Inner radius of hollow cylinder	m
r_o	Outer radius of hollow cylinder	m
D_{fo}	Focal point diameter	m
A_f	Focal point area	m ²
A_r	Area of the receiver	m ²
h_r	Height of the receiver	m
N	Number of PCM tubes	-
M	Mass of the material	kg
C_p	Specific heat of the material	J kg ⁻¹ K ⁻¹
I	Instantaneous solar radiation	W m ⁻²
T	Temperature	°C
Greek symbols		
η	Efficiency	-
π	3.142	-
θ_A	Half acceptance angle of parabola	degree
ϕ	rim angle of parabola	degree
τ	time constant	sec

LIST OF NOMENCLATURE (CONT.)

Symbol	Description	Units
Indices		
PCM	Phase Change Material	-
HTF	Heat Transfer Fluid	-
wf	Final water	-
wi	Initial water	-
wa	Water ambient	-
l	Layer of Receiver	-



CHAPTER I

INTRODUCTION

The technology is developing very vigorously in the last few decades due to globalization and industrialization throughout the world. The usage of resources like coal, oil, petroleum products and natural gas was increased rapidly to meet the demands of the developing technologies. Gradually, this abnormal usage of fossil fuels is effecting the environment and which leads to several problems for the man kind on the earth. Global warming, ozone layer depletion, sea levels increment, resources reduction is some of the major problems that the countries throughout the globe are facing at present. To reduce these problems, all the countries looking for the renewable, clean and green resources. Renewable energy sources like solar, hydro, wind, geothermal, tidal and biomass are able to produce the clean energy which leads to reduction in the CO₂ emission in turn reducing the effect of global warming. The increase in the usage of different renewable energy sources in the past fifteen years is shown in the following Figure 1.

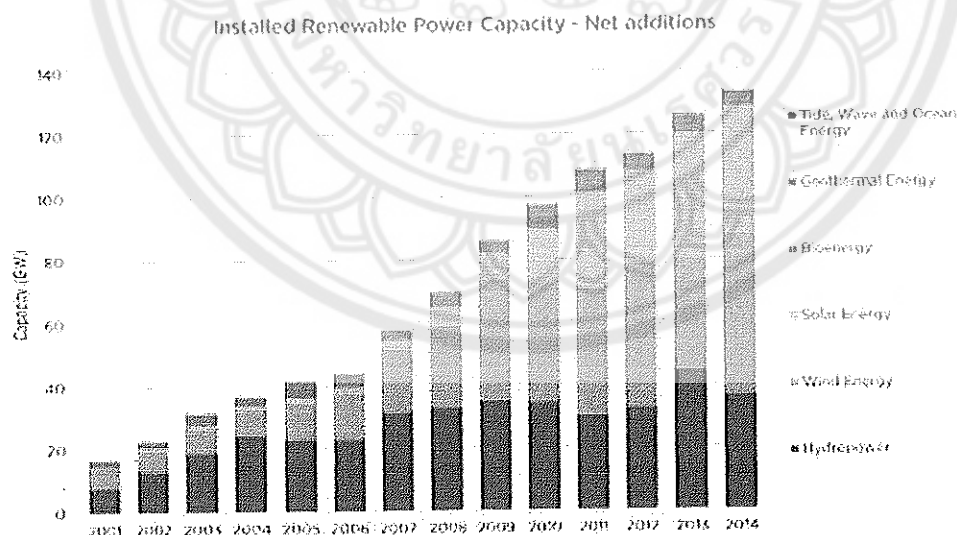


Figure 1 Renewable power capacity since 2001 to 2014 throughout the world

In 2013, 22% of world electricity was produced from the renewable resources. Solar energy is the most promising renewable energy source among the all renewable sources to meet the energy demand of the mankind. At present, solar energy production covers 1% of the global electricity demand. By 2030 China is planning to increase the renewable energy power production up to 20% through solar installations. In 2015, the solar installation capacity in China is increased from 12 GW to 17.8 GW (1).

The enormous potential of solar energy can be used for production of electric power, heating and cooling purposes, drying agriculture products, desalinization of sea water and cooking etc. Solar thermal energy conversion is one of the solar energy conversion technologies to meet the above mentioned needs in the human daily life. In developing countries, from the total energy consumption, noticeable energy is consuming for cooking applications throughout the year. Energy demand for the cooking application was met mostly by wood in rural areas. The sharing of resources in rural and urban areas is shown in Figure 2.

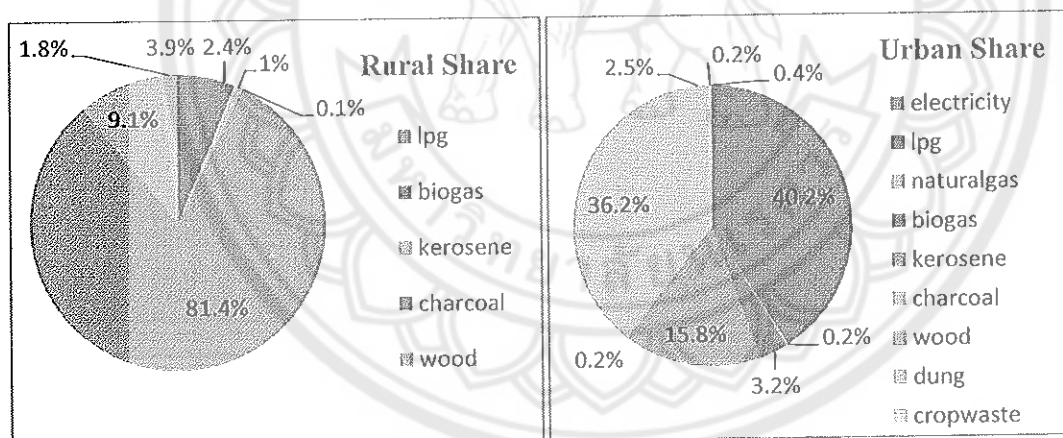


Figure 2 Consumption charts of resources in rural and urban areas

Almost 81.4% of resource sharing is taken by wood in rural areas and 36.2% of wood sharing among all the resources was happening in urban areas. The main purpose of using the wood or biomass resource is for cooking and some heating applications. From the National Family Health Survey of India for 2005 – 2006, NFHS-3, provides the detailed survey about the usage of primary solid fuels for cooking purpose in

households of urban and rural areas of India. 27% urban households and 71% rural households are using biomass as the primary cooking fuel.

The survey was also mentioned that nearly 160 million households nationally using biomass as primary cooking fuel. The detailed statistics about the different primary cooking fuels are mentioned in Table 1 (2).

Table 1 Distribution of primary fuel use for cooking in India, NFHS-3, 2005

Energy source	Urban (%)	Rural (%)	National (%)	Households (million)
Dung	2.80	14.40	10.60	24
Biogas	0.50	0.40	0.50	1.10
Crop waste	1.30	13.00	9.20	21
Wood	22.0	61.80	48.70	110.50
Charcoal	0.50	0.30	0.40	0.90
Coal	4.30	0.80	1.90	4.30
Kerosene	8.20	0.80	3.20	7.20
LPG	58.70	8.20	24.70	56
Electricity	0.90	0.10	0.40	0.90
Other	0.80	0.20	0.40	0.90
Biomass Total	27	90	69	156
Solid Fuel Total		90	71	160

The percentage distribution of households in primary energy sources for the use of cooking in rural and urban India as per the 2009-2010 statistics are shown in Figure 3 (Source: National Sample survey report).

In rural households, 76.30 % firewood and chips together are using as primary energy source for cooking purpose whereas 64.5 % of LPG is using as primary energy source for cooking in urban households. The distribution of other primary energy sources for cooking purpose like dung cake, kerosene in both rural and urban households are shown in Figure 3 (3).

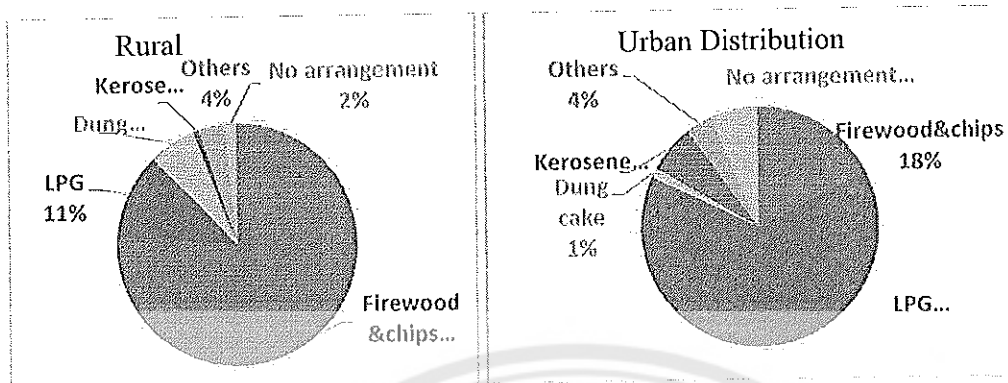


Figure 3 Percentage distribution of Primary energy sources used for cooking in rural and urban areas

The use of these resources causing so many problems like deforestation, health problems due to the smoke and other social and economic issues. The World Health Organization (WHO) estimates 1.5 million deaths per year in worldwide are due to the indoor air pollution because of the usage of solid fuels in households. More than 85% deaths are due to the usage of biomass and the rest are due to the usage of coal as primary fuel (4). The annual worldwide deaths due to different causes like malaria, HIV/AIDS, tuberculosis including biomass are shown in Figure 4.

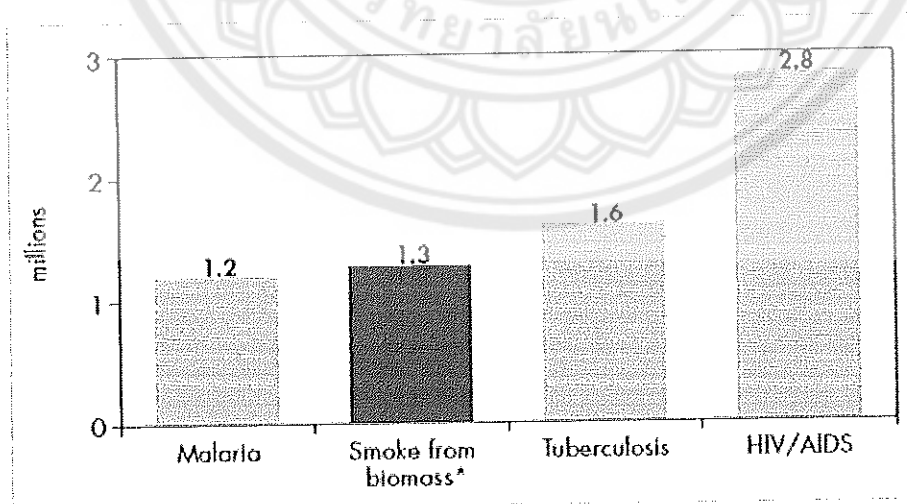


Figure 4 Annual deaths due to different causes

The deaths due to smoke from biomass or solid fuels used in indoors are about 1.3 million per year and which are more than that of the deaths caused by malaria and half of the deaths due to HIV/AIDS. The usage of ineffective cooking stoves and the polluting fuels are the causes for the most premature deaths. The report shows that, the number of deaths due to indoor air pollution because of the solid fuels as primary energy sources is highest in southeast Asian and sub - Saharan African countries (4).

As per 2012 WHO data, the premature deaths caused by indoor air pollution due to the usage of inefficient solid fuels for cooking are increased to 4.3 million per year worldwide. The percentage of different types of diseases caused by the indoor air pollution due to solid fuels usage are mentioned in Figure 5 (5) .

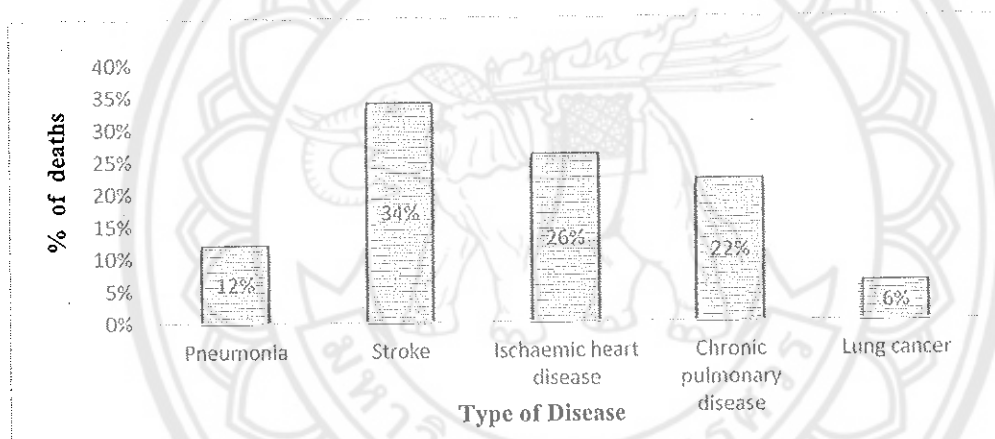


Figure 5 Annual deaths due to diseases caused by indoor air pollution

These issues are leading towards to think about the alternative renewable ways for this application. In the recent years, solar cooking got the importance to avoid all the issues arise with the use of fossil fuels. The main reasons for opting solar energy for cooking application are

1. Solar energy is clean and renewable
2. No carbon footprints like fossil fuels
3. Deforestation can be reduced
4. No economic issues as like with LPG and other fossil fuels
5. No issues regarding health and other social factors.

The above mentioned benefits are the reasons to develop different types of solar cookers which are available in the market to meet the demand of various categories cooking application. The general types of solar cookers are mentioned below (6). Basically the solar cookers classified into three types.

1. Direct or focusing type: In this type a kind of solar concentrator is placed in which the solar radiation is focused and at the focal point of the concentrator cooking vessel or frying pan will be placed. But, this type of cookers having large convective heat loss and it can use only direct radiation from the sun. The following Figure 6 shows this type of solar cooker.

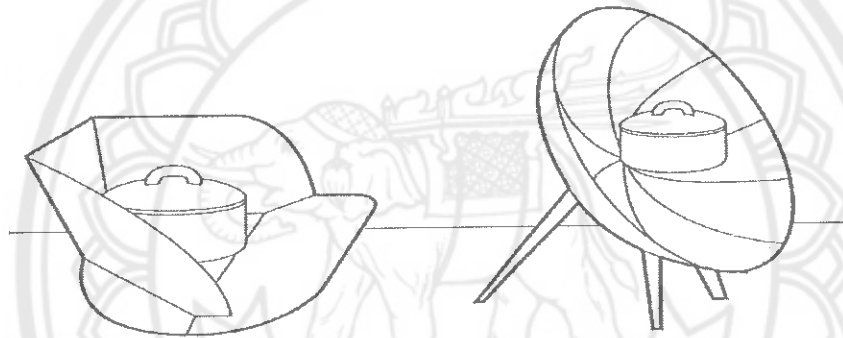


Figure 6 Direct or panel type solar cookers

2. Indirect or box type: This type of cookers is having an insulated box which is painted black from inside and having double glazing and reflector sheet on the top through which the solar radiation is absorbed. The cooking time is long and this type of cooker is not able to prepare so many dishes. The schematic view of the box type solar cooker is shown in Figure 7.

3. Advanced type: These types of cookers are having the heat storing technology. The storage technology provides indoor cooking and having the heat transfer capacity to transfer the heat from the solar collector to the cooking vessel in the kitchen. Figure 8 shows the general view of this type of cookers (source: www.fastonline.org).

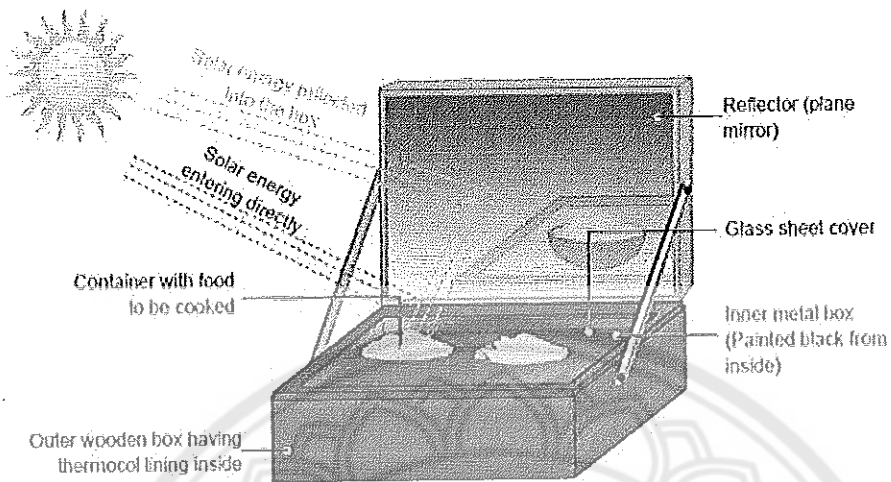


Figure 7 Schematic view of solar box cooker

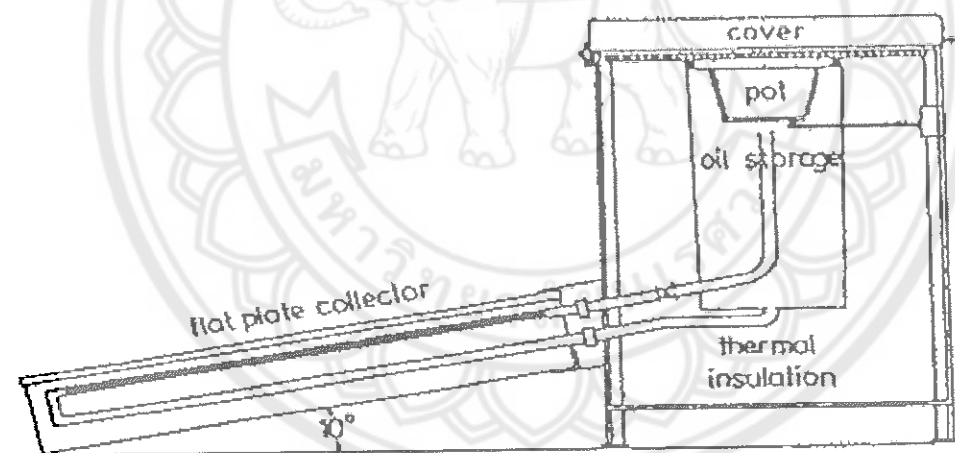


Figure 8 Schematic view of advanced type solar cooker

The development of different types of solar cookers with and without storage is increasing in present conditions. Even though, some non-acceptance of the solar cookers existed in some areas. This dissertation is discussed about the recent developments in the solar cooking with and without storage technology and explains the reasons for the non-acceptance of the solar cookers in wide range.

Solar thermal systems convert the sun's radiation into heat and then transfer that heat to air or water. This process is facilitated by a solar collector. The below mentioned heat transfer methods were happening in the systems to transfer heat from one place to another place (7).

1. Conduction: The process of propagation of energy between the particles of a body which are in direct contact is called conduction. In this phenomenon there is no noticeable movement of particles. The Fourier Law of Conduction is stated in equation 1.

$$Q = -kAdT/dx \quad (1)$$

Q = heat flow rate by conduction, W

K = thermal conductivity of the material, $W m^{-1} K^{-1}$

A = cross sectional area normal to direction of heat flow, m^2

dT/dx = temperature gradient of the section.

2. Convection: The transfer of heat within the fluid by mixing the fluid particles at low temperature is called as convection. Convection is two types as natural convection and forced convection. The rate of heat transfer by convection is expressed as follows.

$$Q = hA(T_s - T_\infty) \quad (2)$$

T_s = surface temperature, $^{\circ}K$

T_∞ = fluid temperature, $^{\circ}K$

h = heat transfer coefficient, $Wm^{-2}K$

3. Radiation: The transfer of heat from a high temperature body to low temperature body by electromagnetic waves is called as radiation. The concept of radiation is expressed with the help of Stefan-Boltzmann Law as follows

$$Q = \sigma \sum T_s^4 \quad (3)$$

T_s = absolute temperature of surface, $^{\circ}K$

\sum = emissivity coefficient, Wm^{-2}

σ = Stefan-Boltzmann constant, $Wm^{-2}K^{-4}$

The above mentioned heat transfer phenomena are important in the storage of solar thermal energy technology. The above mentioned modes of heat transfer and the storage technologies are interrelated to design a storage system for solar thermal energy applications.

Thermal energy storage

The unpredicted solar energy can be utilized efficiently in solar thermal systems by incorporating storage technologies. The storage technologies were developed for the solar thermal energy based on the thermophysical properties of the storage materials like melting, solidification, encapsulation etc. The solar energy is stored with the help of these materials by melting, cooling, solidifying, heating and vaporizing during the sun shine hours and the energy is retrieved back when these cycles are reversed (8). There are so many advantages by incorporating the storage systems for solar thermal applications. The solar thermal applications like water heating, drying, cooking and other heating and cooling applications can be utilized during unseasonal and off sunshine hours. The efficiency and the reliability of the technologies and the adoption of these technologies rather than fossil fuel based technologies will be improved.

Thermal energy systems are mainly classified into three types (9). Figure 9 shows the hierarchical classification of thermal energy storage systems.

1. Sensible heat thermal energy storage
2. Latent heat thermal energy storage
3. Thermo chemical energy storage.

Sensible heat storage: If the storage is based on the temperature change of the material that type of storage is called as sensible heat storage. There is no change of phase for the material. The unit capacity storage is equal to the product of heat capacitance and the temperature change of the medium. The following equation represents the amount of energy stored E in the material (10).

$$E = m \int_{T_2}^{T_1} C_p dT \quad (4)$$

$$E = mC_p (T_1 - T_2) \quad (4a)$$

m = mass, kg

C_p = Specific heat at constant pressure, J/g °C

T_1, T_2 = lower and upper temperature levels, °C

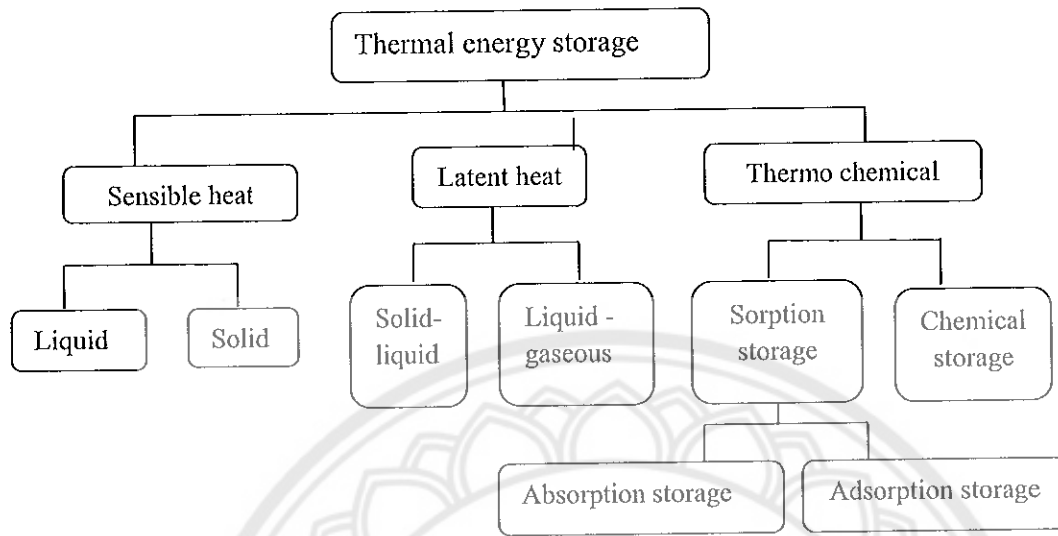


Figure 9 Classification of thermal energy storage systems

Latent heat storage: If the material changes its phase at a certain temperature while heating the substance then the heat is stored in the phase change then that type of heat storage is called latent heat storage. The materials which are used as the storage medium for the latent heat storage technology are called as Phase Change Materials or PCMs. Heat is absorbed by the material while it is heated and the heat is dissipated while the material is cooled. The storage capacity is equal to the phase change enthalpy of the material and the total sensible heat storage of the material. The amount of energy stored E is expressed by the following equation [6].

$$E = m\lambda \quad (5)$$

m = mass, kg

λ = latent heat of fusion, J/g

The amount of energy stored in this technology includes the amount of energy stored when system is operated at melting point which is nothing but the sensible heat storage over temperature ranges of T_1 and T_2 . The equation represents the energy stored in latent heat storage media including sensible heat storage is mentioned below (6). The graphical representation of the above situation is explained in the Figure 10 (6).

$$E = m \left[\left\{ \int_{T_1}^{T^*} C_{ps} dT \right\} + \lambda + \left\{ \int_{T^*}^{T_2} C_{pl} dT \right\} \right] \quad (6)$$

C_{ps}, C_{pl} = Specific heats of solid and liquid phases, J/g °C

T^* = melting temperature of PCM, °C

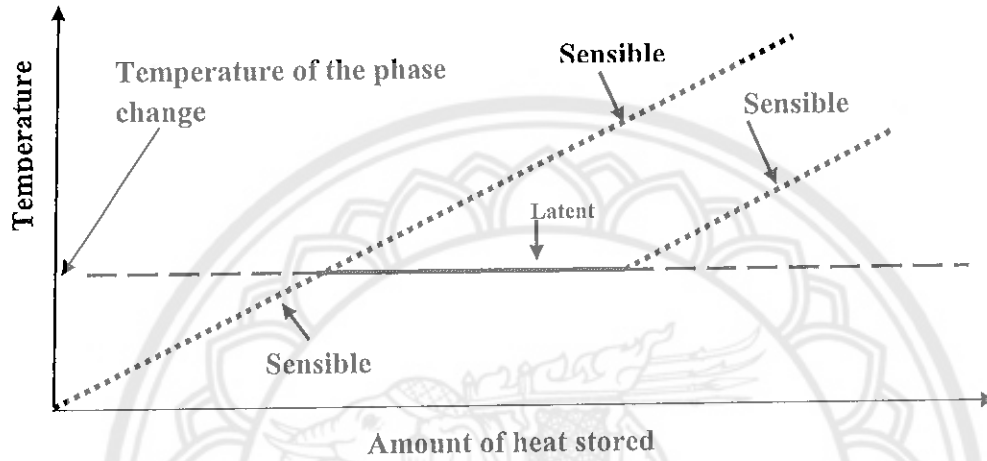


Figure 10 Sensible and latent heat storage

Thermo - chemical heat storage: If the heat storage is possible by breaking and forming any chemical compound with the use of heat then that type of heat storage is called Thermo chemical heat storage. For example, AB is a compound which is broken into two parts A and B with the use of heat and heat is stored separately in A and B, while forming the compound AB again from the two parts A and B then the heat will be released. The heat storage capacity Q is equal to the free energy of the reaction. This can be expressed as follows (6)

$$Q = a_r m \Delta h_r \quad (7)$$

a_r = endothermic heat of reaction, kJ/mol

m = amount of storage material, kg

Δh_r = extent of conversion, moles

Among the three storage systems, latent heat storage technology is suitable and attractive toward the medium range temperature solar thermal energy applications

because of the properties like constant temperature, availability of the materials, chemical stability and other advantages. In the next sections the advantages of latent heat storage technology and different phase change materials were discussed.

Latent heat thermal energy storage

The storage system or the technology is based on the thermophysical properties of the storage medium used within the technology. The phase change materials melt while absorbing the solar radiation and store the energy in the form of heat. When the material is solidifying the absorbed heat is retrieved from the material. The energy is stored and retrieved in the form of heat while the material is changing its phase from one into another (11). Figure 11 shows the schematic change of temperature during melting and solidification cycle (12).

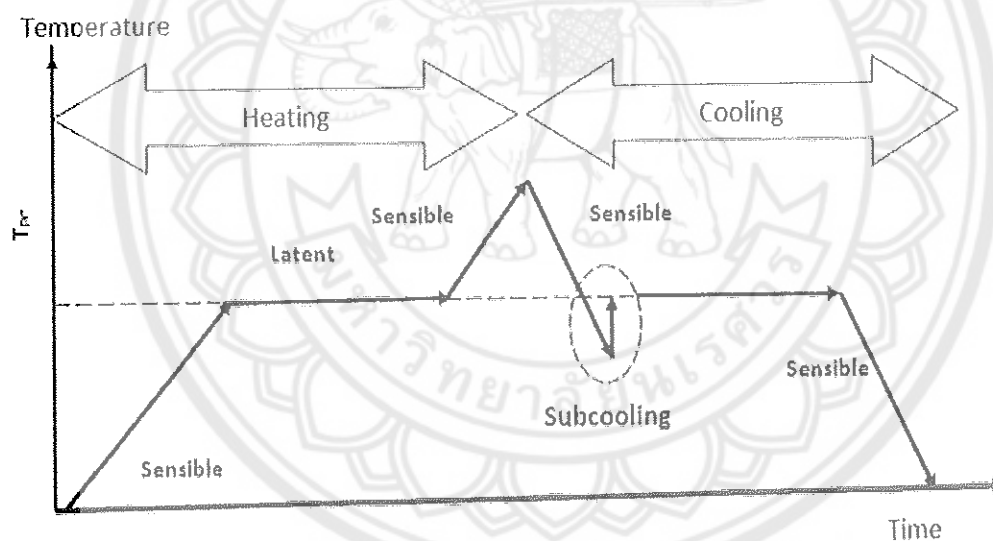


Figure 11 Schematic change of temperature during melting and solidification Cycles

Phase change materials for latent heat storage are classified into three types like organic, inorganic and eutectic phase change materials. These three types of PCMs are further classified as shown in Figure 12 (13).

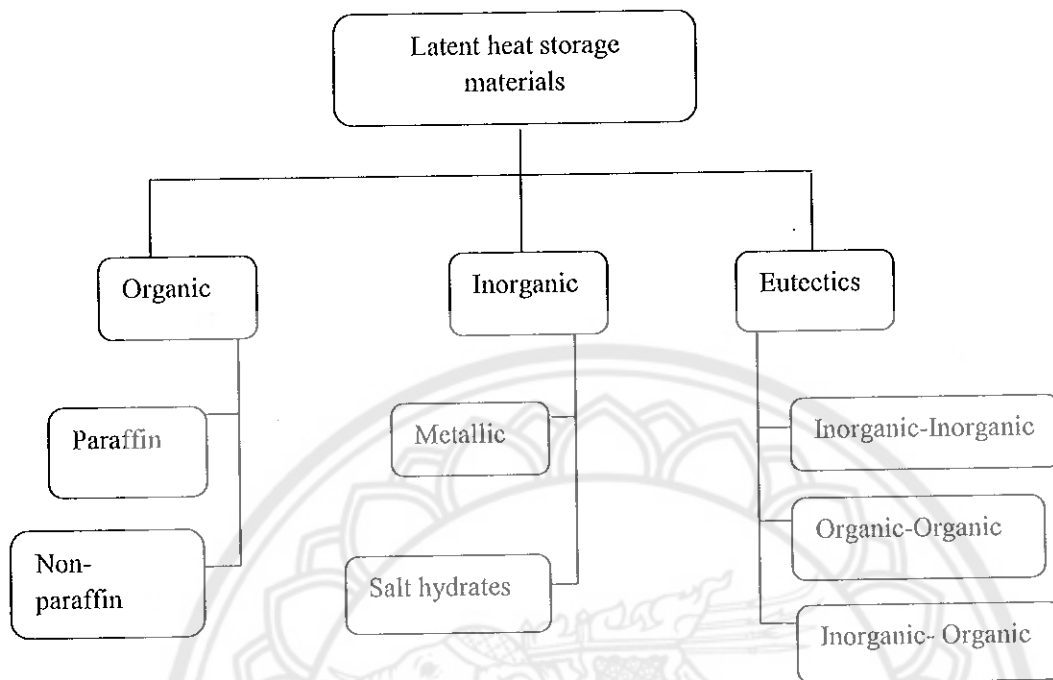


Figure 12 Classification of latent heat storage materials

The advantages and disadvantages of different kinds of PCMs are mentioned in Table 2.

Table 2 Advantages and disadvantages of different PCMs (14)

Type of PCM	Sub-group	Advantage	Disadvantage
Organic compounds	Paraffin's	<ul style="list-style-type: none"> • Can be directly incorporated 	Low thermal conductivity
	Non Paraffin's (fatty acids, esters, alcohol, glycols)	<ul style="list-style-type: none"> • Can be impregnated into porous buildings materials • Chemically stable and inert • Do not suffer from super cooling • Non-corrosive • Non- toxic • High thermal energy storage (latent heat of fusion) • Wide range of melting temperature • Low vapor pressure in phase change process 	(typically $0.2 \text{ W m}^{-1} \text{ K}^{-1}$ for paraffin's) <ul style="list-style-type: none"> • Large volume changes during the phase change process (paraffin's) • Non-paraffin's are three times more expensive than paraffin's • Some are flammable
Inorganic compounds	Salt hydrate	<ul style="list-style-type: none"> • Usually high thermal energy storage (latent heat of fusion) 	<ul style="list-style-type: none"> • Corrosive to more metals
	Metallic	<ul style="list-style-type: none"> • Good thermal conductivity • Less expensive • Non- flammable 	<ul style="list-style-type: none"> • Super cooling and phase segregation • Loss of thermal performance after large thermal cycles • Requires support and container
Inorganic eutectics or eutectic mixtures	Organic-organic	<ul style="list-style-type: none"> • Sharp melting points 	<ul style="list-style-type: none"> • Some suffer from super- cooling effect
	Inorganic-inorganic	<ul style="list-style-type: none"> • Usually high volumetric storage density 	<ul style="list-style-type: none"> • Low total latent heat capacity
	Inorganic-organic		

The proposed work is with the salt hydrate type of phase change material. Some examples of salts which are investigated as phase change material is shown in Table 3.

Table 3 Examples of salts that have been investigated as PCMs (8)

Material	Material Temperature (°C)	Melting enthalpy (kJ/kg)	Thermal Conductivity (W/mK)	Density (kg/m ³)
LiNO ₃	254	360	0.58(liquid)	1780(liquid)
			1.37(solid)	2140(solid)
NaNO ₃	307	172	0.51(liquid)	1900(liquid)
			0.59(solid)	2260(solid)
KNO ₃	333	266	0.50(liquid)	1890(liquid)
			-	1900(solid)
MgCl ₂	714	452	-	2140
NaCl	800	492	-	2160
			-	-
Na ₂ CO ₃	854	276	-	2533
			-	-
KF	857	452	-	2370
			-	-
K ₂ CO ₃	897	236	-	2290
			-	-

Rationale / statement of the problem:

Solar cooking has some challenges because of which the solar cookers are not effectively adopted by the people in some areas of the world even though the solar radiation is noticeably good in those areas. The main reasons for this issue are as follows (2)

1. Economically not viable: In the beginning days of solar cookers development, the cost of the solar cookers is little expensive for an individual family to own the technology instead of wood or fossil fuel technology.

2. In compatible with traditional cooking: This solar cooking was the new technology and the people were not having awareness on the usage of the equipment in the early days. So they continued to use the existed traditional ways for cooking.

3. Direct sun cooking: The early technologies developed for solar cookers are allowed only direct cooking under sunshine. In this case attentive cooking is difficult, so this one of the reason for non-acceptance of the technology.

4. Off sunshine cooking: The cooking is possible only in the sunshine or day light hours of the day and after sunset or night time cooking is not [possible with solar cookers. When the season was changed or cloudy days also solar cooking is not affective. So because of these reasons, people are not interested towards this technology.

5. Danger of getting burnt: The concentrators used in this technology reflecting the sun rays towards the cooking vessel. So, in this case attentive cooking is leads to burning issues and eye damages.

These are the main reasons for the non-effective usage of solar cooking technology. Some of these reasons were raised in the beginning stages of the technology development. But, later on the technology is improved and so many types of designs are available in the markets at present. The main reason for all the above mentioned issues is solar cooking technology without storage systems. The solar cookers with proper heat storage system can overcome the problems like outside cooking, seasonal and daylight cooking, no damage caused by burning and other technical issues.

To develop the solar cooking technology with storage systems depends on solar thermal energy storage materials and the modes of transferring heat from one place to another place. So, the storage of the solar energy for thermal applications gained the attention of scientist to develop different storage systems. Solar energy can be stored during sunshine hours through different techniques and which will be used during off sunshine hours effectively for different solar thermal applications.

Purpose of the study

The objectives of the present study are as follows:

1. Development of $\text{Mg}(\text{NO}_3)_2 \cdot 6\text{H}_2\text{O}$ phase change material based solar thermal energy storage system for solar cooking application and incorporating the storage system with solar concentrator.

2. Performance evaluation of the developed solar concentrator with phase change material solar thermal energy storage system for cooking application.

3. Comparison of economic analysis and carbon emissions of the developed system with the available local fossil fuel based cooking system.

Scope of the study

The scope of the study is limited to:

1. Inorganic phase change materials are considered for this study because of their thermodynamic, technical and economic benefits for thermal energy storage compared with the other types of phase change materials.

2. A parabolic antenna dish of diameter 1.495 m and 0.268 m height is used as solar concentrator to produce the adequate amount of temperature at the focus for cooking application.

3. A stainless steel concentric hollow cylinder with inner and outer radii are 10 cm and 9 cm respectively according to the size and geometrical calculations of solar concentrator.

4. Economic analysis of the developed solar cooker with PCM storage is compared with the other local fossil fuel based cooking methods.

5. The off sunshine cooking time and the type of food can be cooked with this system are limited based on the available temperature of the storage system.

Significance of the study

1. The development of salt hydrate storage system for solar cooking system can reduce the problems facing towards the efficient usage of solar cookers.

2. Off sunshine hours cooking is possible with the help of storage system incorporated solar cooker.

3. Direct sun cooking can be avoided. Attentive and indoor cooking at night times is possible with proper heat transferring mechanism.

4. The corrosion of the and decomposition of the storage vessel or tank can be reduced with the usage of $\text{Mg}(\text{NO}_3)_2 \cdot 6\text{H}_2\text{O}$ as phase change material.

5. The global warming and carbon footprints can be reduced with the use of solar cooking technologies.

6. Economic and social status of the rural communities can be improved with the help of these technologies which are useful in their daily life.



CHAPTER II

LITERATURE REVIEW

Introduction

In recent years, there is noticeable development in the renewable energy technologies. As mentioned earlier, solar energy is the most promising renewable energy among all the renewable energy resources. There are so many technologies to convert solar energy into electricity and for other applications. The main conversion technologies are solar photovoltaic technology and solar thermal technology (15).

Solar thermal technologies are classified based on the range of operating temperature, type of collector and tracking systems. The main four Concentrated Solar Power (CSP) technologies were mentioned in the below table. The descriptions of the technologies, thermodynamic efficiencies of the system and cost comparisons between the systems were mentioned in Table 4.

The four CSP technologies parabolic trough, linear Fresnel, power tower and dish stirling have different land use for the installation depends on the capacity of the plant. Dish stirling technology needs more land requirement than the other CSP technologies for comparatively low capacities of power generation, the different types of efficiencies like peak solar efficiency, annual solar efficiency and thermal cycle efficiency of the four CSP technologies were mentioned in the Table 5.

The load characteristics throughout the day are helpful to design a thermal energy storage system. The heat loss from convection and radiation are high while storing the thermal energy. In such cases, it is necessary to know that the requirement of the heat or load to be demanded by the consumers throughout the day. The present discussed thermal energy application is solar cooking, so which needs the load variation in the residential sector. The daily load variation in the residential sector throughout the week is shown in the following Figure 13 (16).

Table 4 Description and specification of the four main CSP technologies (17)

Collector type	Description	Rel. thermodynamic efficiency	Operating temp range (°C)	Relative cost	Concentration ratio	Technology maturity
Parabolic Trough Collector (PTC)	-Parabolic sheet of reflective material -Linear receiver (metal pipe with heat transfer fluid)	Low	50-400	Low	15-45	Very mature
Linear Fresnel	-Linear Fresnel mirror array focused on tower or high-mounted pipe as receiver	Low	50-300	Very low	10-40	Mature
Solar Tower	-Large heliostat field with tall tower in its center -Receiver: water/HTC boiler at top -Can be used for continuous thermal storage	High	300-2000	High	150-1500	Most recent
Dish Stirling	-Large reflective parabolic dish Stirling engine receiver at focal point -Can be used without HTC	High	150-1500	Very high	100-1000	Recent

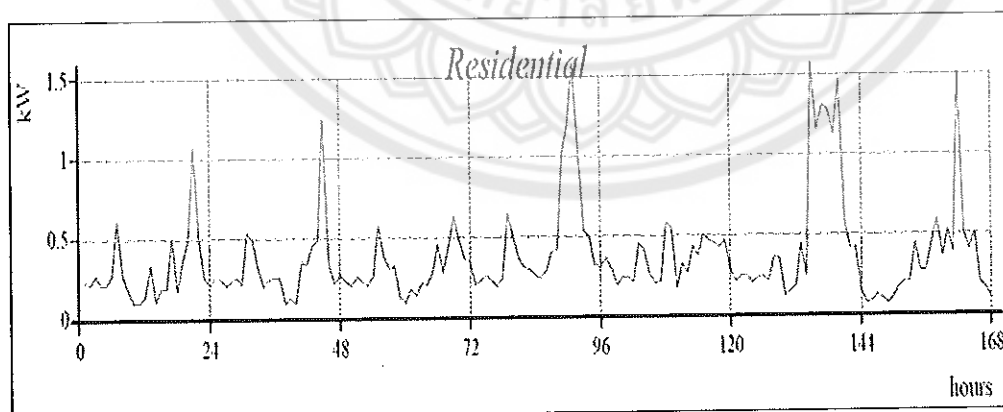


Figure 13 Daily residential load characteristics throughout the week

Table 5 Performance data of various concentrating solar power (CSP) technologies (8, 16)

Collector type	Capacity Unit (MW)	Peak Solar efficiency	Annual Solar efficiency	Thermal Cycle Efficiency	Capacity Factor (solar)	Land Use m ² /MWh
Parabolic Trough	10 – 200	21% (d)	10-15%(d) 17-18%(p)	30-40% ST	24% (d) 25-90%(p)	6 - 8
Fresnel	10 – 200	21% (d)	9-11%(d)	30-40% ST	25-90%(p)	4 - 6
Power Tower	10 – 150	21% (d) 35%(p)	8-10%(d) 15-25%(p)	30-40% ST 45-55%CC	25-90%(p)	8-12
Dish-Stirling	0.01 - 0.04	29% (d)	16-18%(d) 18-23%(p)	30-40% Stir 20-30% GT	25-90%(p)	8 - 12

Note: (d) = demonstrated, (p) = projected, ST steam turbine, GT Gas Turbine, CC = Combined Cycle, Solar efficiency = net power generation / incident beam radiation, Capacity factor = solar operating hours per year / 8760 hours per year.

The storage systems in solar technologies can store the energy during sunshine hours through proper medium and in off sunshine hours the stored energy can meet the power demand of the consumers. Solar energy technologies with storage back up are effective during off sunshine hours (18). The portion of the power requirement supplied by storage during off sunshine hours is shown in Figure 14. The amount of energy is

utilized with direct solar radiation, the amount of energy stored during day time and the amount of energy used from the stored energy are explained throughout the day.

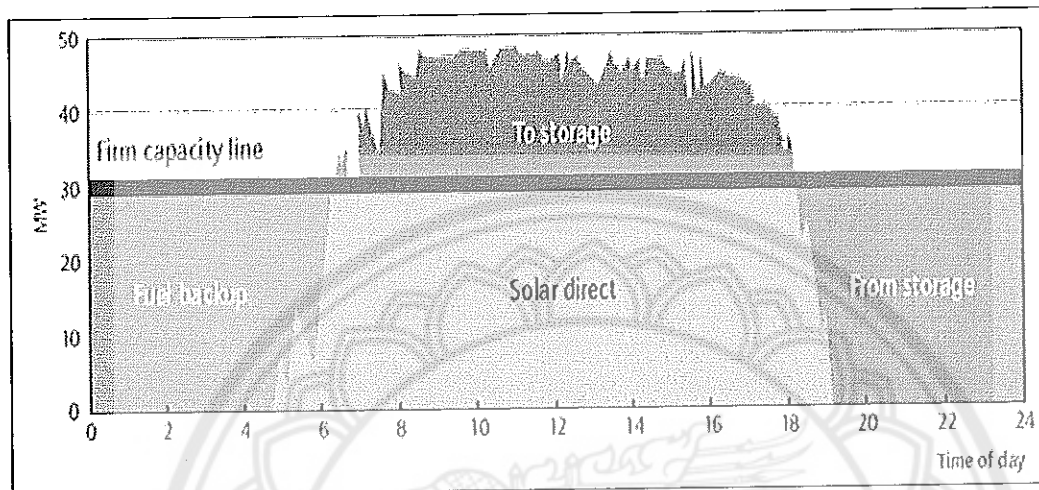


Figure 14 Combination of storage and hybridization in solar plant

Review of related articles

Murat Kenisarin and Khamid Mahkamov presented about the recent developments in the field of solar thermal energy storage with the use of phase change materials. They mainly focused about the thermal properties of the various types of PCMs. They have performed the studies of different phase change materials which are useful for active and passive solar space heating and cooling and solar cooking applications. Recent investigations on organic and inorganic PCMs and how they can be produced commercially and the commercial development of heat storage tanks were presented in this paper. They have studied about the different methods of heat transfer enhancement for the latent heat storage systems and mentioned the two suitable and effective methods for the storage of latent heat. Heat transfer enhancement using fin configurations and embedded high conductive structures are the mainly focused heat transfer configurations for solar heating systems. Application of PCMs in solar cooking and the schematic views of solar box cooker with including the storage system were presented in the paper. They have done the analysis of open literature available on the storage with PCMs and brought out the important conclusions regarding the testing

standards of the PCMs, economic viability of the PCMs, the need of thermal cycling of the PCMs which are used for the latent heat storage applications (19).

Lecuona. A, from Madrid presented about the portable parabolic type solar cooker along with the heat storage facility using phase change materials. They developed an utensil including daily thermal energy storage facility for the cooking purpose. The developed utensil was a two layered coaxial cylindrical cooking pot. The pot contains an inner layer which is small and the outlayer layer which is larger compared to inner layer. The hollow space between the two layers of the pot was filled with phase change material which provides the convective heat transfer of the latent heat stored in the PCM to the cooking material inside the pot. Paraffin and erythritol are the PCMs tested for this application. A numerical model was developed to study the transient behaviour of the system with the climatic conditions of Madrid. The results were attractive and with the developed system it is possible to cook three meals for the family in the summer as well as winter. The utensil can be moved inside the home 2 hours earlier in winter than summer to retain the heat effective for future usage. Paraffin at 100 °C is effectively working than that of erythritol but it is effective for fast cooking indoor applications. The attentive cooking and the hazards with the attentive cooking were reduced with this prototype including heat storage system (20).

A review about the solar cookers with and without thermal storage system was performed by Muthusivagami, R.M. The paper talks about the various development in the solar cookers and especially in the field of solar cookers with storage systems. Solar cookers with and without storage system are compared in this paper. Direct box type and concentrator type and indirect solar cookers without storage system were mentioned in this paper. Different types of sensible and latent heat storage solar cookers were reviewed and the schematic views of those cookers were mentioned. Latent heat storage type concentrating solar cooker using a PCM A – 164 was developed. The PCM is filled in 1 m long and 22 mm diameter tubes functioned as heat exchanger to store the heat during sunshine hours. Cooking surface flat hot plate similar to that of electric cooking and the PCM flows under the hot plate to keep the temperature about 140 °C to 150 °C. The PCM used in this system is economically not viable but with change of PCM the system is effective for residential cooking purposes (21).

John. G, presented their paper about the latent heat storage of solar cooker using Galactitol as a phase change material. The paper is mainly focused about the thermal behaviour of the PCM on bulk cycling. Three bulk samples of the material which are having different upper cycle temperatures compared to each other were taken and melted and frozen repetitively. The properties of the materials like specific heat, temperature and phase change enthalpies were measured with the help of differential scanning calorimetry (DSC) and thermal diffusivity was measured by flash diffusivity instrument. From the results they mentioned that the upper cycle temperature has influence on number of freezing and melting cycles can be attained, phase change enthalpy, the rate of subcooling, etc. The lowest upper cycle temperature is 200°C and with the possibility of 90 thermal cycles for the solar cooking at temperatures greater than 150°C . It was concluded that galactitol as PCM with thermal cycling atleast once in a day can afford of life span less than 100 days for cooking purpose. So galactitol was unstable and short life span PCM for medium range of temperature solar cooking applications (22).

The recent developments particularly in organic solid- liquid phase change materials and their applications in thermal energy storage were presented by Sharma, R.K., et al. The paper mainly focused about the organic solid – liquid materials, encapsulation for the storage systems and the various application of those materials. Because of low thermal conductivity of organic material large surface area is required for the heat transfer, so they paid the attention towards the thermal conductivity enhancement in turn reducing the area of the system. They mentioned about the various material characterization techniques like spectrum electron microscope (SEM), particle size distribution (PSD), Fourier transform infrared spectroscopy technique (FT- IR), Differential scanning calorimeter (DSC) and Differential thermal analysis (DTA) to characterize the thermal and chemical properties of the materials. Different solar thermal applications including heat storage systems were mentioned in this paper collected from the earlier literature. In this paper they concluded that the organic PCMs are useful for the low and medium temperature range of storage systems and they are non corrosive and are able to exhibit nearly constant melting and freezing characteristics after large number of thermal cycles. Organic PCMs are available in the range of 45°C to 70°C , so that they are highly recommended for solar energy applications like drying the food products (23).

Sharma, S.D, designed and developed a latent heat storage unit for evening cooking. They further evaluated the performance of the developed system. In this developed system acetamide was used as the latent heat storage material. They conducted the experiments with different loads and different loading times in summer as well as winter. The thermal performance of the developed unit was compared with the standard solar cooker. In this paper they mentioned the cooking vessel dimensions along with schematic view and the cooker is similar to that of solar box cooker. The first Figure of merit F_1 and second Figure of merit F_2 were calculated for both the cookers. From the experiment it was concluded that the developed unit is capable for cooking purpose in the evening time and the PCM did not affect the cooking process in the afternoon. If the used PCMs in this unit having the melting temperature range of 105°C to 110°C are able to provide evening cooking (24).

Buddhi, D., S.D. Sharma, and A. Sharma performed the thermal performance evaluation of a latent heat storage unit for late evening cooking in a solar cooker having three reflectors. Acetanilide with melting point 118.9°C was used as a PCM material in this developed system. Evaluation of the cooker was performed with different loads and loading times in the winter. In this system the three reflectors are used to enhance the solar radiation incident on the solar cooker during sunshine hours. First and second Figure of merits of the system were calculated. These experiments were conducted at Indore in India with the latitude of 22.7°N . While conducting the experiment the direction and orientation of the cooker and the reflectors were adjusted for every 30 minutes along with the motion of the sun. From the results it was concluded that the set up is effectively working for the evening cooking about 8:00 P.M with 4 kg of PCM (25).

Thermal performance of evacuated tube solar collector based solar cooker with a PCM storage unit was conducted by Sharma, S.D. The proposed design has separate parts for energy collection and cooking which were coupled to PCM storage unit. Energy collector was the evacuated tube collector and the PCM used in this prototype for storage purpose is commercial grade erythritol. Different loads with different loading times were experimented in this prototype but the cooking and PCM processing were carried out simultaneously. These experiments were carried out at Mie in Japan where the evening cooking with the PCM storage unit is faster than that of noon cooking. From

the results it was concluded that, the PCM reaches 110°C in the summer at the time of evening cooking but the system is expensive because of the cost of the PCM. This kind of PCM units have good potential for community cooking applications with temperature range about 130°C with out tracking the cooker (26).

El-Sebaili, A. A, performed one thousand thermal cycles of magnesium chloride hexahydrate as a PCM for indoor cooking purpose. This paper mainly focused about the variation in thermo physical properties like melting point and latent heat of fusion of the PCM material on fast melting and freezing cycles and the properties are measured with DSC. In a sealed container one thousand thermal cycles have been performed with the help of extra water principle. 463 g of the PCM was taken for the thermal cyclings and for every regular period of cycles 4 mg of PCM sample was tested under DSC. The DSC results were mentioned in the paper and from the results it was concluded that $\text{MgCl}_2 \cdot 6\text{H}_2\text{O}$ solidifies with small range of super cooling about 0.1°C to 3.5°C and this PCM was a promising material for latent heat storage for solar cooking indoor applications (27).

Tyagi, V.V. and D. Buddhi, performed thermal cycle testing of calcium chloride hexahydrate $\text{CaCl}_2 \cdot 6\text{H}_2\text{O}$ as a PCM for latent heat storage. In this study they performed thousand thermal cycles of the material to observe the variations in the melting point and latent heat of fusion of the selected inorganic salt hydrate. 26.38 mg of sample was tested under DSC for every 100 cycles of the total thermal cycles. After 1000 accelerated thermal cyclings calcium chloride hexa hydrate undergone small variation in latent heat of fusion but it maintains the constant temperature range after large number of thermal cyclings. All the DSC results were mentioned in the paper from the analysis of those results it was concluded that $\text{CaCl}_2 \cdot 6\text{H}_2\text{O}$ can be a promising PCM for latent heat storage applications (28).

For solar thermal latent heat storage applications, accelerated thermal cycle test were performed on acetamide, stearic acid and paraffin wax by Sharma, A., S.D. Sharma, and D. Buddhi. Total 1500 thermal cycles were conducted on these materials to observe the variations in the latent heat of fusion and melting point of those materials. 130 g, 90 g and 150 g of acetamide, stearic acid and paraffin wax were taken respectively for the testing. The melting time taken by those materials are 40 min, 35 min and 25 min respectively and the solidifying times are 70 min, 50 min and 40 min respectively for

actamide, stearic acid and paraffin wax. The samples were tested under DSC after 1500 cycles and from the results it was concluded that the three samples did not have degradation in the melting point after 1500 repeated thermal cycles. Actamide and paraffin wax shown good stability for the thermal cyclings but actamide absorbs moisture from the surroundings. Stearic acid melts over a range of temperatures. So from these results , it is better to test the PCM for thermal cyclings before using as a latent heat storage systems (29).

Pia Piroshka Otte presented a study about the cultural turn towards to the solar cooking in two countries Burkina Faso and India. For this work they installed a type of solar cooker with Scheffler reflectors in different places like bakeries and steam kitchens. Six case studies were presented in this paper and explained how the cultural factors affecting in the adoption – enhancing or limitation of using solar cookers. From the work he concluded that the foreign technology image for solar cookers was moved away from the installations of the solar cookers within the frame of cultural network (30).

Raam Dheep. G and Sreekumar. A, presented a review about the various studies on latent heat storage using phase change materials and the classification of the PCMs, properties of the PCMs, selection criteria of the studies involved to analyze the thermophysical properties of PCMs. The paper also presents the possible research areas on latent heat thermal energy storage (31).

Kevin Merlin, discussed about the heat transfer enhancement in latent heat thermal energy storage. They also presented the comparative study of different solutions and thermal contact investigation between the exchanger and PCM. They conducted the experiments with conductive structures like finned exchangers, graphite powder and Expanded Natural Graphite (ENG) matrix. The practical set up consists of heat exchanger tube and the outer annular of the heat exchanger filled with PCM. The overall heat transfer coefficient is measured for each configuration. The study concludes that the PCM embedded in ENG matrix is the best storage configuration for industrial purposes with the overall heat transfer coefficient about $3000 \text{ Wm}^{-2} \text{ K}^{-1}$. Thermal conductivity of the ENG/PCM composite is 100 times more than that of PCM alone. The numerical simulations are compared with the experimental results which are helpful

for the further investigations for the thermal contact resistance on the heat transfer process of latent heat thermal storage systems (32).

Different experimental test procedures of paraboloid concentrator solar cooker to determine the optical efficiency factor were presented by Subodh and Mullick (33). The heat loss factor ($F'U_L$), optical efficiency factor ($F'\eta_0$) were calculated with three different experimental procedures. The first process uses sensible water heating curve of the water in the cooking pot placed at the focus of the paraboloid. The second process uses the steady flow of water through the focal zone of the cooker and the third process is the combination of the above two processes. 0.335, 0.273 and 0.347 are the optical efficiency factors of the paraboloid solar cooker from the first, second and third test procedures respectively. From this study they concluded that, the first and second procedures are good whereas the first procedure is recommended for the accurate determination of optical efficiency factor.

The heat transfer enhancement of solar parabolic cooker by a porous medium was designed and analyzed by Lokeswaran and Eswaramoorthy (34). Waste metal chips made of copper with size 1.5 cm length and 0.5 to 1 cm thickness were used as porous medium. This porous medium was placed in a cylindrical container of height 8 cm and diameter is equal to the cooking utensil. That container is filled with porous medium upto 5 cm and is placed below the cooking utensil. Stagnation temperature test, water heating and cooling tests were performed with this parabolic cooker. The stagnation temperature was 80 °C more than that of the utensil without porous medium. The minimum heat loss factor with and without porous medium was 20 Wm⁻² and 14 Wm⁻² respectively. The optical efficiency factor increases upto a maximum value of 61 with porous medium.

A parabolic dish solar cooker of 1.25 m diameter and height 0.23 m with a cylindrical receiver of diameter 0.215 m and height 0.15 m was designed and analyzed for the climatic conditions in Yola, Nigeria by Aidan (35). 0.4 kg mass of cooking pot containing 0.37 kg of water placed at the focal point and the temperature of water is recorded for every 5 min time interval. ($F'U_L$), ($F'\eta_0$), combined heat capacity and cooking power were calculated. For a combined heat capacity of 1914.3 J K⁻¹, the optical efficiency factor, heat loss factor and the cooking power are 0.0198, 4.404 W m⁻² and 96.530 W respectively.

From the above mentioned related review articles, it was summarized that, in recent years the research and development of thermal energy storage got the attention of the researchers throughout the world. In developing countries like south Asian and African countries solar cooking got the noticeable demand as same as that of traditional cooking ways with in the cultural frame of the situations in those countries. To make the technology more user friendly and efficient researchers are concentrated their research on the storage of thermal energy with different technologies like sensible heat storage, latent heat storage and the thermo-chemical storage. From the reviewed articles it is clearly understood that the latent heat storage technology is got the attention of the research than the other two technologies. The advantages and the different latent heat or phase change materials experimental studies for the use of solar thermal energy storage were mentioned in the articles. The studies which were conducted till now on PCMs are shown that less number of researchers performed their studies on $\text{Mg}(\text{NO}_3)_2$ based salt hydrate phase change material.

The storage technologies developed for cooking application are limited to an individual family but not for community or institutional based cooking applications. So, from the literature scope this dissertation is discussed on the $\text{Mg}(\text{NO}_3)_2$ based phase change material solar thermal energy storage system for the community solar cooking applications. The advantages of the selected PCM, background of the thermal energy storage systems, different classifications of phase change materials and the experimental methods to conduct research are mentioned in the next chapters.

CHAPTER III

RESEARCH METHODOLOGY

This dissertation was conducted in five phases.

1. Development of PCM storage system
2. Design of solar cooking system
3. Incorporating PCM storage with solar cooking system
4. Performance evaluation of the developed system
5. Economic and emission analysis of the system

Figure 15 shows the complete flow chart of research methodology for this dissertation. The Selection and testing of PCM and design of solar concentrator are the main phases of the methodology. After completion of these two phases, the remaining three phases are performed on the developed system.

The flow chart for development of PCM storage system is shown in Figure 16. All particulars of the different criteria in the selection of the PCM are mentioned in the next sections.

Development of PCM storage system

The development of PCM storage system was performed in the following steps.

1. Confirmation criteria of PCMs
2. Preliminary testing of PCMs
3. Thermal cycling method
4. Instrument analysis
5. Corrosion analysis

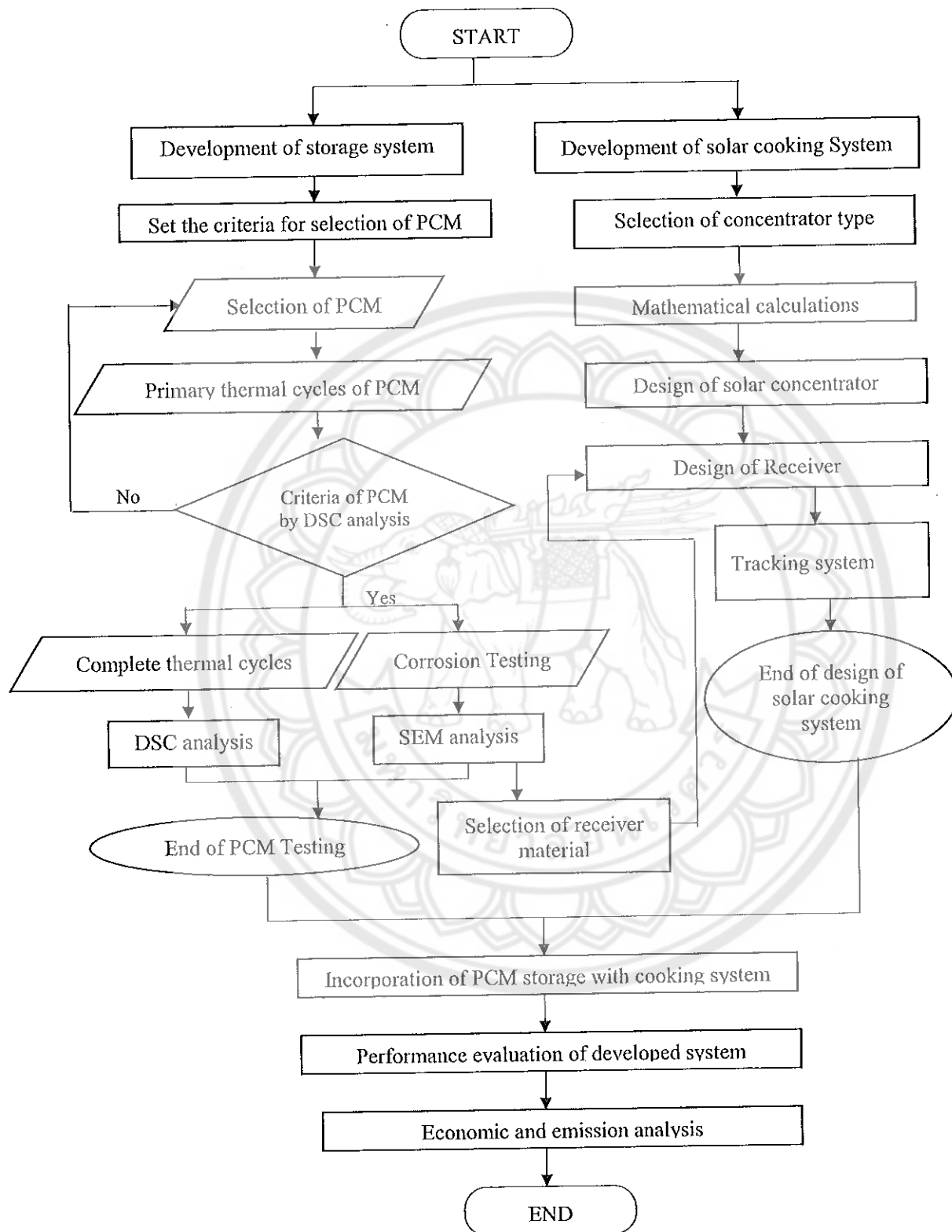
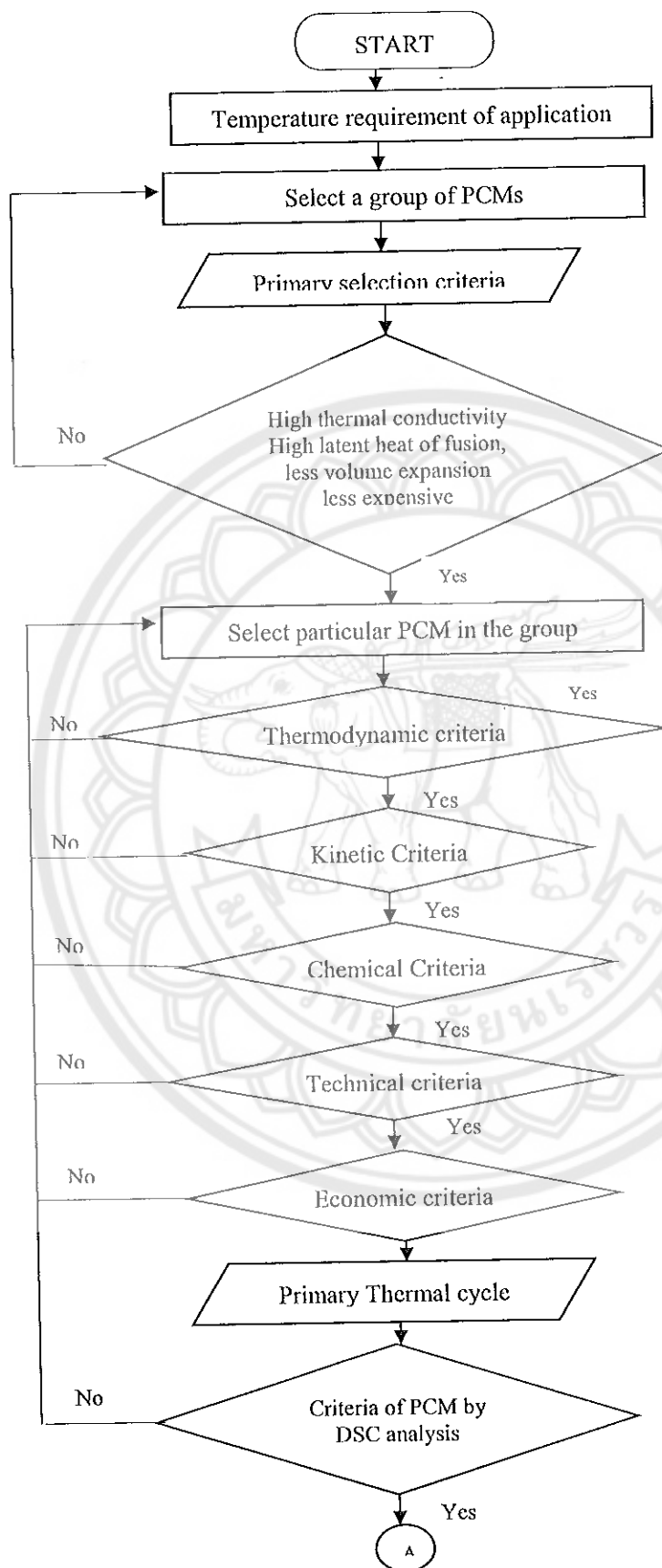


Figure 15 Flow chart of complete research methodology



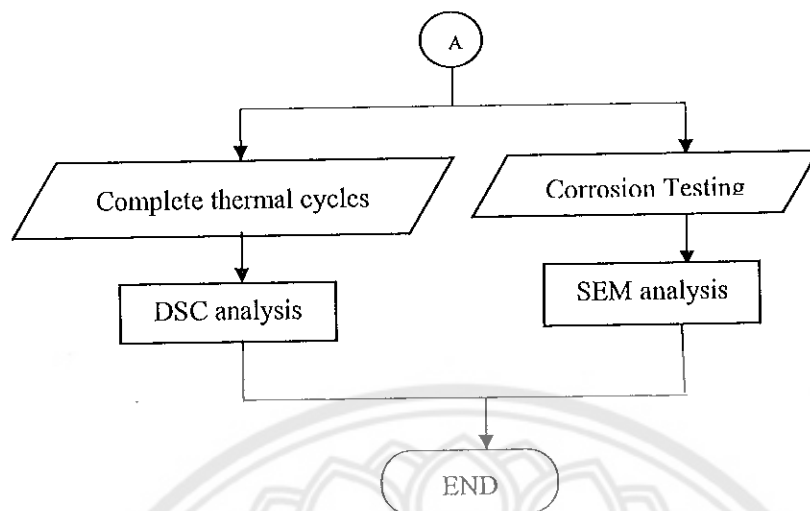


Figure 16 Flowchart of development of storage system

Confirmation criteria of PCMs: The phase change materials are selected based on the melting point of the materials and the type of application for which the storage system will be incorporated. Different criteria a PCM should have are explained below (11).

Thermodynamic criteria:

1. PCM should have the melting point in desired operating range about 90°C to 110°C
2. High latent heat of fusion per unit mass in the range of 150 J g^{-1} to 200 J g^{-1}
3. High density in the range of 1.5 g cm^{-3} to 1.7 g cm^{-3} so that volume of the material is reduced
4. High thermal conductivity in between $0.5\text{ W m}^{-1}\text{ }^{\circ}\text{C}^{-1}$ to $0.7\text{ W m}^{-1}\text{ }^{\circ}\text{C}^{-1}$
5. High specific heat in the range of $1.8\text{ J g}^{-1}\text{ }^{\circ}\text{C}^{-1}$ to $2.5\text{ J g}^{-1}\text{ }^{\circ}\text{C}^{-1}$
6. Small volume changes during phase transition

Kinetic criteria:

The PCM should have very low super cooling phenomenon during freezing cycle.

Chemical criteria:

1. Chemical stability
2. Non corrosive to the storage tank material
3. Nontoxic, nonflammable and non-explosive

Technical and economic criteria:

1. Applicability
2. Compactness and effectiveness
3. Reliability and viability
4. Commercial availability
5. Economically viable

From the above mentioned criteria, some inorganic phase change materials were selected and different properties of those materials were mentioned in Table 6.

Table 6 Properties of inorganic phase change materials

Inorganic PCM	Melting temp T_m ($^{\circ}\text{C}$)	Heat of fusion (J g^{-1})	Specific heat capacity C_p ($\text{J g}^{-1} \text{ }^{\circ}\text{C}^{-1}$)	Density (g cm^{-3})	Thermal conductivity ($\text{W m}^{-1} \text{ }^{\circ}\text{C}^{-1}$)
CaCl₂.6H₂O	29.5	170	1.42(S)	1.802(S)	1.088(S)
			2.10(L)	1.562(L)	0.540(L)
Na₂SO₄.10H₂O	32.4	251	-	-	0.5
			-	-	-
Mg(NO₃)₂.6H₂O	90	163	1.81(S)	1.636(S)	0.669(S)
			2.48(L)	1.55(L)	0.49(L)
MgCl₂.6H₂O	116.7	169	2.25(S)	1.57(S)	0.704(S)
			2.61(L)	1.45(L)	0.570(L)

Applications of PCMs: There are different types of implicational requirements for a PCM to be selected for a particular application. Table 7 shows the characteristics of different PCMs for Different applications (7).

For the above mentioned different applications design considerations of thermal energy storage systems at each level were shown in the Figure 17 (36).

Table 7 Different applications of PCMs

Required PCM melting temp (°C)	PCM can be used	Melting point temp of PCM (°C)	Application of PCM
Room Temperature	$\text{CaCl}_2 \cdot 6\text{H}_2\text{O}$	27	Diurnal storage for building structure
20 - 35	$\text{CaCl}_2 \cdot 6\text{H}_2\text{O}$	27	Building heating using heat pumps
25 - 30	$\text{CaCl}_2 \cdot 6\text{H}_2\text{O}$	27	Solar hot air systems
40 - 60	$\text{Mg}(\text{NO}_3)_2 \cdot 6\text{H}_2\text{O}$ $\text{MgCl}_2 \cdot 6\text{H}_2\text{O}$	About 58	Day and night solar hot air heating systems
55- 70	$\text{Mg}(\text{NO}_3)_2 \cdot 6\text{H}_2\text{O}$ $\text{MgCl}_2 \cdot 6\text{H}_2\text{O}$	About 58	Domestic solar hot water system
60 - 95	$\text{Mg}(\text{NO}_3)_2 \cdot 6\text{H}_2\text{O}$	89	Solar hot water base board systems
100 - 175	$\text{Mg}(\text{NO}_3)_2 \cdot 6\text{H}_2\text{O}$	117	Concentrated solar systems

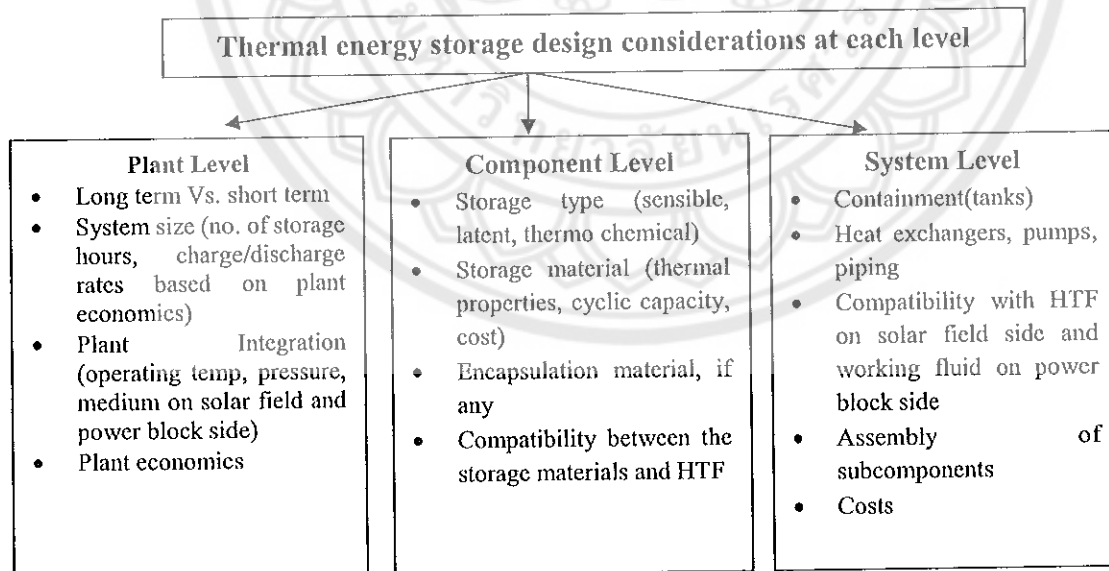


Figure 17 Thermal energy storage design considerations at each level

From the literature and different criteria for the selection of PCM, $\text{Mg}(\text{NO}_3)_2 \cdot 6\text{H}_2\text{O}$ was qualified thermodynamic, kinetic, chemical, technical and economic criteria. So, the materials selected for the further testing procedure to use it as storage material for the proposed dissertation.

Magnesium Nitrate Hexahydrate ($\text{Mg}(\text{NO}_3)_2 \cdot 6\text{H}_2\text{O}$):

1. Molecular weight of $\text{Mg}(\text{NO}_3)_2 \cdot 6\text{H}_2\text{O}$ is $256.41 \text{ g mol}^{-1}$
2. Salt and water proportions by weight are 57.84% and 42.16% respectively
3. $\text{Mg}(\text{NO}_3)_2 \cdot 6\text{H}_2\text{O}$ will be dehydrated if heated above 95°C
4. Melting temperature, latent heat of fusion, specific heat capacity, thermal conductivity and density of $\text{Mg}(\text{NO}_3)_2 \cdot 6\text{H}_2\text{O}$ are mention in table 5.
5. $\text{Mg}(\text{NO}_3)_2 \cdot 6\text{H}_2\text{O}$ has super cooling characteristics which can be avoided b adding additives

The testing and analysis methods for $\text{Mg}(\text{NO}_3)_2 \cdot 6\text{H}_2\text{O}$ PCM are explained in next sections.

Testing methods of PCM

To incorporate the PCM storage system with the solar thermal applications some tests are to be performed on the PCMs. The main order of the tests performed on a PCM which can be used for a storage system are as follows (37).

1. Preliminary testing of PCMs
2. Thermal cycling method
3. Instrument analysis
4. Corrosion analysis

Preliminary testing of PCMs

In this step, among the certain type of phase change materials, melting point of the materials is examined with the use hot plate or any other heating source. From the observation of the melting points of all the considered PCMs, required operating range temperature PCM is selected for the further tests to finalize the PCM for storage applications. From the literature, based on the melting point and the operating range of temperature $\text{Mg}(\text{NO}_3)_2 \cdot 6\text{H}_2\text{O}$ is selected as the storage material for the cooking application of this dissertation. To compare the properties of this PCM with other inorganic PCMs, a preliminary test is needed.

Salt hydrate PCMs calcium chloride hexahydrate ($\text{CaCl}_2 \cdot 6\text{H}_2\text{O}$), magnesium chloride hexahydrate ($\text{MgCl}_2 \cdot 6\text{H}_2\text{O}$), sodium sulphate decahydrate ($\text{Na}_2\text{SO}_4 \cdot 10\text{H}_2\text{O}$) and magnesium nitrate hexahydrate ($\text{Mg}(\text{NO}_3)_2 \cdot 6\text{H}_2\text{O}$) were considered. Primarily, the melting point temperature of the salt hydrates will be observed. From the observation and the literature PCM which suitable for the community solar coking application will be considered for further tests. From the above mentioned tables from literature it is shown that $\text{Mg}(\text{NO}_3)_2 \cdot 6\text{H}_2\text{O}$ has high melting point compared to the remaining salt hydrate materials.

Thermal cycling method

This is the important part of testing a PCM. For the selected PCM from the preliminary tests, thermal cycling method will be conducted. In this method The PCM will undergo for repetitive thermal cycling in order to observe the variation in the properties of the PCM. A relatively more quantity of the PCM about 200 g to 500 g should be taken to conduct the thermal cycling. A hot plate is required to heat the PCM container and a natural cooling water environment is to be set up for the solidification cycle immediately after the heating cycle of the PCM. The water cooling environment helps to freeze the PCM in less time so that duration of a single heating and cooling process can be reduced.

While performing the thermal cycling the PCM container should be closed to avoid the other foreign materials and the heat losses. The sample of the PCM should be collected before starting the thermal cycling of the PCM and store it as 0th cycle. Then after, for every regular interval of thermal cycle's small amount of the sample about 0.5 mg to 100 mg is to be collected for the instrument analysis. The collected 11 samples of the PCM were analyzed in the nest step of testing of PCMs (27) (28) (29).

A 227 g of $\text{Mg}(\text{NO}_3)_2 \cdot 6\text{H}_2\text{O}$ is taken for the thermal cycling process in this dissertation. From 0th cycle the weight of the material is measured for every 100 cycles. The sample of $\text{Mg}(\text{NO}_3)_2 \cdot 6\text{H}_2\text{O}$ is allowed to heat for in the process of thermal cycles for melting with the help of hotplate which is known as melting cycle. After the melting cycle the sample is allowed to cool down in the cooling water environment which is known as solidification or freezing cycle. A complete melting and solidification cycle is known as a thermal cycle and such a 1000 cycles are performed for the taken sample of $\text{Mg}(\text{NO}_3)_2 \cdot 6\text{H}_2\text{O}$. For every 100 cycles, the time taken for the melting cycle and

solidification cycle are observed and noted. The sample is taken in an aluminum container with closed lid to conduct the thermal cycling process. The initial sample of the material at 0th cycle and the weighing process of the sample after melting process are shown in Figure 18 a, b. The melting cycle of the sample with the help of hot plate and the freezing cycle in the cooling water environment is shown in Figure 19 (a) and (b).

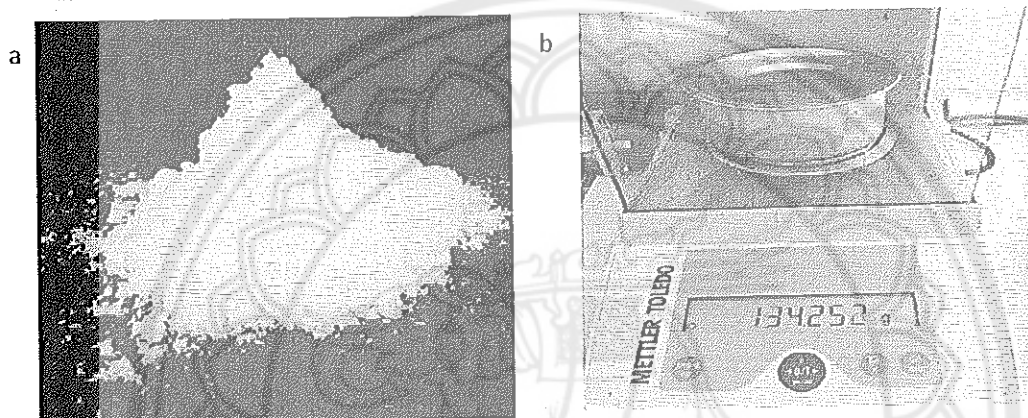


Figure 18 $\text{Mg}(\text{NO}_3)_2 \cdot 6\text{H}_2\text{O}$ (a) Sample at 0th cycle (b) Weight measurement of the sample

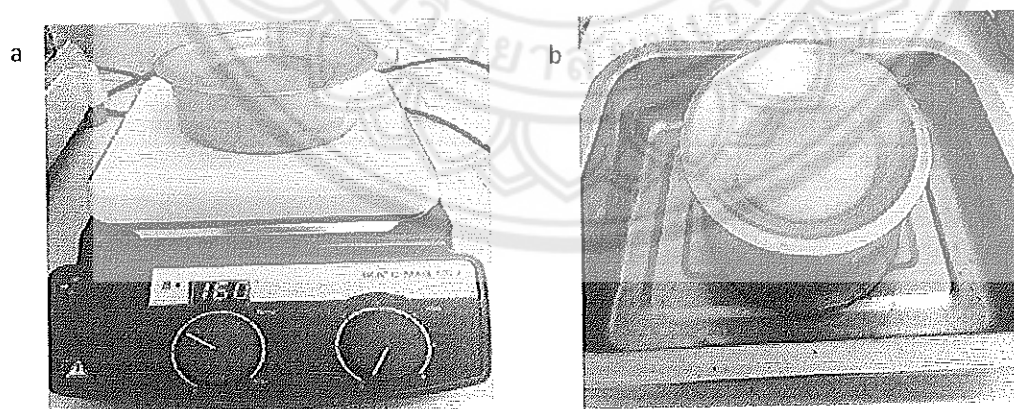


Figure 19 $\text{Mg}(\text{NO}_3)_2 \cdot 6\text{H}_2\text{O}$ (a) Melting cycle (b) Solidification cycle

Instrument analysis

Instrument analysis of the sample is conducted at two levels of the thermal cycling process. After 100 thermal cycles a primary Differential Scanning Calorimeter (DSC) analysis is conducted to check the thermal criteria of the PCM sample as shown in the flow chart of the PCM storage system. If the material is satisfied with the mentioned criteria the sample is continued for the remaining thermal cycles. If the sample is not stable in the primary testing, then the other PCM materials are considered for the storage system. The $\text{Mg}(\text{NO}_3)_2 \cdot 6\text{H}_2\text{O}$ sample is collected after 100 cycles and tested with DSC. The criteria for PCM as storage system are satisfied for the $\text{Mg}(\text{NO}_3)_2 \cdot 6\text{H}_2\text{O}$ sample and the results are shown in chapter 4. The $\text{Mg}(\text{NO}_3)_2 \cdot 6\text{H}_2\text{O}$ sample is continued for the remaining thermal cycles. After every 100 cycles about 100 mg of the sample is collected for the DSC analysis.

After 1000 thermal cycles of the selected PCM the collected samples are to be analyzed to observe the variations in the melting point and latent heat of fusion of the material. In DSC the sample will be placed in aluminum pan and the empty pan is placed in the of reference pan. Thermocouples sensors were placed below the plans. A schematic view of DSC is shown in Figure 20. The original DSC instrument and the DSC with samples inside the DSC are shown in Figure 21.

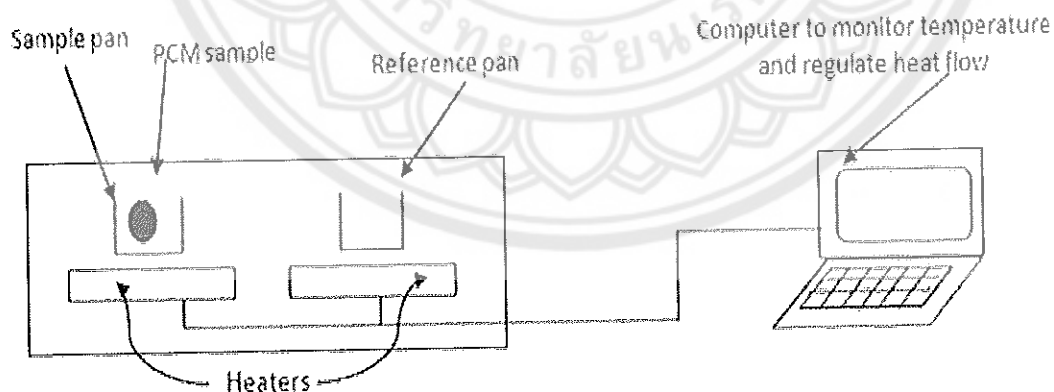


Figure 20 Schematic view of interior view of DSC

The measurements of DSC are two types

1. Measuring the electrical energy provided to the heaters to maintain the same temperature between the two pans.

2. By measuring the heat flow as a function of temperature.

From the two ways ultimately, the DSC gives the output as the differential heat flow between the sample and reference pan. Heat capacity is to be determined with the following equation.

$$C_p = q / \Delta T \quad (8)$$

C_p = material heat capacity, $J g^{-1} ^\circ C^{-1}$

q = heat flow, W

ΔT = change in temperature, $^\circ C$

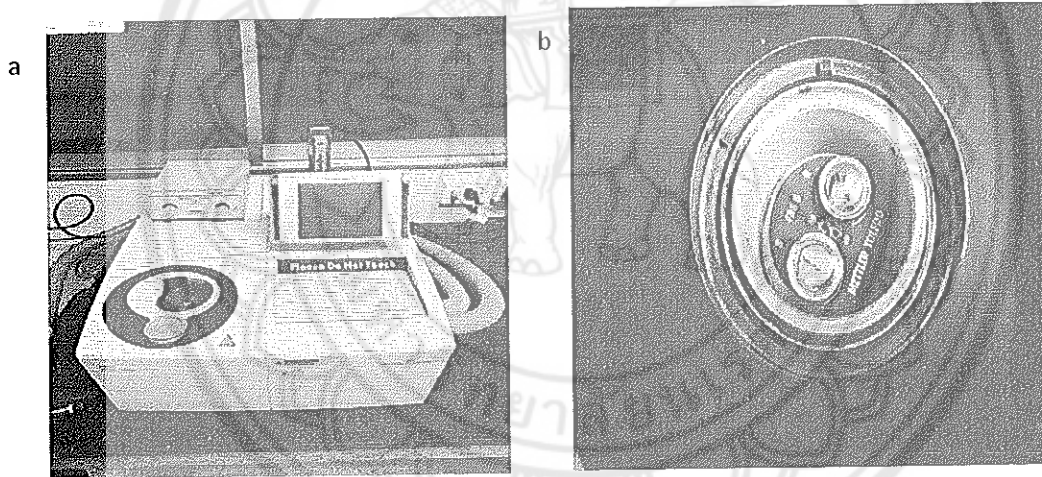


Figure 21 (a) DSC (b) DSC loaded with $Mg(NO_3)_2 \cdot 6H_2O$ sample

After the arrangement of the sample DSC is operated for the thermogram. Thermogram is a graph between temperature in x- axis and heat flow in y- axis. It will give the information about the glass transition temperature T_g , crystallization temperature T_c , melting point temperature and oxidation temperature (38). The schematic of a DSC thermogram is shown in Figure 22. After the observation of the results the PCM can be finalized for the storage system.

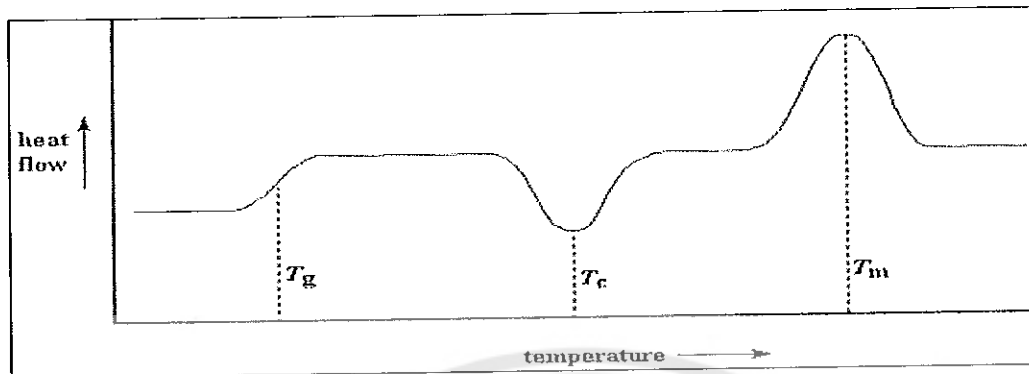


Figure 22 Schematic graph of a DSC thermogram

Corrosion analysis:

In the thermal energy storage systems storage tank or the container also plays an important role. The container is always in the contact with storage medium. For solar thermal energy applications either stainless steel or aluminum containers are commonly used. So, container material analysis after repetitive thermal cycles of the PCM will provide the corrosion effect of the PCM on the container. A small piece of stainless steel and aluminum are placed in the PCM in different experimental vessels. Before starting the thermal cycling for corrosion testing Scanning Electron Microscopy (SEM) images of the metal samples should be collected. After thermal cycling process at 500th cycle and 1000th cycle again SEM images of the metal pieces should be collected. From those observations the corrosive effect of the PCM on the storage container will be analyzed (13).

A 3 cm x 3 cm aluminum and stainless steel samples are kept in the $\text{Mg}(\text{NO}_3)_2 \cdot 6\text{H}_2\text{O}$ sample for corrosion analysis. The PCM sample is allowed for thermal cycling process including aluminum and stainless samples. After 500, 1000 thermal cycles the samples are taken out and analyzed with the help of SEM. The results are shown in chapter 4. After the analysis of the SEM results, the receiver material is selected to design the receiver or cooking pot of the solar cooking system. The SEM practical image and the PCM with container material samples are shown in Figure 23.

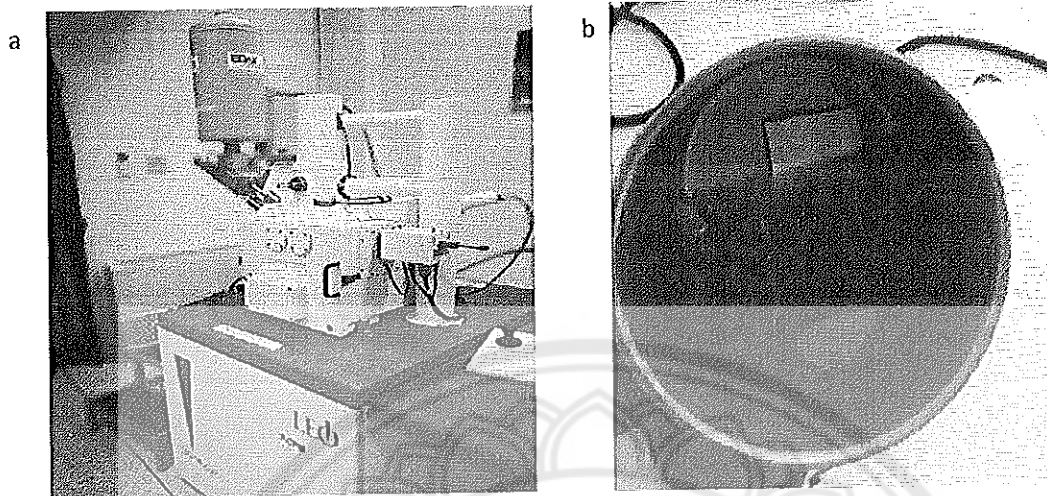


Figure 23 (a) Image of SEM (b) Container materials inside $\text{Mg}(\text{NO}_3)_2 \cdot 6\text{H}_2\text{O}$

Design of solar cooking system

The phase change material storage system is going to develop will be incorporated with the solar cooking system which contains solar concentrator and receiver or cooking pot as the main components. A parabolic dish is designed as a solar concentrator and the receiver is placed at the focal point of the parabolic dish. The different calculations of the cooking system including heat transfer methods are also mentioned in this section.

1. Mathematical calculations for solar concentrator and receiver
2. Heat Transfer network
3. Tracking of the system

Mathematical calculations for solar concentrator and receiver

A parabolic antenna dish with a diameter of 1.495 m and a depth or height of 0.268 m is considered to design the solar concentrator. The surface of the parabolic dish is covered by a number of high reflective solar parabolic mirrors of size 2.5 sq. cm. The design and construction solar concentrator is shown in Figure 24.

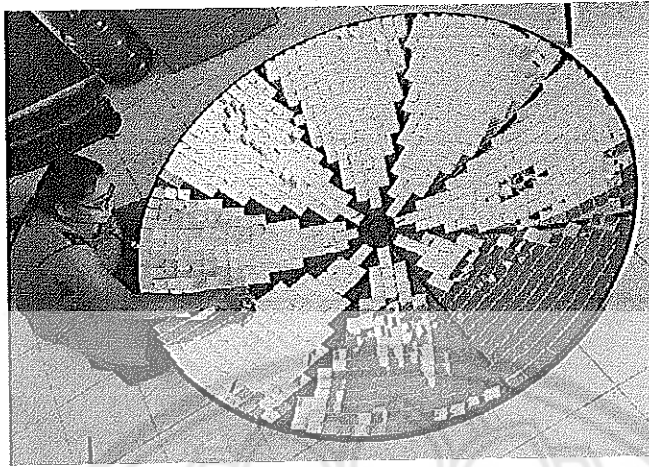


Figure 24 Construction of solar concentrator

Different parameters of the parabolic dish like focal length, rim angle, acceptance angle, concentration ratio, arc length, surface and aperture areas and the focus area of the receiver pot were calculated with the following sequence of expressions (6, 39-42).

The focal length ' f ' of solar concentrator, is the distance from the vertex to the focus point F. It is calculated using equation 9.

$$f = \frac{D^2}{16h} \quad (9)$$

After finding the value of focal length, rim angle of the parabolic solar concentrator is found using equation 10.

$$\phi = 2 \tan^{-1} \left[\frac{D}{4f} \right] \quad (10)$$

Half acceptance angle of the parabolic concentrator is the half of the angular limit to which the incident ray may deviate from the normal to the aperture plane and still reach the absorber or receiver, is calculated using equation 11.

$$\theta_A = \frac{90 - \phi}{2} \quad (11)$$

Concentration ratio is an important factor for the parabolic concentrators which is expressed as a function of rim angle and is also expressed as the ratio of aperture area

of the solar concentrator the surface area of the receiver. Concentration ratio is calculated using equation 12.

$$C = \frac{1}{\sin^2 \phi} \quad \text{or} \quad C = A_a/A_r \quad (12)$$

The maximum radius of the parabolic concentrator is calculated using equation 13. It is a function of focal length and rim angle.

$$P = \frac{2f}{1 + \cos \phi} \quad (13)$$

Surface area of the parabolic concentrator is the outer area of the parabolic concentrator and is calculated using equation 14.

$$A_s = \frac{8\pi f^2}{3} \left\{ \left[\left(\frac{D}{4f} \right)^2 + 1 \right]^{\frac{3}{2}} - 1 \right\} \quad (14)$$

Aperture area of the solar concentrator is the area where the solar radiation incident on the parabolic concentrator. It is calculated using equation 15 and is a sin function of maximum radius and rim angle of the concentrator.

$$A_a = \frac{\pi}{4} (2P \sin \phi)^2 \quad (15)$$

The diameter of the focal point of the concentrator is calculated using equation 16.

$$D_{fo} = 2P \sin \theta_A \quad (16)$$

After finding the diameter of the focal point, area of the focal point is calculated by equation 17. These both parameters are useful to calculate and design the receiver or cooking pot.

$$A_f = \frac{\pi}{4} (D_{fo})^2 \quad (17)$$

The geometrical representation of the above mentioned parameters are shown in Figure 25.

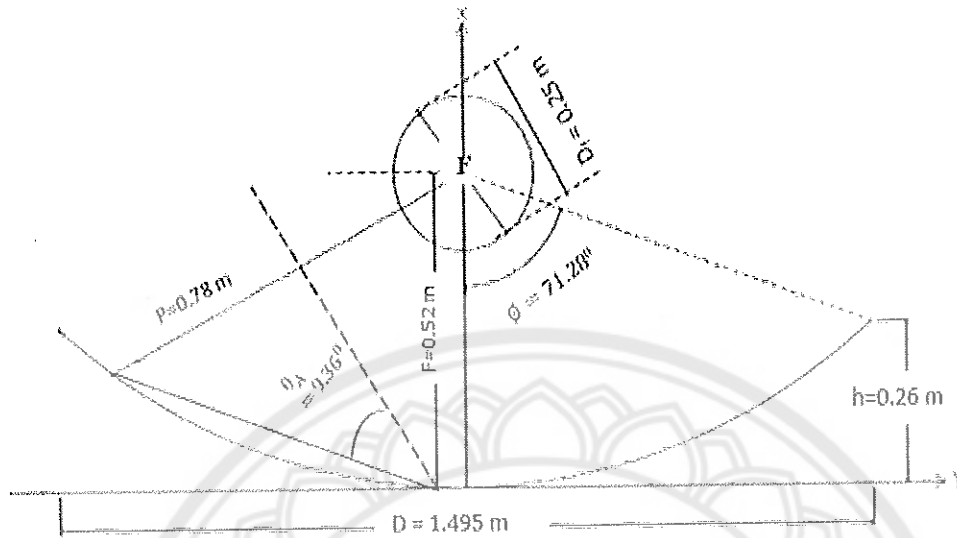


Figure 25 Geometrical representation of design parameters of solar concentrator

The receiver or cooking pot of the solar cooker is made up of stainless steel which is in the shape of hollow concentric cylinder with outer and inner radii are 10 cm and 9 cm respectively.

The gap or thickness between the layers of the receiver is 1 cm and height of the receiver is 25 cm. This gap between the layers is filled by heat transfer oil. A cylindrical tube of diameter 2.5 cm and height of 23 cm is used as phase change material (PCM) tube and is filled with selected PCM. Number of such tubes are placed on the surface of the outer layer of the receiver. The PCM is filled in the tubes up to a height of 20 cm.

Area of the receiver or cooking pot is calculated using expression 18.

$$A_r = 2\pi r_p (r_p + h_p) \quad (18)$$

The gap or thickness between the layers of the receiver is 1 cm and height of the receiver is 25 cm. This gap between the layers is filled by heat transfer oil. A cylindrical tube of diameter 2.5 cm and height of 23 cm is used as PCM tube and is filled with $\text{Mg}(\text{NO}_3)_2 \cdot 6\text{H}_2\text{O}$. The schematic view of the cooking pot or receiver is shown in Figure 26 with the help of sketch-up software. The surface area calculations of the cooking pot are mentioned in appendix B.

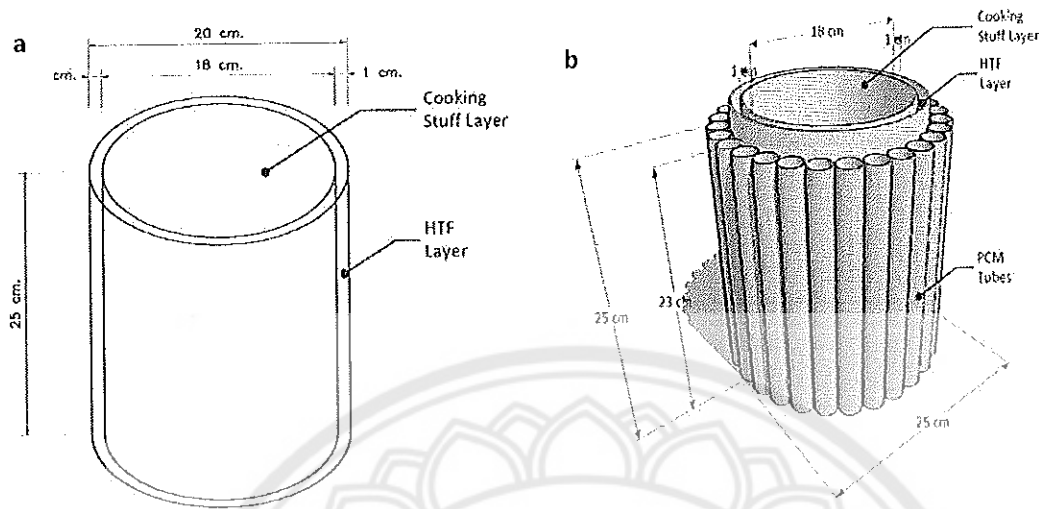


Figure 26 Schematic view of (a) Cooking pot layers (b) Cooking pot with PCM tubes

Heat Transfer network

In the solar cookers with heat storage technology, the heat from the solar collector to the receiver or cooking pot is transferred in the form of three modes namely radiation, convection and conduction (7). In most of the solar cookers, radiation and convection are the two modes of heat transfers involved to transfer heat. But, in this solar cooker with PCM as storage, conductive mode of heat transfer also involves while storing and transferring heat from the solar collector to the cooking stuff inside the receiver which is explained with the help of heat transfer network. The heat transfer network is the combination of different thermal resistances which represents the conductive, convective and radiative heat transfer modes involved in the system. The complete heat transfer network for PCM solar cooker is shown in Figure 27.

The solar energy reflected from the solar collector is transferred to the receiver at the focal point of the parabolic collector by radiative and convective heat transfer modes. The radiative and convective heat transfer resistances are represented as h_r and h_l in the heat transfer network. As the outermost part of the receiver is covered with PCM tubes, the mode of heat transfer involved between the outer wall of the PCM and surroundings is conduction and is denoted by k_l . The heat is transferred to the entire PCM inside the tube by convection and from the last layer of the PCM to PCM wall heat is transferred by conduction which are represented by h_2 and k_2 respectively. The

heat is transferred from the wall of PCM tube to outer layer of the receiver by conduction and is represented as k_3 . The heat from the outer layer of the receiver is transferred by convection to the entire oil which presents in the gap between the layers of the receiver pot which is denoted by h_3 . The heat is transferred from the oil to the inner layer of the receiver by conduction and is represented as k_4 and that heat is transferred to the cooking material inside the pot by convection which is represented as h_4 in the heat transfer network. These are the complete modes of heat transfer and are explained at each stage with the help of heat transfer network.

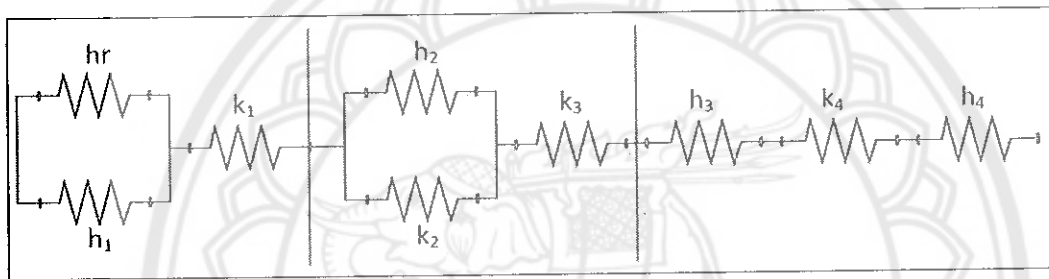


Figure 27 Heat transfer network of PCM solar cooker

In PCM tubes, the PCM is filled completely in the tubes except a little gap for the small volume expansion after the melting cycle of the PCM. As $\text{Mg}(\text{NO}_3)_2 \cdot 6\text{H}_2\text{O}$ comes under inorganic salt hydrate PCMs, it has the advantage of small volume expansion so the PCM tubes are filled completely. So, the mode heat transfer through convection is not possible in PCM tubes. The heat transfer oil which presents in the gap of the concentric cylindrical receiver is also filled completely inside the gap and the layer vent is tightly closed. In this case also, the convective mode of heat transfer is not possible. The above mentioned heat transfer network is modified based on this consideration and the modified heat transfer network is shown in Figure 28.

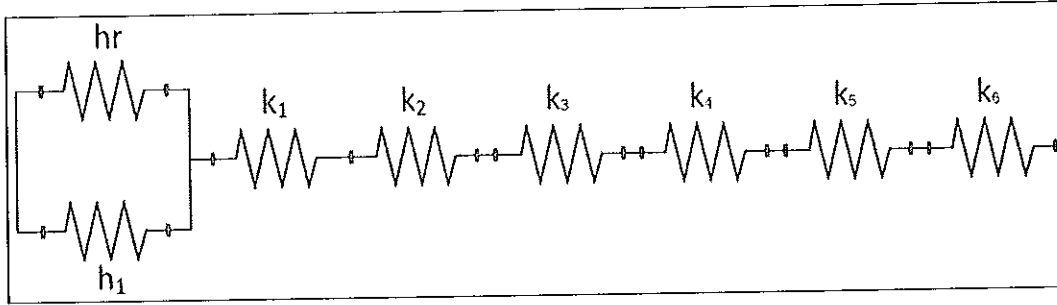


Figure 28 Modified heat transfer network

In Figure 30, k_1 is the conductive heat transfer resistance inside the PCM tube, k_2 is the conductive heat transfer resistance between PCM tube to heat transfer oil layer, k_3 is the conductive heat transfer resistance inside heat transfer layer, k_4 is the conductive resistance heat transfer oil layer to cooking stuff layer and k_5 is the conductive heat transfer resistance inside the cooking stuff layer.

Modes of heat transfer:

As mentioned in chapter 1, there are three modes of heat transfer conduction, convection and radiation. From the solar concentrator to the receiver or cooking pot the heat is transferred by radiation and convection. From the above heat transfer network h_r is the radiative heat transfer coefficient.

The radiative heat transfer coefficient is can be calculated using equation 19 (39, 43, 44).

$$h_r = \sigma \epsilon_c F_{cr} (T_c^2 + T_s^2)(T_c + T_s) \quad (19)$$

T_c = Temperature of the solar concentrator, $^{\circ}\text{C}$

T_s = Sky temperature, $^{\circ}\text{C}$

$$T_s = 0.0552 T_a^{1.5} \quad (20)$$

T_a = ambient temperature, $^{\circ}\text{C}$

ϵ_c = emissivity of the solar concentrator

F_{cr} = view factor from the solar concentrator to the receiver

The convective heat transfer coefficient from the solar concentrator and the receiver h_1 is calculated from the simple equation 21 (39).

$$h_1 = 5.7 + 3.8W_s \quad (21)$$

W_s = wind speed, $m\ s^{-1}$

The convective heat transfer coefficient between the concentrator and the receiver by considering Nusselts number N_u , Grasshof number G_r and Prandlt number P_r is expressed as equation 22 (44).

$$h_1 = \frac{K}{L} N_u \quad (22)$$

K = thermal conductivity of air, $Wm^{-1}\ K^{-1}$

L = length of air fluid stream, m

$$N_u = a(G_r \times P_r)^n \quad (23)$$

$$G_r = \frac{g\beta\rho^2 L^3 (T_c - T_a)}{\mu^2} \quad (24)$$

$$P_r = \frac{C_p \mu}{K} \quad (25)$$

C_p = specific heat of air, $kJ\ kg^{-1}\ K^{-1}$

The PCM tube is in cylindrical shape and the heat transfer method inside the tube is conduction. The conductive heat transfer coefficient for the cylindrical PCM tube is shown in equation 26. The schematic view of cylinder is shown in Figure 29. a.

$$k_1 = \frac{\ln\left(\frac{r_1}{r_2}\right)}{2\pi LK} \quad (26)$$

The receiver or cooking pot is a hollow concentric cylindrical shape and the gap is filled with heat transfer oil. The conductive heat transfer of the concentric cylinder is shown in equation 27 and the schematic view of layers of the concentric cylinder is shown in Figure 29. b.

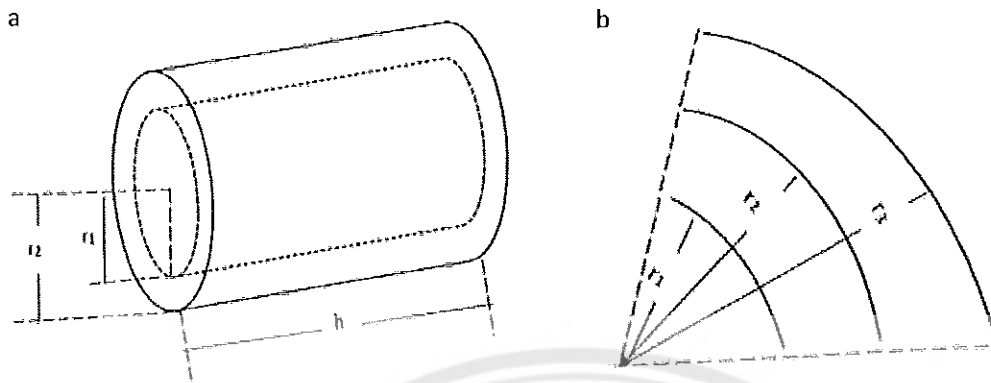


Figure 29 Schematic view of (a) cylinder (b) concentric cylinder

$$k_3 = \frac{\ln\left(\frac{r_2}{r_1}\right)}{2\pi L K_1} + \frac{\ln\left(\frac{r_3}{r_2}\right)}{2\pi L K_2} \quad (27)$$

Tracking system

The proposed application in this dissertation deals with a real time application like cooking which takes less strong sunshine hours. This proposed system developing to meet the cooking needs of rural communities in developing countries. The system should be economical for such kind of communities or individual families to use the system. So, to fulfill that economical viabilities and the requirement of tracking for less sun shine hours, a simple manual tracking is designed for the solar concentrator.

The receiver pot is not in contact with the solar concentrator directly. The solar concentrator is constructed with the dragging wheels. The solar concentrator and the receiver are constructed in a way that it is possible to track the system manually by adjusting the screws on the movable arms of the solar concentrator and receiver.

The solar concentrator can be tracked according to the position of the sun by the help of moving wheels and the screws on the support rod of concentrator frame. The receiver of the cooking system can be adjusted with the help of vertical and horizontal arms to achieve the proper point focus on the bottom of the cooking pot. The solar cooking system is tracked manually for every half an hour to get the efficient focus at the bottom

of the receiver. The vertical and horizontal adjustable arms of the receiver are shown in Figure 30.

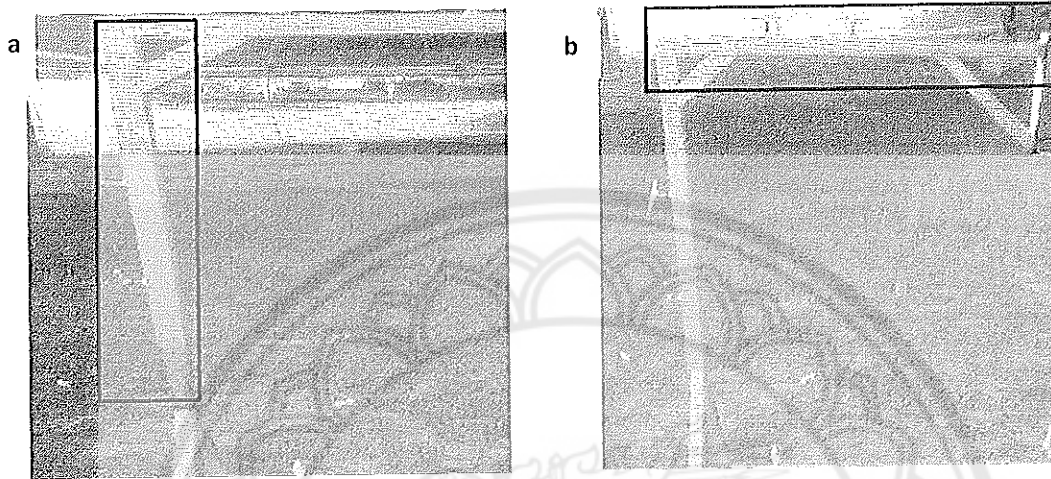


Figure 30 Manual tracking system with (a) Vertical arm (b) horizontal arm

Incorporating storage system with solar cooking system

After designing the solar cooking system, it was incorporated with the PCM storage system. The material of the PCM storage container is selected from the corrosion analysis of the PCM on container material. The PCM, $\text{Mg}(\text{NO}_3)_2 \cdot 6\text{H}_2\text{O}$ is filled in the stainless steel cylindrical tubes of height 23 cm and 2.5 cm diameter and the vents of the tubes are closed tightly with screws. 28 PCM tubes are welded on the surface of the cooking pot which were increased the contact surface area of the of the PCM material with the heat transfer fluid layer. The PCM is filled in the tubes up to a height of 20 cm. The top and side view of receiver or cooking pot are shown in Figure 31.

Instead of a single concentric layer, this individual tubes design will help to increase the heat storage capacity and to avoid the problems of food contamination because of the PCM material. The surface area of the PCM tubes is calculated with the help of basic cylinder mathematical expressions. The developed complete solar cooking system is shown in Chapter IV.

After developing the complete PCM solar cooking system, performance evaluation of the system has been conducted by calculating different parameters. The complete performance analysis of the solar cooking system is explained in next section.

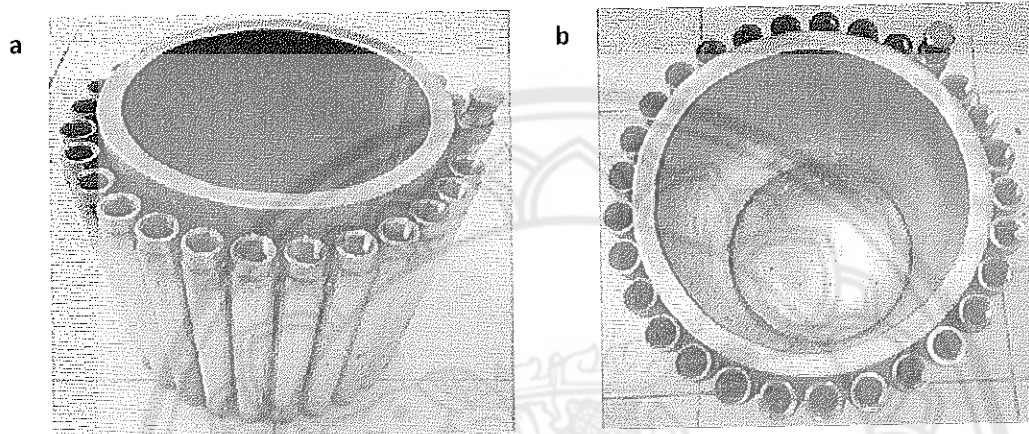


Figure 31 Design of the receiver (a) front view (b) top view

Performance Evaluation of the developed system

The performance analysis of developed system is performed three steps

1. Calculation of solar cooking parameters
2. Experimental testing of the system
3. Real time applications on the system

Calculation of solar cooking parameters

The efficient solar concentrator cooker should provide sufficient amount of energy for cooking processes. The performance of this solar cooker is analyzed by calculating some major parameters like combined heat capacity $((MC)_r)$, heat loss factor $(F'U_L)$, optical efficiency factor $(F'\eta_o)$, cooking power (P) and standard cooking Power (P_s) . A salt hydrate within the above mentioned ranges of thermodynamic properties was used as PCM. Palm oil is taken as heat transfer fluid and the cooking stuff is considered as water.

The combined heat capacity of the receiver is the combination of individual heat capacities of the materials presented in each layer of the receiver and the heat capacity

of the stainless steel receiver. The combined heat capacity is calculated from equation 28.

$$(MC)_r = (MC)_{l1} + (MC)_{l2} + (MC)_{l3} + (MC)_{pot} \quad (28)$$

Where l_1 , l_2 and l_3 represents the layers of the receiver.

Heat loss factor is the ratio of combined heat capacity of the receiver to the surface area and the time taken for cooking. It is expressed as in the equation 29.

$$F'U_L = \frac{(MC)_r}{\tau_0 A_r} \quad (29)$$

Where τ_0 is the time constant determined from the temperature difference falls to $1/e$ of its initial value (45).

The theoretical maximum limit of the overall efficiency of a concentrator solar cooker is defined as the optical efficiency factor $F'\eta_0$. It is expressed in equation 30 (33).

$$F'\eta_0 = \frac{F'U_L}{C} \left[\frac{\left(\frac{T_{wf} - T_a}{\bar{I}} \right) - \left(\frac{T_{wi} - T_a}{\bar{I}} \right) e^{-\frac{\tau}{\tau_0}}}{1 - e^{-\frac{\tau}{\tau_0}}} \right] \quad (30)$$

Where τ is the time required for the water temperature to increase from initial to final temperature. The rate of useful energy available during heating period of the concentrator solar cooker is known as the cooking power P [46]. It is expressed in equation 31.

$$P = M_w C_w \frac{(T_{wf} - T_{wa})}{\tau} \quad (31)$$

The corrected cooking power P at each interval to a standard irradiance of 700 W m^{-2} defines the standardized cooking power P_s of the solar concentrating cooker [46]. It is mentioned in equation 32.

$$P_s = M_w C_w \frac{(T_{wf} - T_{wa}) \times 700}{\tau I} \quad (32)$$

The overall heat loss coefficient U_L can be determined from the plot between standardized cooking power and $(T_w - T_a)$.

$$U_L = \frac{\text{slope}(P_s, (T_{wf} - T_{wa}))}{A_r} \quad (33)$$

Slope of the plot between P_s and $(T_{wf} - T_{wa})$ can be obtained from the linear regression of the graph by considering P_s on Y-axis and $(T_{wf} - T_{wa})$ on X-axis.

The simplified energy balance of the solar concentrating PCM cooker is expressed in equation 34 (46).

$$Q_i = Q_u + Q_{PCM} + Q_{loss} \quad (34)$$

Q_i is the heat gain by the solar radiation and is expressed in equation 35 [47].

$$Q_i = \eta_{opt} A_a I \Delta t \quad (35)$$

The amount of heat stored in PCM is Q_{PCM} is calculated from the equation 36 (24).

$$Q_{PCM} = M_{PCM} [C_{PCM}(T_m - T_a) + H + C_{PCM}(T_{PCMmax} - T_m)] \quad (36)$$

The heat stored or used to boil or cook food is the useful heat gain Q_u of the system and is expressed as in equation 37 [25].

$$Q_u = M_f C_w (T_f - T_m) \quad (37)$$

From the equations 35, 36 and 37, the heat loss Q_{loss} from the solar receiver can be calculated by substituting Q_i , Q_{PCM} , Q_u in equation 33.

Mathematical heat balance modelling of the PCM solar cooking system

The complete heat balance equations for every stage of the solar cooking system is explained in this section. The solar irradiation is captured by solar parabolic concentrator and is reflected to the cooking pot or the receiver which is placed at its focal point. The reflected radiation from the concentrator reaches receiver by convection and radiation modes of heat transfer. Some part of the absorbed heat is reradiated to the surroundings as heat losses from the receiver. The solar irradiation to the solar concentrator is transferred by convective radiative modes of heat transfer. The heat transfer balancing equation between parabolic concentrator and receiver is shown in equation 38. The schematic diagram is shown in Figure 32.

$$IA_p \eta_o F \sigma \epsilon (T_{fp}^4 - T_{ip}^4) + A_p h_1 (T_{fp} - T_{ip}) = IA_c F \sigma \epsilon \Delta t (T_{PCM,f}^4 - T_{PCM,i}^4) + A_c h_1 (T_{PCM,f} - T_{PCM,i}) + U_L (T_{PCM} - T_a) \quad (38)$$

η_o = optical efficiency of solar concentrator

F = view factor

σ = Stefan Boltzmann constant, $\text{Wm}^{-2}\text{K}^{-4}$

ε = emissivity coefficient, W/m^2

U_L = overall heat loss coefficient, $\text{W/m}^2\text{K}$

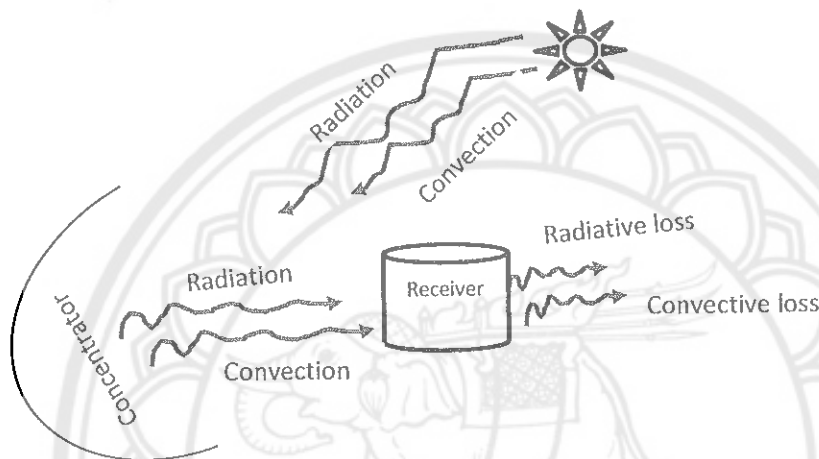


Figure 32 Schematic diagram of heat balance network for first stage

As the outer layer of the cooking pot is PCM tubes, the thermal energy reflected from the concentrator receives by PCM tubes by radiation and convection. After that heat is transferred to HTF layer from PCM tubes by conduction. The schematic heat view of heat transfers from PCM to HTF layer is shown in Figure 33.

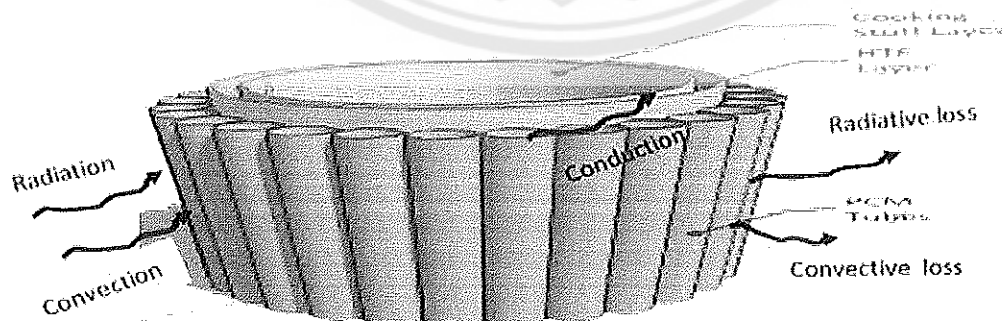


Figure 33 Schematic diagram of heat balance network for second stage

The heat balance equation for second stage is shown in equation 39.

$$IA_c F \sigma \epsilon (T_{PCM,f}^4 - T_{PCM,i}^4) + A_p h_1 (T_{PCM,f} - T_{PCM,i}) = A_{PCM} k_1 (T_f - T_i) + A_{HTF} k_2 (T_{HTF,f} - T_{HTF,i}) + U_L (T_{PCM} - T_a) \quad (39)$$

Where A_{PCM} = total area of PCM of tubes, m^2

A_{HTF} = area of heat transfer layer, m^2

Heat from the HTF layer will be transferred to cooking stuff layer by conduction. This heat transfer is shown schematically in Figure 34 and the heat balance equation for this stage is shown in equation 40.

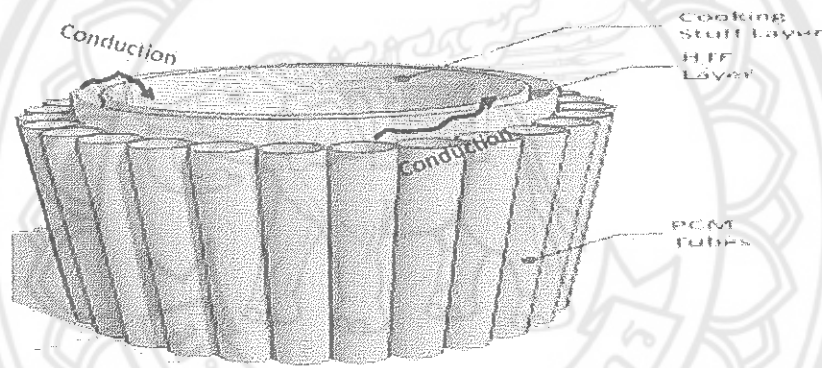


Figure 34 Schematic diagram of heat balance network for third stage

$$A_{PCM} k_1 (T_f - T_i) + A_{HTF} k_2 (T_{HTF,f} - T_{HTF,i}) = A_{HTF} k_3 (T_{HTF,f} - T_{HTF,i}) + A_{cl} k_4 (T_{HT} - T_{HT}) \quad (40)$$

The heat balance equation and the schematic diagram for the fourth stage of the receiver are shown in equation 41 and Figure 35.

$$A_{HTF} k_3 (T_{HTF,f} - T_{HTF,i}) + A_{cl} k_4 (T_{HT} - T_{HT}) = A_{cl} (k_5 + k_6) (T_{HT} - T_{HT}) \quad (41)$$

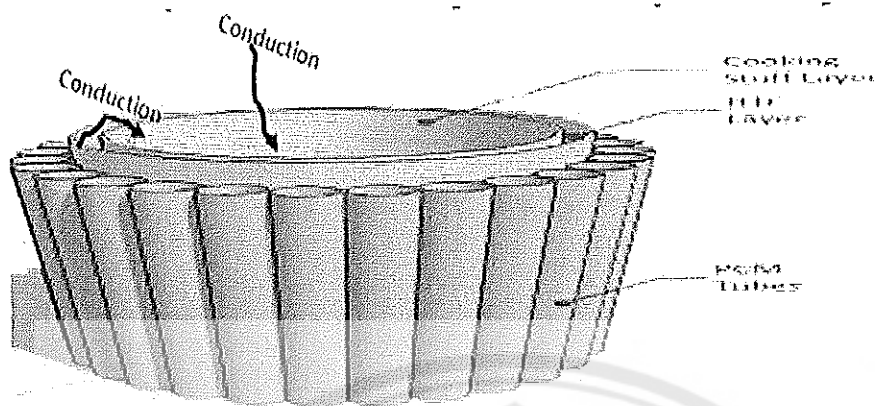


Figure 35 Schematic diagram of heat balance network for fourth stage

Experimental testing of the system

The experimental testing of the system is performed in three sets by keeping the 10 kg mass of receiver or cooking pot at the focus of the parabolic dish. Water heating test and cooling test were performed in the three sets of the experiment.

In the first set, the experiment is performed in different loadings of the materials in the receiver. The temperature profile of all the layers of the empty receiver is observed in the first set. Later, the heat transfer layer is filled with water as heat transfer fluid and the other two layers are left as empty. Later, HTF layer and PCM tubes are filled with water and with no load in cooking stuff layer, the temperature profile was observed during sunshine hours. In this set later, The HTF layer is filled with palm oil and the PCM tubes are filled with $\text{Mg}(\text{NO}_3)_2 \cdot 6\text{H}_2\text{O}$ and the and with no load in the cooking stuff layer the experiment was performed which is considered as the no load test of the cooking system. In the next step, water is filled in the cooking stuff layer and the temperature profile of all the layers of the receiver during sunshine hours. This step is called as the load test of the cooking system.

The temperature of the water inside the receiver is recorded again from the 40 °C to boiling temperature of the water is recorded. The temperature profile curve of the water inside the cooking layer is from the 40 °C to boiling temperature is known as heating curve. The temperature profile curve of the water inside the cooking layer is from the boiling temperature to 40 °C is known as cooling curve. The heating curve and cooling curve are plotted for this set of data which is measured and recorded with the

help of thermocouples and data logger respectively. The plots are shown and analyzed in the next chapter.

In the second and third sets, the receiver PCM tubes are filled with $\text{Mg}(\text{NO}_3)_2 \cdot 6\text{H}_2\text{O}$ and the HTF layer is filled with palm oil. In these two tests the experiment is performed in two cases. One is no load test and second is load test. No load is again performed by allowing the receiver inside the insulation box and without allowing into the insulation box. Load test of the system is also performed in two ways same as that of the no load test. The cooking stuff layer is filled with 2 liters of water for the load test of the system. For both no load and load test, after sunshine hours the receiver is placed inside insulation box to observe and record the temperature profile of the different layers of the receiver. In this case the temperature profiles are recorded from the evening to the next day morning. The data was collected for both the sets in no load cases with and without allowing receiver inside the insulation box.

The heating and cooling curves of the two sets are plotted with the help of recorded data. The complete temperature profiles of the solar cooking system in no load and load cases with and without allowing receiver inside the insulation box are also plotted with the help of recorded data.

28 PCM tubes are placed on the surface of concentric receiver, for every 4 PCM tubes, a thermocouple is placed to record the temperature of the PCM. The temperature of the PCM is recorded uniformly throughout the surface of the receiver. The Temperature profiles of all the PCM tubes with thermocouples were recorded and the storage capacity of the PCM was plotted in no load and load cases when the receiver is kept inside the insulation box.

The temperature of HTF, temperature of cooking layer, focal point temperature at the bottom of the receiver, temperature on the lid of the receiver, aperture temperature of solar concentrator and the ambient temperature of the surroundings are the other temperature observed and recorded positions of the solar concentrator. The schematic view of thermocouples positions in the receiver and solar concentrator are shown in Figure 36. The calibrated K and J type thermocouples are used to measure the temperature and pyranometer, anemometer are used to record the solar radiation intensity and wind speed respectively. All the temperature profiles and other parameters

are shown in chapter 4. The complete experimental procedure is mentioned in Appendix C.

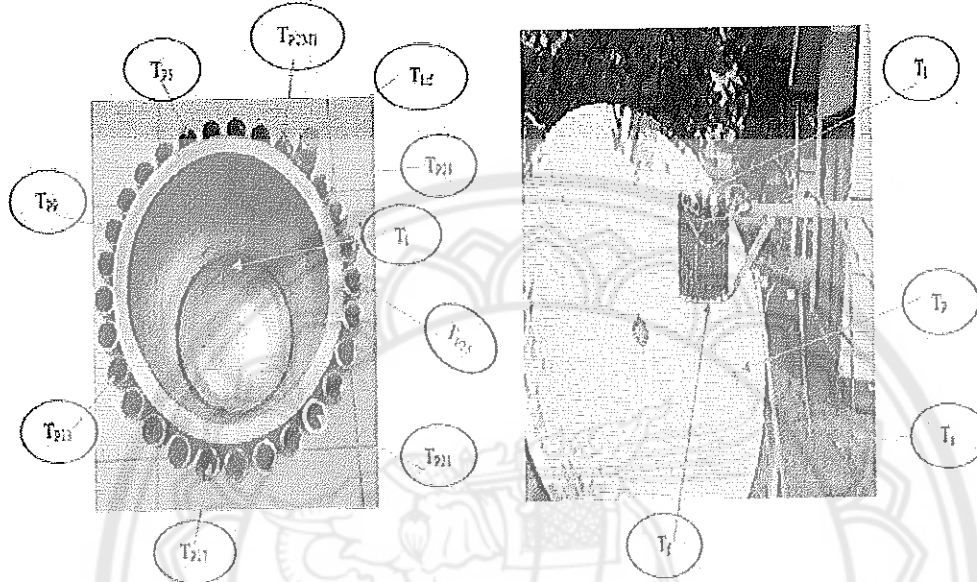


Figure 36 Various positions of the thermocouples placed in receiver and solar Concentrator

Complete efficiency Analysis of the system

The efficiency of the solar cooking system is the ratio of the useful thermal energy obtained from the system to the thermal energy used by the system. In other words, efficiency of the system is the ratio of output energy to the input energy.

$$\eta_{\text{system}} = \frac{Q_{\text{output}}}{Q_{\text{input}}} \quad (42)$$

Q_{output} is the energy stored in the cooking material which is placed in the cooking stuff layer. The developed solar cooking system has three layers and each layer is filled with the corresponding material inside the layer as cooking stuff layer is filled with water. HTF layer is filled with palm oil and the PCM tubes are filled with $\text{Mg}(\text{NO}_3)_2 \cdot 6\text{H}_2\text{O}$.

The useful energy of the developed solar cooker Q_{output} is expressed as in equation 43.

$$Q_{\text{output}} = Q_{\text{water}} + Q_{\text{oil}} + Q_{\text{PCM}} \quad (43)$$

$$Q_{\text{water}} = M_w C_w (T_{\text{fw}} - T_{\text{iw}}) \quad (44)$$

Where M_w = mass of water, kg

C_w = specific heat of water, kJ/(kg·K)

T_{fw} = final temperature of water, °C

T_{iw} = initial temperature of water, °C

$$Q_{\text{oil}} = M_{\text{oil}} C_{\text{oil}} (T_{\text{f,oil}} - T_{\text{i,oil}}) \quad (45)$$

Where M_{oil} = mass of oil, kg

C_{oil} = specific heat of oil, kJ/(kg·K)

T_{foil} = final temperature of oil, °C

T_{ioil} = initial temperature of oil, °C

$\text{Mg}(\text{NO}_3)_2 \cdot 6\text{H}_2\text{O}$ is a latent heat material. These type of materials store the energy in three phases. Sensible heat storage for melting purpose in the first phase, latent heat storage for phase change purpose in second phase and again the sensible heat storage while discharging the heat in third phase. So the useful thermal energy stored in PCM is the combination sensible, latent and sensible heat storages. Q_{PCM} is expressed as in equation 46.

$$Q_{\text{PCM}} = M_{\text{PCM}} C_{\text{PCM}} (T_{\text{PCM}} - T_{\text{m,PCM}}) + M_{\text{PCM}} L_{\text{PCM}} + M_{\text{PCM}} C_{\text{PCM}} (T_{\text{PCM,max}} - T_{\text{PCM}}) \quad (46)$$

Where M_{PCM} = mass of PCM, kg

C_{PCM} = Specific heat of oil, kJ/(kg·K)

L_{PCM} = Latent heat capacity of PCM, J/kg

T_{PCM} = Temperature of PCM, °C

T_{mPCM} = melting temperature of PCM, °C

T_{PCMmax} = maximum temperature of PCM, °C

Q_{useful} or Q_{output} can be obtained by adding equations 44, 45 and 46 to equation 43.

The input heat energy to solar cooking system is also divided into two parts for this proposed solar cooker. The first part is the amount of thermal energy captured by the solar concentrator. The second part is the amount of thermal energy reflected from the solar concentrator to the receiver or the amount of thermal energy received by the receiver from the concentrator.

$$Q_{\text{in}} = I_{\text{no}} (A_p + A_c) \Delta t \quad (47)$$

Where I = solar irradiation, W/m^2

η_o = optical efficiency of solar concentrator

A_p = aperture area of the solar concentrator, m^2

A_c = area of cooking pot r receiver, m^2

Δt = time of operation, sec

Case 1: Efficiency of the solar cooker without storage

For all the cases of the developed solar cooking system, Q_{in} can be calculated by using equation 44. But Q_{out} will change depending upon the materials in the cooking pot layers. In this case the receiver is filled with water in cooking stuff layer and the other two layers are empty. Then Q_{out} in this case is only the thermal energy stored in the water as expressed in equation 44. Therefore, efficiency of the system in this case is expressed in equation 48.

$$\eta_1 = \frac{Q_{out}}{Q_{in}} = \frac{M_w C_w (T_{fw} - T_{iw})}{I \eta_o (A_p + A_c) \Delta t} \quad (48)$$

Case 2: Efficiency of the solar cooker with heat transfer fluid in HTF layer

In this case the HTF layer is filled with palm oil as heat transfer fluid and water inside the cooking layer. Then Q_{out} can be obtained by adding equations 44 and 45 in equation 43. The efficiency of the system in this case is expressed as in equation 49.

$$\eta_1 = \frac{Q_{out}}{Q_{in}} = \frac{M_w C_w (T_{fw} - T_{iw}) + M_{oil} C_{oil} (T_{f,oil} - T_{i,oil})}{I \eta_o (A_p + A_c) \Delta t} \quad (49)$$

Case 3: Efficiency of the system with PCM, HTF and water in respective layers

In this case Q_{out} can be obtained by adding equations 44, 45 and 46 to equation 43. But as per the design of the receiver 28 PCM tubes are welded on the surface of the two layered cooking pot. To measure the temperature of PCM in the tubes throughout the experiment period, thermocouples are placed inside the PCM tubes as shown in Figure 36. Total 7 thermocouples are used to measure the temperature in 28 PCM tubes. The 7 thermocouples are placed symmetrically for every 4 PCM tubes. So, one thermocouple temperature is used for 4 PCM tubes calculation of heat stored in that

tube. After every 4 PCM tubes, another thermocouple is used to recorded the next 4 PCM tubes temperature.

In Q_{PCM} , sensible heat storage part is modified according to the thermocouple placement inside the PCM tubes. The modified sensible heat stored in the PCM tube can be expressed as in equation 50 and 51.

$$Q_{PCM\text{sensible}1} = 3M_{PCM} C_{PCM} \sum_{J=1}^6 [(T_{PCM,m} - T_{J,PCM}) + (T_{PCM,m} - T_{(J+1),PCM})] \quad (50)$$

$$Q_{PCM\text{sensible}2} = 3M_{PCM} C_{PCM} \sum_{J=1}^6 [(T_{PCM,max} - T_{J,PCM}) + (T_{PCM,max} - T_{(J+1),PCM})] \quad (51)$$

$$Q_{PCM} = Q_{PCM\text{sensible}1} + M_{PCM} L_{PCM} + Q_{PCM\text{sensible}2} \quad (52)$$

Efficiency in this case is the ratio of equations 47 and 52.

Real time applications on the system

After performance of the experimental test procedure, some real time cooking applications like boiling and frying of different types food materials are performed. The temperature profiles of both the applications are recorded and plotted corresponding to solar radiation on that particular day.

The boiling and frying applications are performed in batches by loading different types of food materials inside the cooking stuff layer of the receiver. After sunshine hours the receiver is placed inside the insulation box and the applications performed again with the help of energy stored in the PCM. Different types of beans, rice, potato, sweet potato and eggs are boiled in this solar cooker. Vegetables and eggs are fried in the PCM solar cooker. The time taken for the complete cooking of the food materials in both the applications was recorded and results are plotted. The amount of energy required to cook the food can be calculated from equation 53.

$$Q_{\text{food}} = m C_p (T_{f,\text{food}} - T_{i,\text{food}}) \quad (53)$$

Where Q_{food} = Energy required to cook food, kJ

m = Mass of food, kg

$T_{f,\text{food}}$ = Final temperature of food, °C

$T_{i,\text{food}}$ = Initial temperature of food, °C

The results of real time applications like time taken to cook food, number batches per day can be cooked and the number of batches cooked after sunshine hours are mentioned in chapter IV.

Economic and emission analysis of the system

Economic analysis of the system

The economic analysis of the developed system will be considered to evaluate the financial viability of the developed system. Economic analysis of the system, net present cost, payback period and minimum number of cooking times will be considered. Some assumptions like discount rate and repair or maintenance cost rate need to be considered for the economic analysis (47). In this dissertation the economic analysis is compared with Liquefied Petroleum Gas (LPG) which is a fossil fuel based cooking technology.

The proposed PCM solar cooker capital cost or the annualized cost of the system includes concentrator glass sheet cost, mechanical structure cost and PCM cost. The costs of above materials depend on the local market conditions.

The following assumptions were made to calculate the economic feasibility of the developed PCM solar cooker(47).

1. Life time of the project 10 years. As the structural design of the solar cooker is not robust and complicated, the life time of the developed system can be long enough to serve the proposed application.
2. Discount rate is 5%. In the proposed design the cost of the materials like reflecting glass, mechanical structure of the system and chemical used for storage are the main components. The cost of these materials and the discount rate on those materials depends on the local market conditions. So, the discount rate is considered as 5%.
3. Maintenance and repair cost is 10%. As already mentioned, the design of the system is compact and no electrical and electronic parts are involved in the design of the system. But, the after a certain period, the PCM should in the tubes should be checked and refill into the tubes. This is the major maintenance cost of this system. The cost of the PCM has major share in the total capital cost of the system. So, the maintenance and repair cost is assumed to be 10%.

Net Present Cost: The total amount of expenditures involved in a renewable energy project throughout its life time is called as Net Present Cost (NPV). The NPV can be calculated by the following equation 54 (48).

$$NPV = \frac{C_{total}}{CRF(d, N)} \quad (54)$$

Where, C_{total} = total annualized cost of the system, \$

CRF = capital recovery factor

d = discount rate, %

N = project life time, years

Capital recovery factor: The factor which converts the present value into series of equal cash flow by considering discount rate and life time of the project is called as the capital recovery factor [43]. The following equation 55 represents the capital recovery factor.

$$CRF = \frac{d(1+d)^N}{(1+d)^N - 1} \quad (55)$$

The minimum number of meals (n_m) cooked by the solar cooker with storage system is expressed in equation 56 as follows [42]

$$n_m = \frac{C_0}{p} \left[\alpha + \frac{d(1+d)^N}{(1+d)^N - 1} \right] \quad (56)$$

Where, C_0 = capital cost, \$

P = money value of the saved fuel per cook, \$

α = maintenance and repair cost rate, %

The money value of the saved fuel per year P is expressed as in equation 57 (49).

$$P_y = P_r \cdot M_{LPG} \cdot P_{LPG} \quad (57)$$

Where P_r = % of time where solar cooker is used per month

The payback period (PP) of the developed system can be calculated with the help of the following equation 58 (42). The simplified expression for the payback period is expressed as in equation 59 (50).

$$PP = \frac{C_0}{(n_m P - \alpha C_0)} \quad (58)$$

$$PP = \frac{C_0}{P_y} \quad (59)$$

The economic analysis of the developed system is calculated for Thailand and India by considering the present day cost of LPG for cooking application in respective countries. The current price of 1 kg of LPG in Thailand is 0.71 \$ (50) and 0.79 \$ (51) in India statistical values of the economic analysis of the system are presented in the Chapter IV.

Emission analysis of the system

In this dissertation LPG is considered to compare the CO₂ emissions and the reduced emissions of CO₂ to that of the developed solar cooking system. After LPG is allowed to complete combustion can produce 80% of butane and 20% of propane. One kg of butane and propane produces 3.03 kg and 3.00 kg of CO₂ respectively. From the above values it was calculated that one kg of LPG produces 3.02 kg of CO₂ [50].

The annual CO₂ emissions reduced from LPG by replacing the LPG cooking system with the developed PCM solar cooking system is expressed following equation 60 [50].

$$M_{\text{redCO}_2} = P_r \cdot M_{\text{CO}_2, \text{total}} \quad (60)$$

Where $M_{\text{CO}_2, \text{total}}$ = total amount of CO₂ produced in kg/month. The statistics of emission analysis are mentioned in Chapter IV.

CHAPTER IV

RESULTS AND DISCUSSION

The design, development and evaluation of the $\text{Mg}(\text{NO}_3)_2 \cdot 6\text{H}_2\text{O}$ phase change material storage system for community solar cooking application was performed in School of Renewable Energy Technology (SERT), Naresuan University, Thailand. The latitude and longitude of this location place where the system was developed are 16.7678° N , 100.1953° E . In this chapter, the results are mentioned in six parts as follows.

1. Design parameters of solar cooking system
2. PCM analysis
3. Experimental data analysis
4. Real time applications analysis
5. Thermal imager analysis
6. Economic and emission analysis

Design parameters of solar cooking system

From the above mentioned mathematical calculations of solar cooking system in Chapter III, the design parameters of the solar concentrator and the receiver are calculated. The different design parameters are presented in Table 8. The complete developed solar cooking system with PCM storage in PCM tubes on the surface of the receiver is shown in Figure 37.

Table 8 Parameters of solar concentrator and receiver

Parameter	f	ϕ	θ_A	C	P	A_s	A_a	D_{fo}	A_f	A_r	N
(units)	(m)	($^\circ$)	($^\circ$)		(m)	(m^2)	(m^2)	(m)	(m^2)	(m^2)	
Value	0.52	71.28	9.36	5.97	0.789	1.9647	1.7554	0.256	0.05173	0.294	25

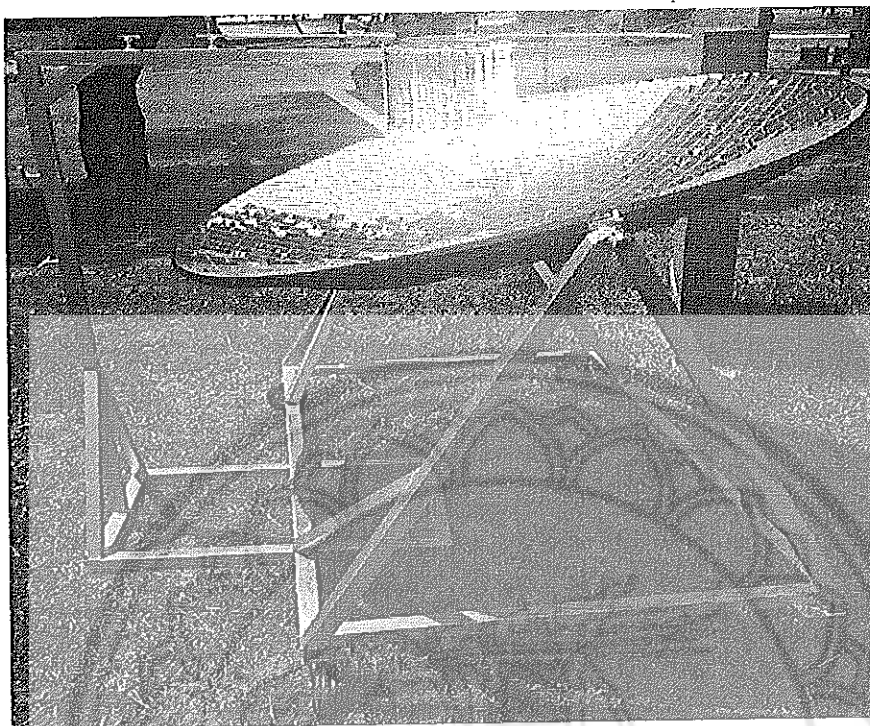


Figure 37 The complete design of developed PCM solar cooking system

PCM analysis

The 1000 thermal cycles of $\text{Mg}(\text{NO}_3)_2 \cdot 6\text{H}_2\text{O}$ was performed by using the hotplate. The variation in the weight and time taken for $\text{Mg}(\text{NO}_3)_2 \cdot 6\text{H}_2\text{O}$ sample after melting and solidification cycles after every 100 thermal cycles is mentioned in Table 9. It is observed that the weight of the sample is reducing gradually from 0th cycle to 1000th cycle. After 1000 thermal cycles, about 24.00% of initial weight of the sample is left in the testing container.

The time taken for the melting and solidification cycles after every 100 thermal cycles is noted and the values are plotted in the graph. The variation of weight and time taken after melting and solidification cycles are shown in Figure 38 and Figure 39.

From Figure 38, it is observed that the weight of the PCM sample after the solidification cycle is greater than the weight of the sample after melting cycle. The $\text{Mg}(\text{NO}_3)_2 \cdot 6\text{H}_2\text{O}$ absorbs heat for the melting process and stores heat in its liquid phase while melting. The hydroxide atoms will evaporate during melting process. In solidification cycle, $\text{Mg}(\text{NO}_3)_2 \cdot 6\text{H}_2\text{O}$ releases heat by forming the chemical bonds

between the molecules and the material was solidified completely after retrieving the heat to the water in the cooling water environment. So, the weight of melting cycle is less than that of the weight of solidification cycle. After repetitive thermal cycles from 0th to 1000th cycle, the weight of the material is reduced in both melting and solidification cycles due to the evaporation of water molecules in the chemical compound. This variation shows that the volume changes of the $\text{Mg}(\text{NO}_3)_2 \cdot 6\text{H}_2\text{O}$ is less which is the effective desired criteria of the inorganic PCMs.

Table 9 Variation in weight and time for $\text{Mg}(\text{NO}_3)_2 \cdot 6\text{H}_2\text{O}$ thermal cycling process

No. of cycles	Weight after melting (g)	Weight (%)	Weight after solidification (g)	Melting time (min)	Solidification Time (min)
0	227.20	100.00	227.20		
100	205.39	90.40	205.40	75	82
200	200.35	88.18	200.37	60	73
300	190.99	84.06	191.01	54	68
400	182.83	80.40	182.91	52	63
500	176.13	77.52	176.92	45	57
600	170.15	74.80	170.06	41	52
700	126.95	55.80	127.07	30	41
800	84.77	37.30	84.92	23	35
900	67.71	29.80	68.01	21	33
1000	54.96	24.10	55.01	15	28

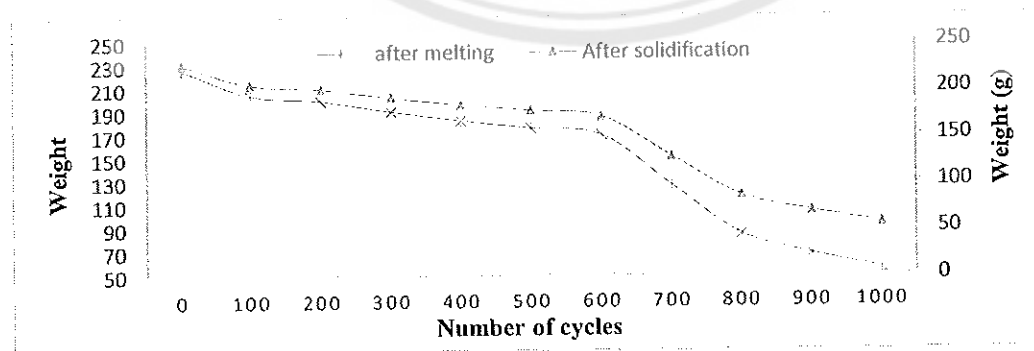


Figure 38 Variation in weight of PCM

From Figure 39, it is observed that the time taken for the solidification cycle is more than that of the melting cycle. The formation of chemical bonds while retrieving heat from the material by allowing the material to solidify completely takes more time compared to that of breaking the chemical bonds and storing the heat by melting the material. Time taken for both melting and solidification cycles from 0th cycle to 1000th cycle are reduced gradually due to the repeated cycles and the loss in the material weight over a continuous 1000 thermal cycles as shown in Figure 38.

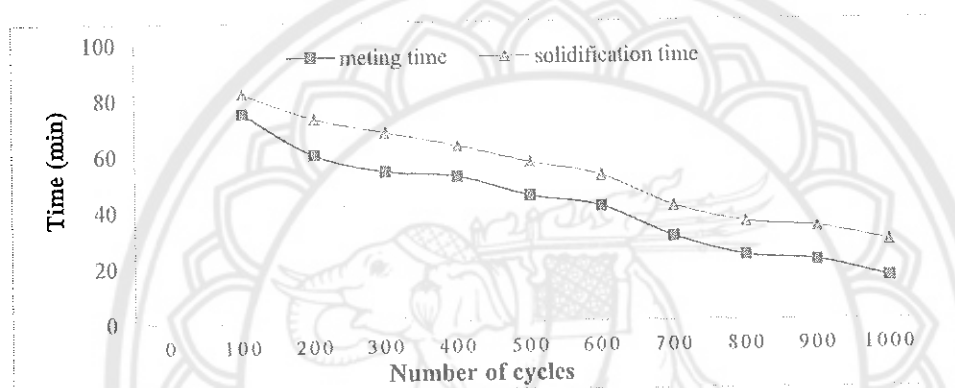


Figure 39 Variation in time taken for melting and solidification of PCM

After 1000 thermal cycles the collected sample of the $\text{Mg}(\text{NO}_3)_2 \cdot 6\text{H}_2\text{O}$ were analyzed with DSC. The DSC thermograms are taken after 0, 100, 200, 400, 600, 800 and 1000 thermal cycles. Figure 40 shows the DSC thermogram of 0th cycle of $\text{Mg}(\text{NO}_3)_2 \cdot 6\text{H}_2\text{O}$. 10.26 mg of $\text{Mg}(\text{NO}_3)_2 \cdot 6\text{H}_2\text{O}$ sample was placed in the aluminum holder of the DSC. 25 °C to 200 °C was the melting temperature range with 7 K/min heating rate. 200 °C to 25 °C was the solidification temperature range with 5 K/min heating rate are the test conditions sample.

The Peak in the DSC thermogram shows the melting temperature of the material and the area under the peak gives the latent heat capacity of the material. Figure 40, it is observed that the material shows two peaks while melting process. First peak represents the melting process of the water molecules present in the sample and the second peak shows the melting process of the magnesium nitrate compound. The complete is considered to analyze the melting point and latent heat capacity of the material at 0th cycle.

Figure 41 shows the DSC thermogram of $\text{Mg}(\text{NO}_3)_2 \cdot 6\text{H}_2\text{O}$ sample after 100th cycle. 9.86 mg of the PCM sample is placed in the aluminum holder of the DSC.

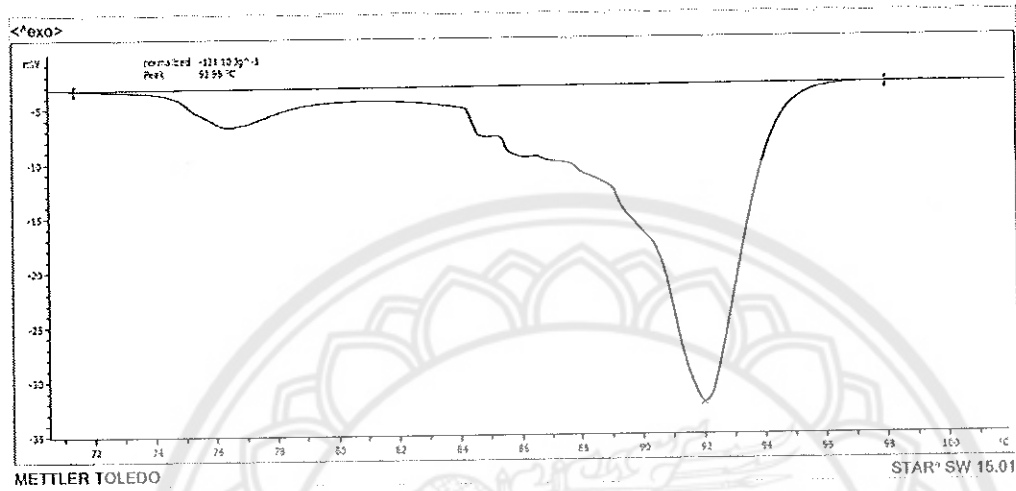


Figure 40 DSC thermogram of $\text{Mg}(\text{NO}_3)_2 \cdot 6\text{H}_2\text{O}$ sample at 0th cycle

The DSC test conditions of 100th cycle are same as that of 0th cycle's test conditions. From 0th cycle to 100th cycle the material in DSC thermogram, the first melting peak is shifting near to the second melting peak. So, the area under the peaks is reduced which is the reason for the reduction in the latent heat capacity of the 100th cycle sample.

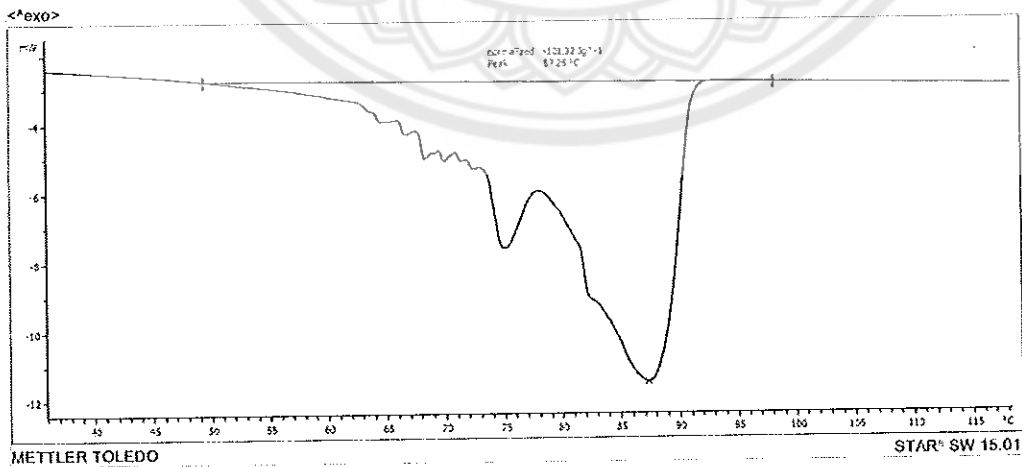


Figure 41 DSC thermogram of $\text{Mg}(\text{NO}_3)_2 \cdot 6\text{H}_2\text{O}$ sample after 100th cycle

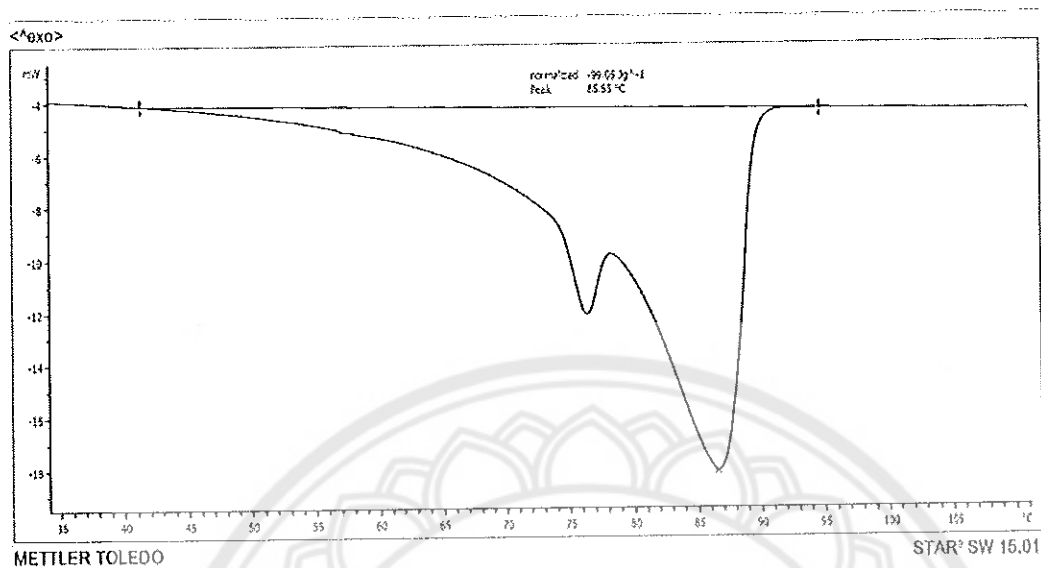


Figure 42 DSC thermogram of $\text{Mg}(\text{NO}_3)_2 \cdot 6\text{H}_2\text{O}$ sample after 200th cycle

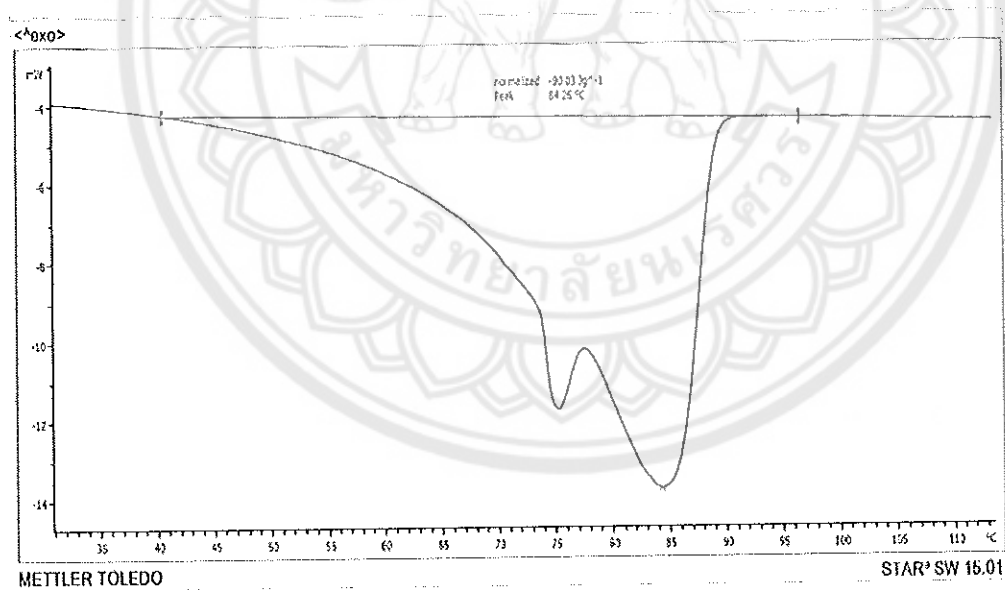


Figure 43 DSC thermogram of $\text{Mg}(\text{NO}_3)_2 \cdot 6\text{H}_2\text{O}$ sample after 400th cycle

Figure 42 shows the DSC thermogram of $\text{Mg}(\text{NO}_3)_2 \cdot 6\text{H}_2\text{O}$ sample after 200th cycle. 15.09 mg of the PCM sample is placed in the aluminum holder of the DSC. Figure 38 illustrates the small peaks due to the presence of water molecules in the compound

were smoothed over a repetitive 200 thermal cycles. The DSC test condition are same for the remaining 400, 600, 800 and 1000 cycles DSC thermograms.

DSC thermogram for 400th cycle of $\text{Mg}(\text{NO}_3)_2 \cdot 6\text{H}_2\text{O}$ sample is shown in Figure 43. 15.01 mg of the PCM sample is placed in the aluminum holder of the DSC for 400th cycle. The DSC thermogram of the 400th cycle appears even smoother than that of 200th cycle DSC thermogram of the $\text{Mg}(\text{NO}_3)_2 \cdot 6\text{H}_2\text{O}$ sample due to the adjustment of chemical bonds in the compound over repetitive thermal cycles.

DSC thermogram for 600th cycle of $\text{Mg}(\text{NO}_3)_2 \cdot 6\text{H}_2\text{O}$ sample is shown in Figure 44. 14.04 mg of the PCM sample is placed in the aluminum holder of the DSC. The DSC thermogram for 600th cycle is appeared as narrow compared to the before cycles DSC thermograms. The reduction in weight of the material and time take for melting and solidification from 400 to 600 cycles effects the DSC thermogram of the $\text{Mg}(\text{NO}_3)_2 \cdot 6\text{H}_2\text{O}$ sample collected at 600th cycle for DSC analysis.

DSC thermogram for 800th cycle of $\text{Mg}(\text{NO}_3)_2 \cdot 6\text{H}_2\text{O}$ sample is shown in Figure 45. 14.27 mg of the PCM sample is placed in the aluminum holder of the DSC to obtain the DSC thermogram. The figure shows that the first melting peak is sharp compared to the DSC thermogram of before cycles. After 800 repetitive thermal cycles the evaporation or melting process of hydrate molecules is takes less time over a narrow temperature range causes the sharp peak in the first peak of DSC thermogram. The complete peak is wide but the area under the peak is less than that of the 600th cycle. So, the latent heat of fusion for 800th cycle is less than that of 600th cycle.

DSC thermogram for 1000th cycle of $\text{Mg}(\text{NO}_3)_2 \cdot 6\text{H}_2\text{O}$ sample is shown in Figure 46. 15.02 mg of the PCM sample is placed in the aluminum holder of the DSC. The first peak in the 1000th cycle DSC thermogram is even more sharp and the second peak is not smooth as compared to that of 800th cycle. The bulk repetitive cycles caused to break the hydrate molecules from the compound easily and the magnesium nitrate compound crystallizes in the absence of hydrate molecules are the reason for the sharp and unsmooth peaks in 1000th thermal cycle.

From the DSC thermograms, the melting point temperature, latent heat of fusion for all the above mentioned DSC thermograms are summarized in Table 10.

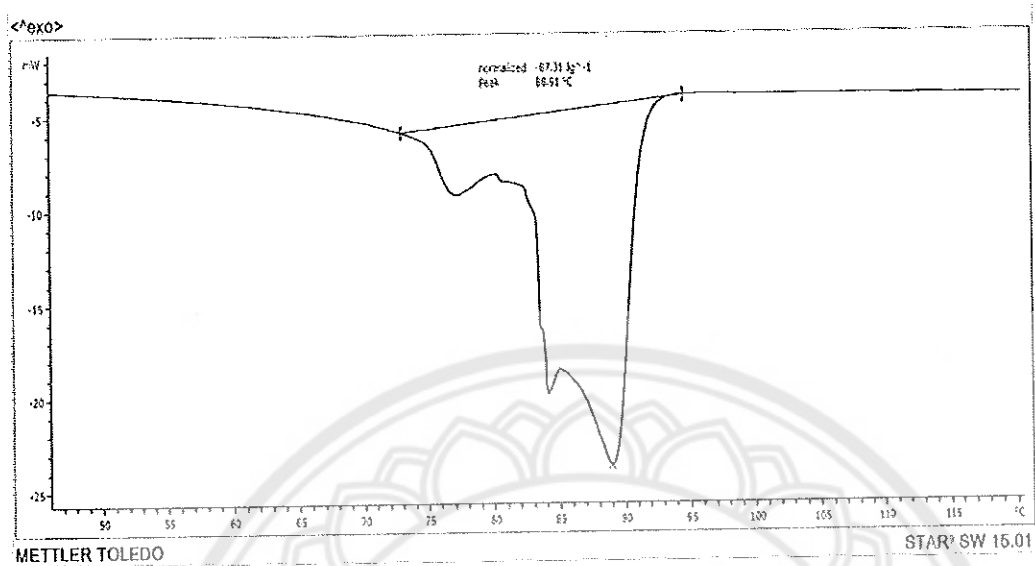


Figure 44 DSC thermogram of $\text{Mg}(\text{NO}_3)_2 \cdot 6\text{H}_2\text{O}$ sample after 600th cycle

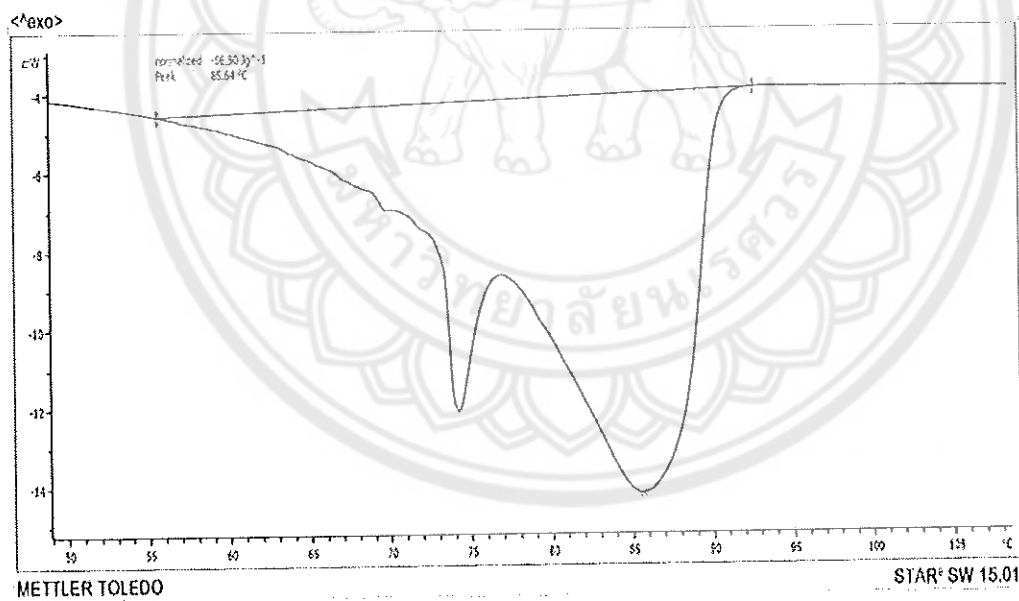


Figure 45 DSC thermogram of $\text{Mg}(\text{NO}_3)_2 \cdot 6\text{H}_2\text{O}$ sample after 800th cycle

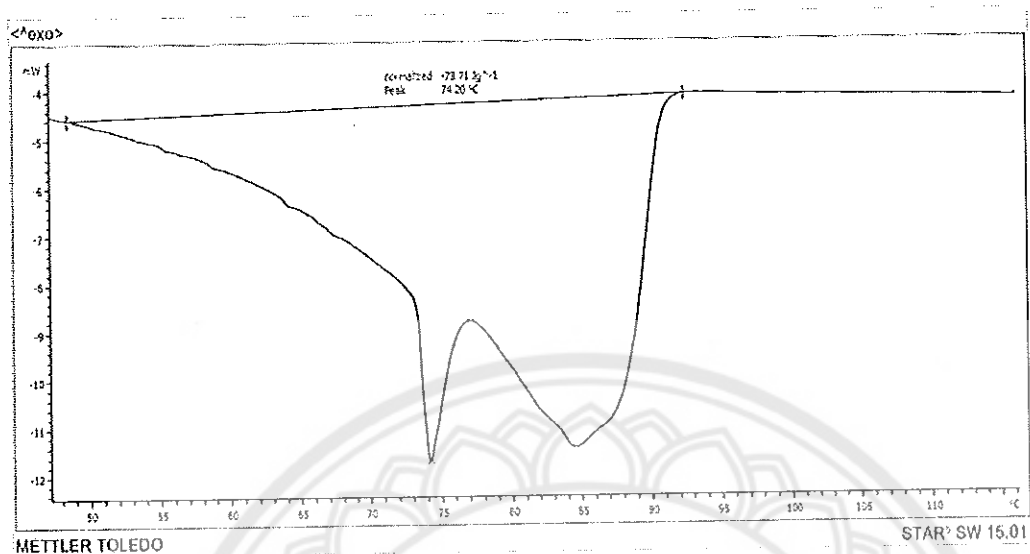


Figure 46 DSC thermogram of $\text{Mg}(\text{NO}_3)_2 \cdot 6\text{H}_2\text{O}$ sample after 1000th cycle

Table 10 Results of DSC thermograms

Number of cycles	Melting Point (°C)	Latent heat of fusion (Jg ⁻¹)	Latent heat of fusion (%)
0	91.98	121.00	100.00
100	87.25	101.32	83.70
200	85.85	99.05	81.80
400	84.26	90.03	74.40
600	88.91	87.31	72.15
800	85.64	86.50	71.40
1000	74.20	78.71	65.00

From the above table it is shown that, after 1000 thermal cycles the melting temperature of the PCM sample is reduced from 91.98 °C to 74.20 °C and the latent heat of fusion is reduced gradually from 0th cycle to 1000th cycle. After 1000th thermal cycle the capacity of latent heat of fusion in the PCM sample is about 65% from the initial value of the latent heat of fusion.

The $\text{Mg}(\text{NO}_3)_2 \cdot 6\text{H}_2\text{O}$ material is tested with container materials and the aluminum and stainless steel material samples are analyzed with SEM. Figure. 47 (a) and (b) shows the SEM images of steel and aluminum samples before starting the thermal cycling for corrosion analysis respectively.

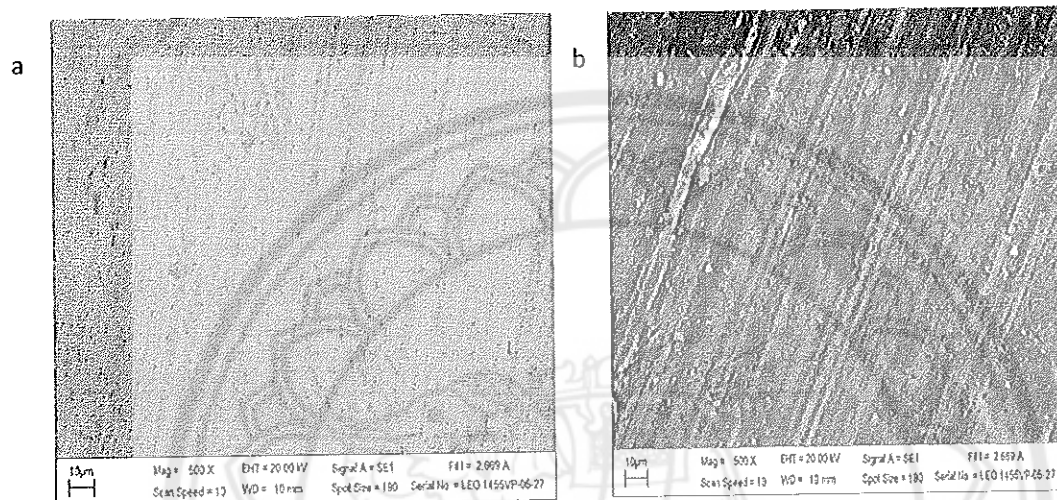


Figure 47 SEM images of zeroth cycle (a) Stainless steel (b) Aluminum

Figure 48 and 49 show the SEM images of the stainless steel and aluminum after 500th and 1000th cycles respectively.

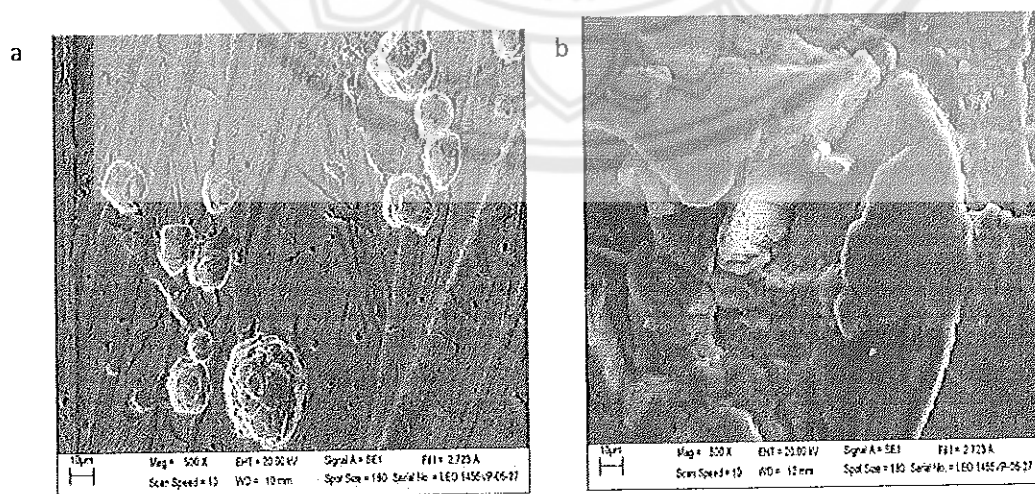


Figure 48 SEM images of 500th cycle (a) Stainless steel (b) Aluminum

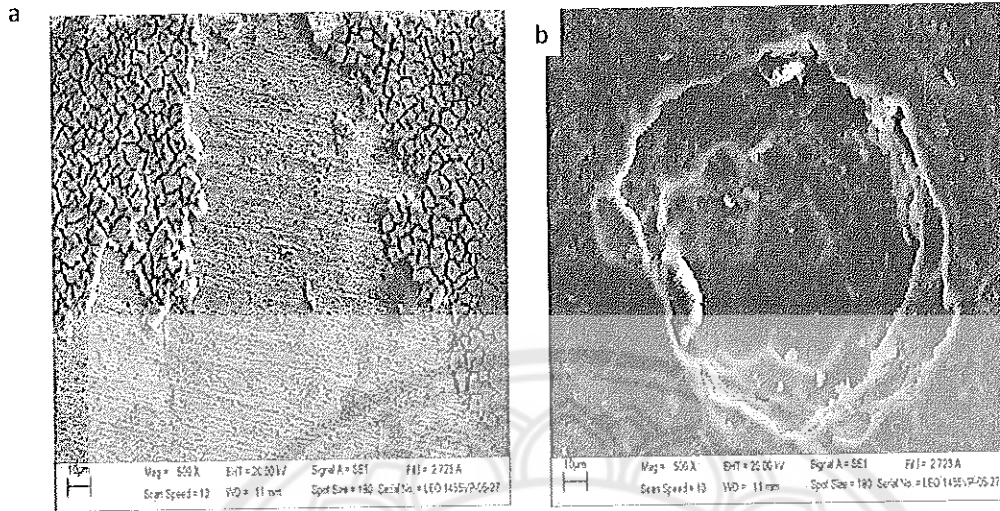


Figure 49 SEM images of 1000th cycle (a) Stainless steel (b) Aluminum

All the above SEM images at different cycles illustrates, the stainless steel is corroded layer by layer whereas aluminum is corroded deeply after 1000 thermal cycles with $\text{Mg}(\text{NO}_3)_2 \cdot 6\text{H}_2\text{O}$ sample. So, stainless steel material is selected for the receiver material and PCM tubes for the storage of $\text{Mg}(\text{NO}_3)_2 \cdot 6\text{H}_2\text{O}$ as storage medium.

Experimental data analysis

The experiment procedure is performed to mainly calculate the heating and cooling curves for the temperature inside the cooking stuff layer. The temperature profiles of the experiment in the three sets are plotted and analyzed in this section. The heating and cooling time constants τ , τ_0 respectively for all the sets of data are mentioned in Table 11. All the plots are drawn with local time in horizontal axis and the temperature on the primary vertical axis and solar radiation on the secondary vertical axis.

Figure 50 shows the temperature profile of the solar cooking system with no materials loaded in the receiver. T_f , T_i , T_p and T_a are the focal temperature at the outside bottom of the receiver, cooking stuff layer temperature, aperture temperature of solar concentrator and ambient temperature respectively. The receiver layers are empty in this case, the temperature inside the cooking layer depends on the focal point temperature. The T_i curve follows the temperature pattern of T_f and where temperature profile of the

focus is depending on the solar radiation and the tracking of the system according to the position of the sun throughout the day.

From the Figure 50 it is observed that, as the cooking layer is surrounded by two more layers, the temperature inside the cooking layer is not much affected by the variations in the focal temperature and solar radiation.

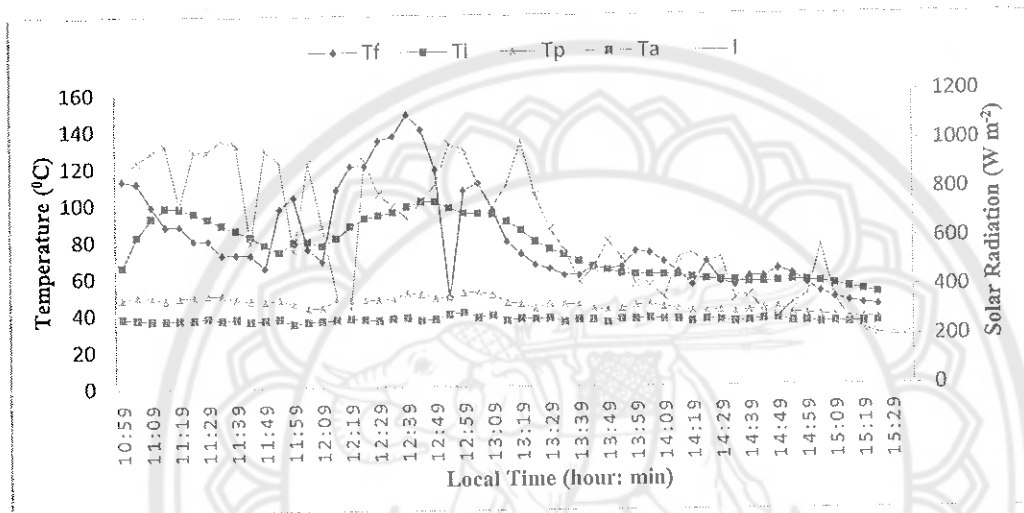


Figure 50 Temperature profile of the solar cooking system with empty receiver

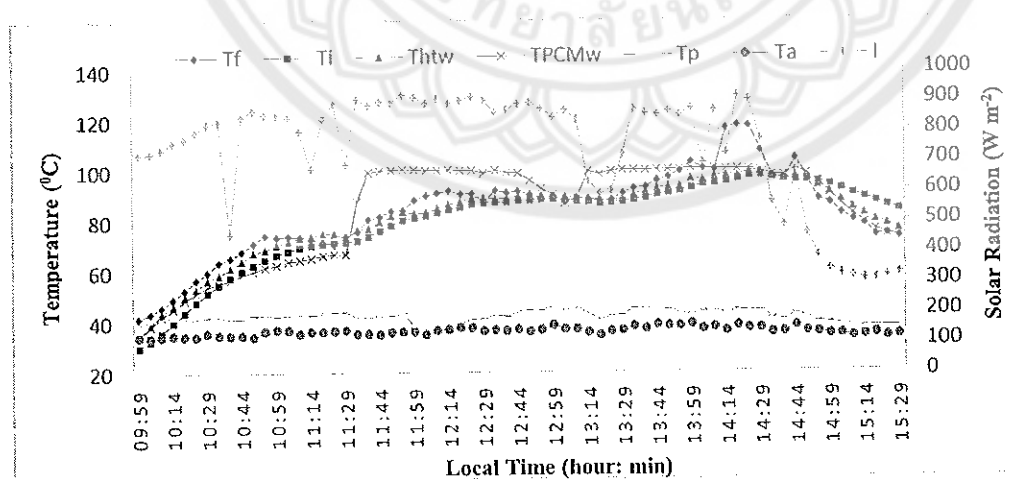


Figure 51 Temperature profile of the system with water inside the HTF layer and PCM tubes

Figure 51 shows the temperature profile of the cooking system with water inside the HTF layer and PCM tubes of the receiver. The cooking stuff layer of the receiver is empty in this case. T_{htw} , T_{PCMw} are the temperature of the water inside HTF layer and PCM tubes respectively. The figure shows, that temperature profile of the water in PCM tubes is more compared to the temperature profiles of other layers because PCM tubes are the outermost layer of the cooking pot and are also directly absorbing the solar radiation. Temperature profile inside the HTF layer and cooking pot are similar to the temperature profile of the focal point and the temperature profiles are nearly uniform irrespective of the variation in the solar radiation because of the presence of water in HTF layer and PCM tubes. As the solar radiation is decreasing after sunshine hours, the temperature profiles are also decreasing smoothly.

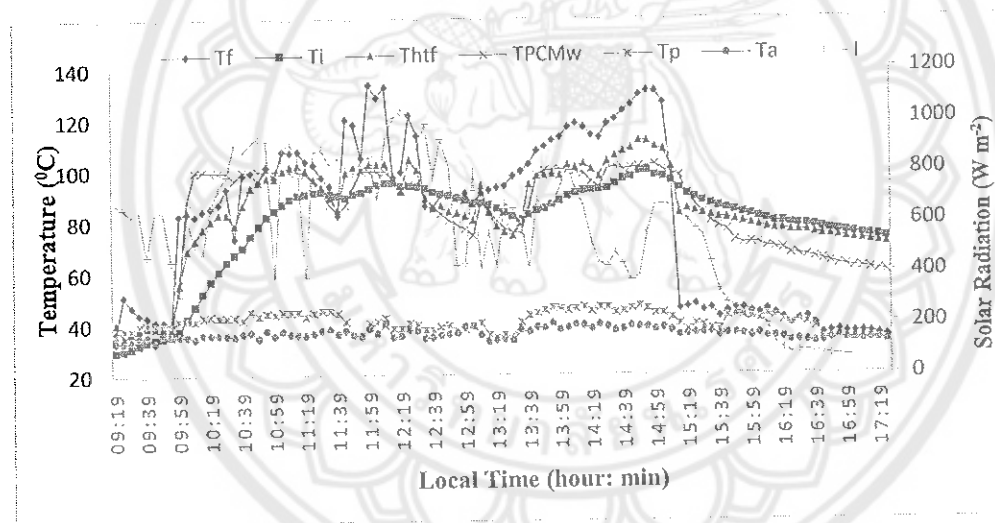


Figure 52 Temperature profile of the system with palm oil in HTF layer and water inside PCM tubes

Figure 52 shows the temperature profile of the system with palm oil in HTF layer and water inside PCM tubes. In this case, the cooking stuff layer is left empty. T_{htf} is the temperature of oil inside the HTF layer of the receiver. The graph shows that the temperature inside the HTF layer with palm oil as heat transfer fluid is more than that of the temperature in HTF layer in the Figure 51. Temperature of the water inside the PCM tubes is also more than that of Figure 51 due to the presence of heat transfer oil.

Temperature inside cooking layer is more due to the presence of oil in HTF layer and water in PCM tubes compared to that of Figure 51. After 3 PM, the solar concentrator is covered with big umbrella to avoid the focus of solar radiation on cooking pot to observe the heat holding capacity of the cooking layer with the presence of Oil and water in HTF layer and PCM tubes respectively. The figure illustrates that after avoiding focus of solar radiation the temperature profile of focal point is reduced whereas the temperature profiles of cooking layer, HTF layer and PCM tubes is still maintained due to the presence of oil in HTF layer. The temperature of cooking layer is more than that of HTF layer and PCM tubes even after the removal of solar radiation.

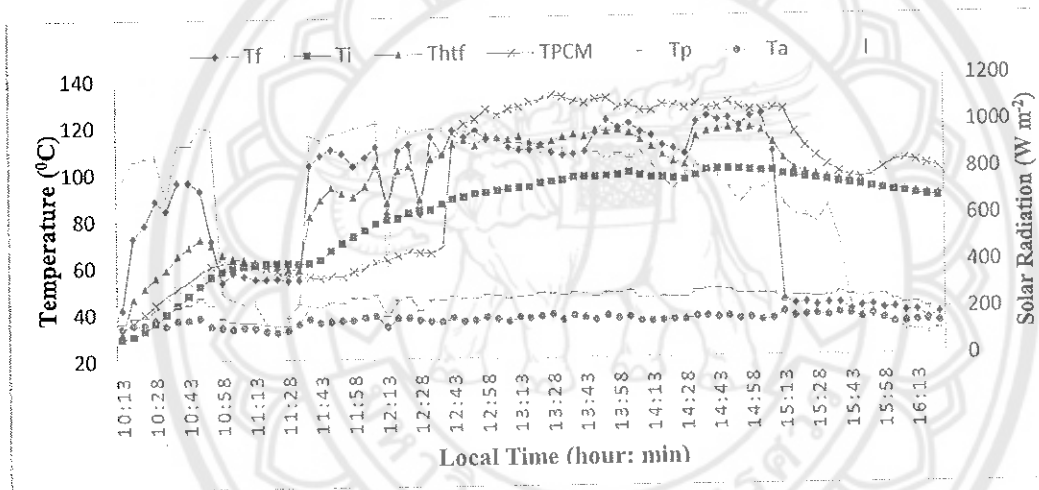


Figure 53 Temperature profile of the system with water, oil and PCM respective layers of the receiver

Figure 53 shows the temperature profile of the system with oil inside HTF layer, $\text{Mg}(\text{NO}_3)_2 \cdot 6\text{H}_2\text{O}$ filled in PCM tubes and cooking stuff layer is filled with 2 liters of the water. T_{PCM} is the temperature of PCM. 100.2°C , 117.9°C and 183.9°C are the maximum temperatures of the water inside cooking stuff layer, oil inside the HTF layer and PCM inside PCM tubes respectively. From Figure 53 it is noticed that, the temperature in PCM tubes with $\text{Mg}(\text{NO}_3)_2 \cdot 6\text{H}_2\text{O}$ as storage medium is more than that of the temperature of PCM tubes in above cases. The temperature of the cooking layer in this case is more uniform than the previous cases irrespective of the variations in the solar radiation. Temperature profile of the focal point is similar to that of solar radiation

profile. The Storage Material $\text{Mg}(\text{NO}_3)_2 \cdot 6\text{H}_2\text{O}$ temperature curve is low in the beginning due to the time of charging of the storage material. After the charging period the material started melting process and absorbs heat from solar radiation focused to the cooking pot. The temperature of the PCM is uniform after charging period. After removal of focus on the cooking pot, the temperature of the focal point is dropped rapidly whereas the temperature profile of cooking layer is maintained uniform due to the presence of PCM and oil in PCM tubes and HTF layer.

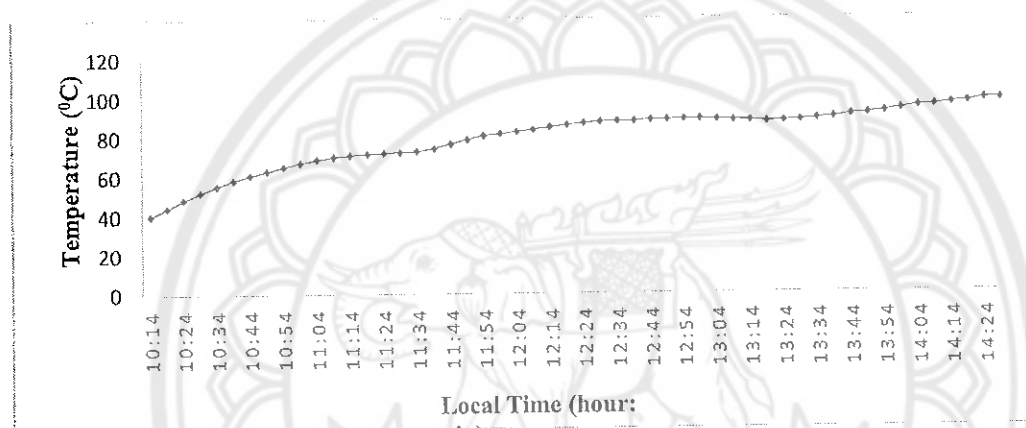


Figure 54 Heating curve of the system with no load conditions in the first set

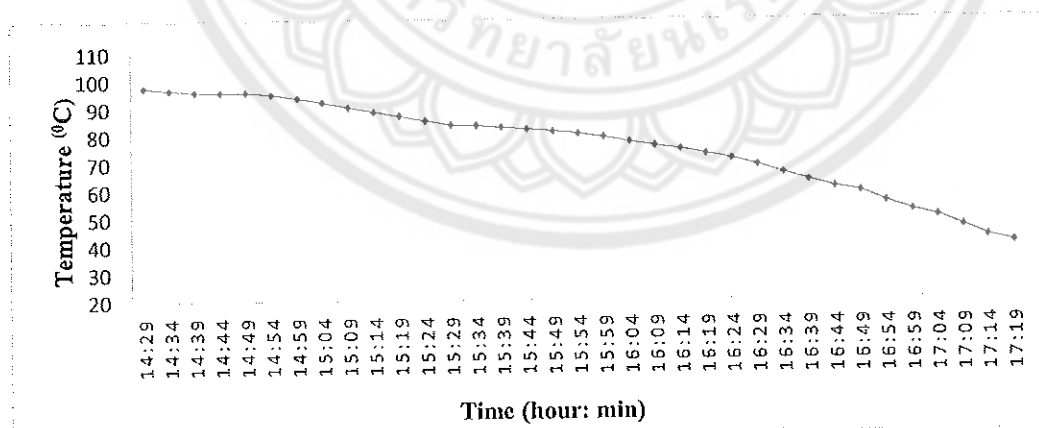


Figure 55 Cooling curve of the system with no load conditions in the first set

Figures 54 and 55 shows the heating and cooling curves of the system with no-load test conditions in the first set of data. Figure 54, illustrates the time taken for the empty pot to reach maximum temperature is long due to the presence of two more layers on the surface of the cooking layer of the receiver pot. Figure 55 shows, the time taken to cool the cooking layer up to 40 °C is also long because of the presence of two more layers on the surface of the cooking layer.

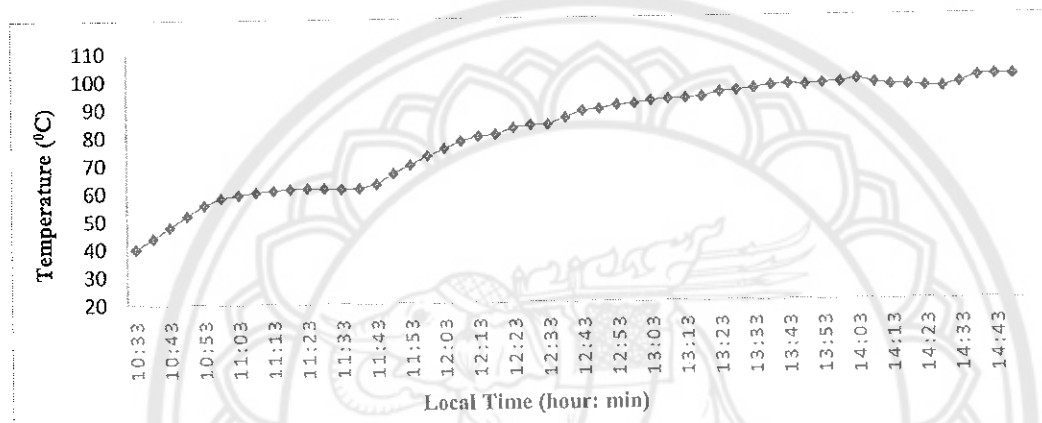


Figure 56 Heating curve of the system with load conditions in the first set

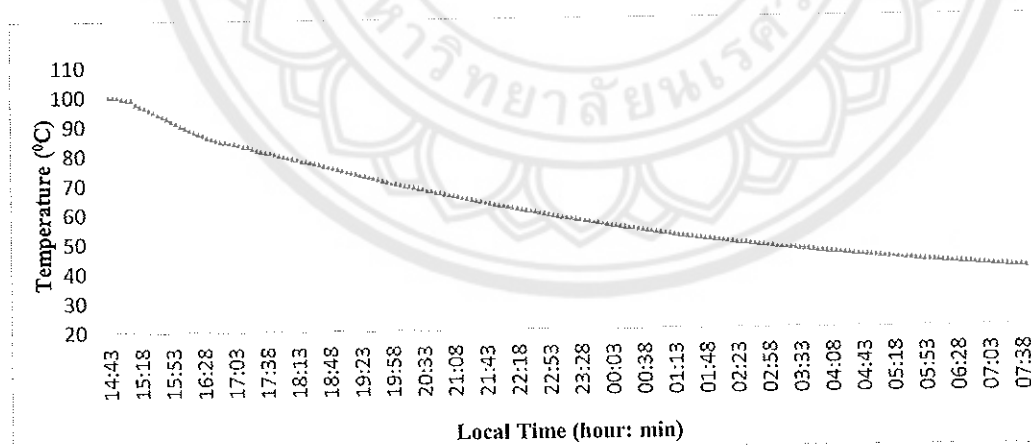


Figure 57 Cooling curve of the system with load conditions in the first set

Figures 56 and 57 shows the heating and cooling curves of the system with load conditions in the first set of data. Figure 56, shows the time taken for the water to reach boiling point is more similar to that of no-load test conditions. In this case, PCM needs

more time to charge and absorb the heat from the solar radiation after that the heat will be transferred to the HTF oil and to the water. From Figure 57, it is noticed that the time taken to bring the water temperature up to 40°C is very long due even compared with the no-load case because of the presence of PCM in PCM tubes and after the sunshine hours the cooking pot is placed inside the insulation box.

Figure 58 shows the temperature profile of the system with no load conditions in second set of data of the experiment. The figure illustrates the complete charging period of the PCM, temperature profiles of the HTF layer and cooking layer are uniform irrespective of the variation in the solar radiation. But, temperature of the focal point depends on the solar radiation. Till the PCM get charged the temperature profiles of HTF layer and cooking pot depends on focal point temperature. From the figure it is also observed that the temperature profiles of the cooking and HTF layers and the PCM are uniform and overlapped on each other after the removal of focusing the solar radiation on the cooking point.

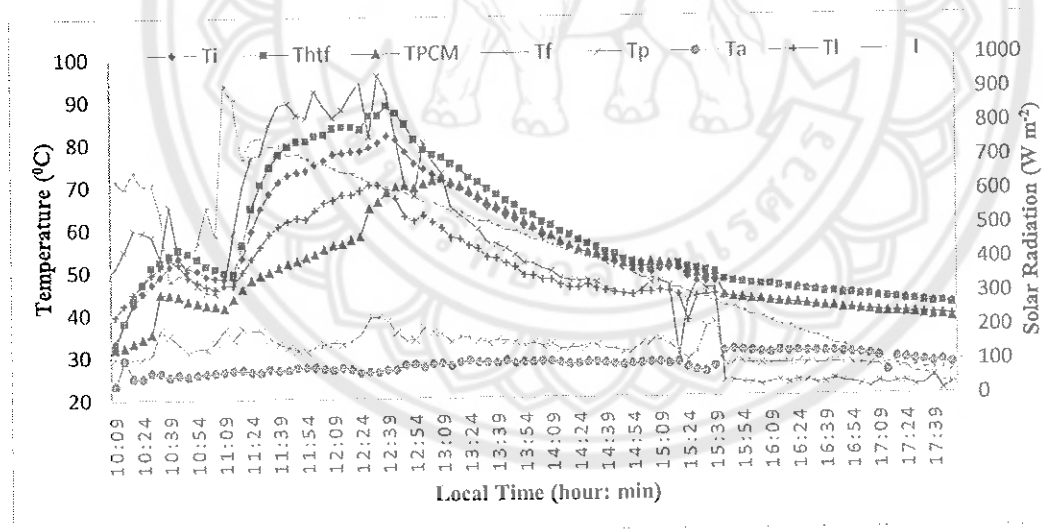


Figure 58 Temperature profile of the system with no load conditions in second set

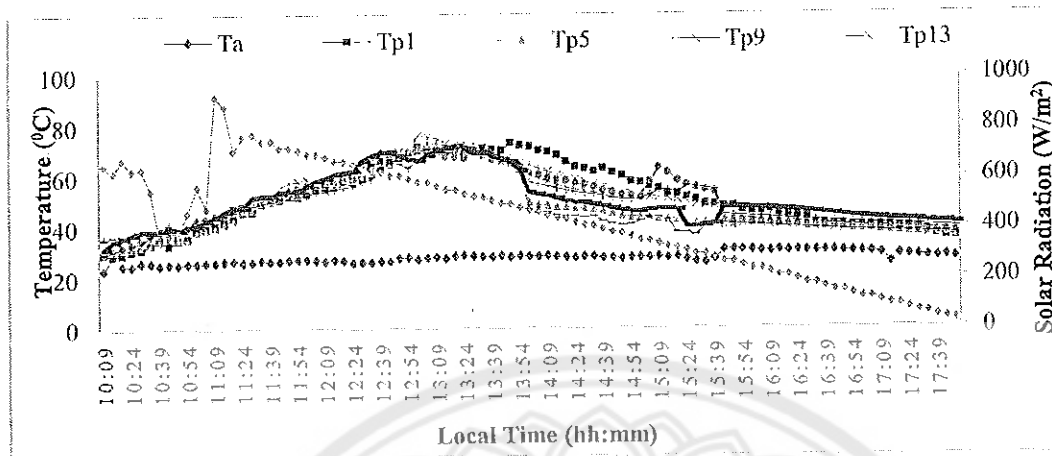


Figure 59 Temperature profile of the PCM with no load conditions in second set

The complete temperature profile of the PCM with no load conditions is shown in Figure 59. The temperatures in all tubes is almost similar and are overlapped on each other till the charging period. After the charging period of the PCM, the temperature in all the tubes is not similar but most of the tubes have the similar temperature profile. The peaks in some PCM tubes temperature profiles is due to the increase in focal temperature at that particular tube while adjusting the focal point by manual tracking system. After removing the cooking pot from the focal point of the concentrator, the temperature profile of PCM in all tubes is similar and overlapped on each other.

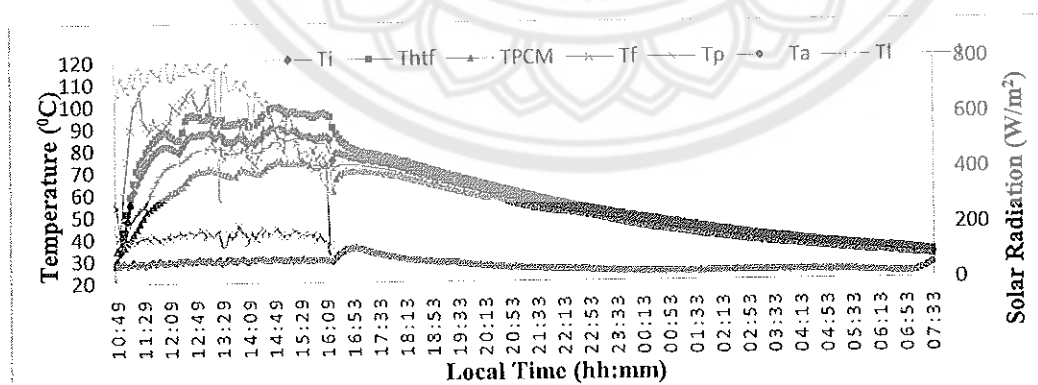


Figure 60 Temperature profile of the system with no load conditions in second set by placing receiver inside insulation box

Figure 60 shows the temperature profile of the system with no load conditions in second set by placing receiver inside insulation box. It is noticed that, the temperature profile of water and oil in cooking layer and HTF layer are similar with the PCM temperature profile after charging. Before charging, those temperature profiles are similar to that of focal point temperature profile. After sunshine hours the cooking pot is placed inside the insulation box. The temperature profiles of the HTF layer, cooking layer and PCM are overlapped on each other in the next day morning. The water temperature is maintained for long time due to the presence of PCM in PCM tubes and oil in HTF layer and the heat holding capacities of PCM and Heat transfer oil.

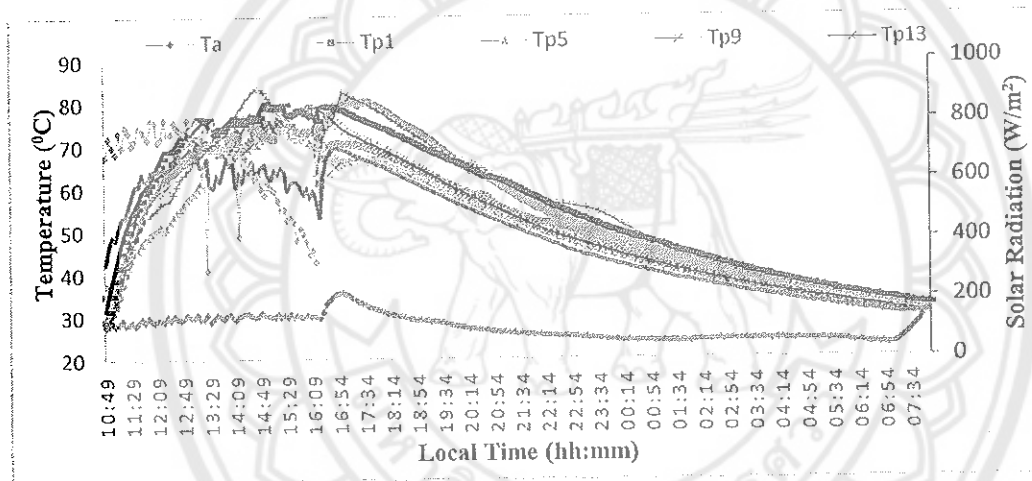


Figure 61 Temperature profile of the PCM with no load conditions in second set by placing receiver inside insulation box

The complete temperature profile of the PCM with no load conditions second set by placing receiver inside insulation box is shown in Figure 61. The temperatures in all tubes is almost similar and are overlapped on each other till the charging period. After the charging period of the PCM, the temperature in all the tubes is not similar but most of the tubes have the similar temperature profile. The peaks in some PCM tubes temperature profiles is due to the increase in focal temperature at that particular tube while adjusting the focal point by manual tracking system. After removing the cooking pot from the focal point of the concentrator and placing it in insulation box the temperature of water reaches minimum temperature in the next day morning. The

temperature profile of PCM in all tubes is similar and overlapped on each other at the end of the heat holding capacity of the PCM.

Figure 62 shows the temperature profile of the system with load conditions in second set. 2 liters of water is placed in the cooking layer for the load test experiment. It is observed that, the charging time of the PCM is less compared to the other cases of the experiment and the temperature profile of the PCM is similar to that of focal point temperature. The temperature of water inside the cooking layer is increased constantly after the charging period of the PCM. The temperature of the PCM, oil and water are maintained similar profile with the decrease in solar radiation in the evening hours of the day.

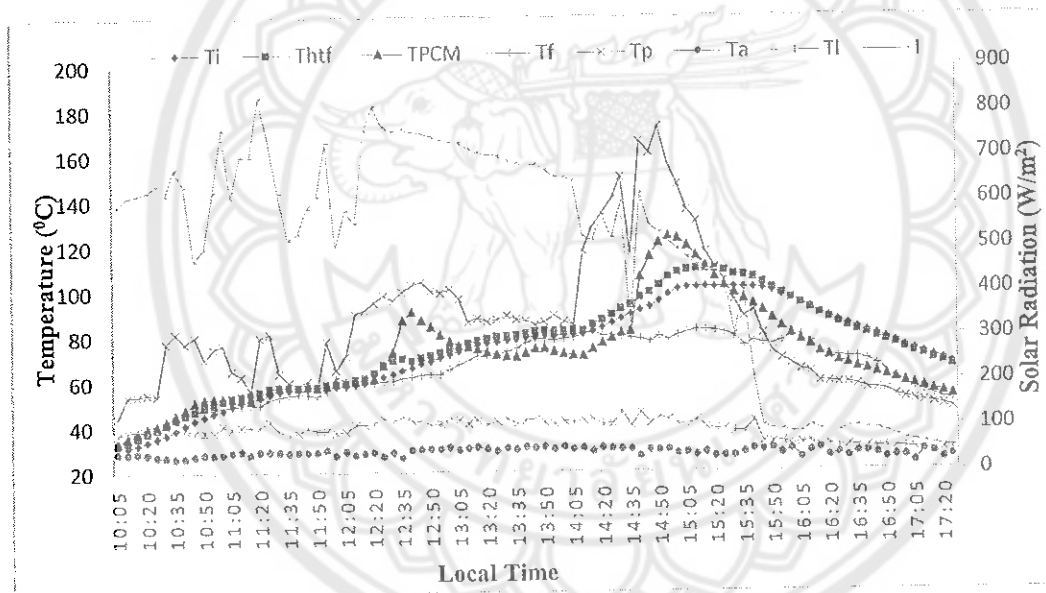


Figure 62 Temperature profile of the system with load conditions in second set

The complete temperature profile of PCM with load conditions in second set of data is shown in Figure 63. The temperature profiles of the PCM in the PCM tubes is more than that of the PCM tubes in Figure 59. With water inside the cooking layer absorbs temperature from the focal point quickly compared to that of empty vessel and which in turn helps to absorb the heat from the focal point by heat transfer oil and PCM. After sunshine hours the Temperature profile of the PCM tubes are overlapped with each other.

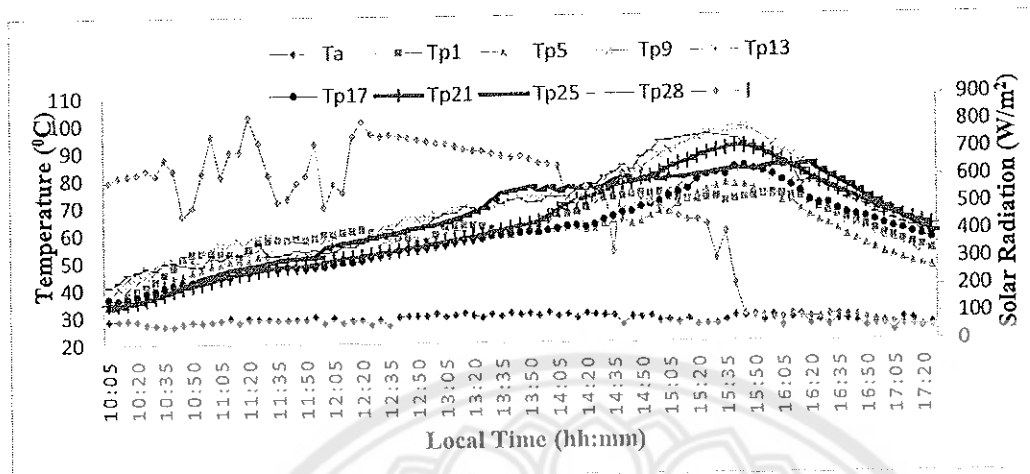


Figure 63 Temperature profile of the PCM with load conditions in second set

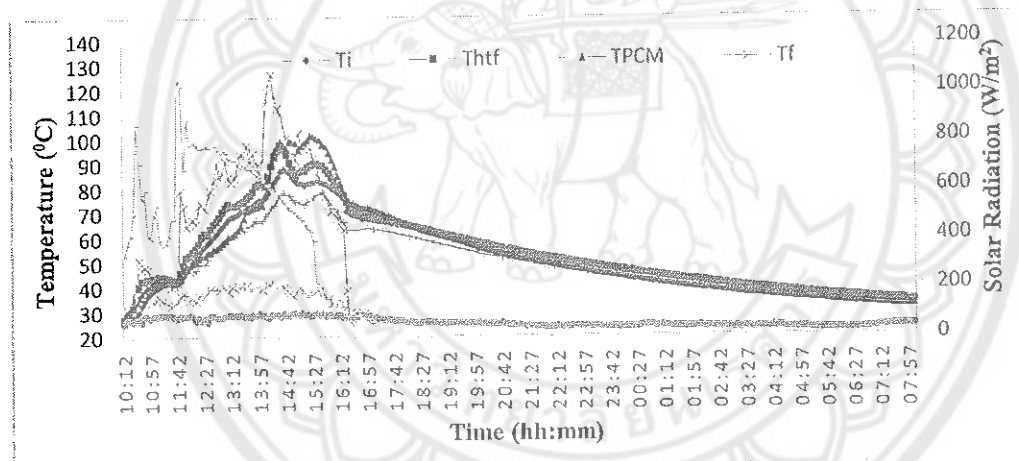


Figure 64 Temperature profile of the system with load conditions in second set by placing receiver inside insulation box

Figure 64 shows the temperature profile of the system with load conditions in second set by placing receiver inside insulation box. The figure illustrates the focal point temperature curve and solar radiation curve throughout the day are similar. Temperature of PCM, oil and water are more than that of the case in Figure 59 which is due to the variation in the solar radiation for that two particular days. From the figure, it is also noticed that the HTF layer and cooking layer temperature profiles are overlapped on each other due to the heat holding capacity of the PCM inside the PCM tubes. The

temperature profile of the PCM is less than that of oil and water due to the transfer of stored heat from the PCM to the oil and water.

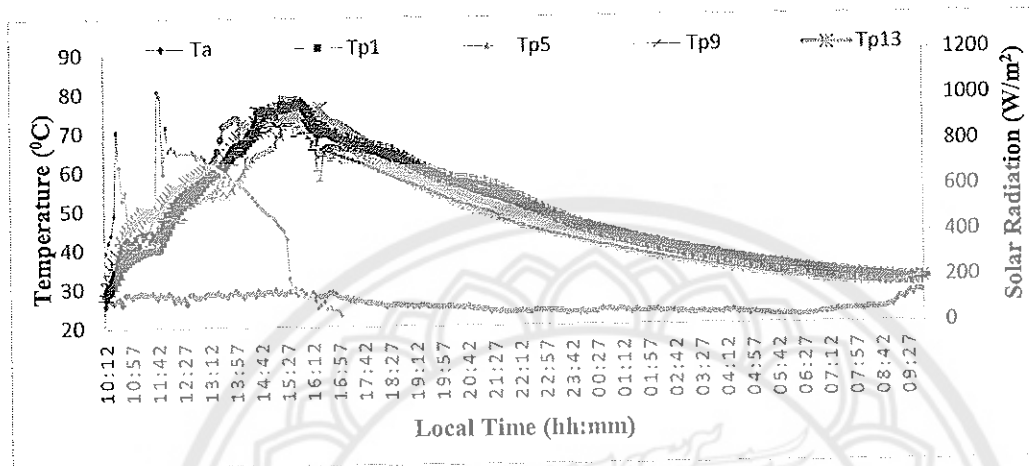


Figure 65 Temperature profile of the PCM with load conditions in second set by placing receiver inside insulation box

Figure 65 shows the temperature profile of the PCM with load conditions in second set by placing receiver inside insulation box. In this case, the temperature profiles are greater than that of the case in Figure 61 due to the presence of water inside the cooking layer. From the Figure 65, it is observed that the temperature profile of the PCM in all the tubes is similar and most of the tubes profile is overlapped with another throughout the day. After placing the cooking pot in the insulation box, the temperature of PCM is reduced gradually but maintains the uniform reduction in all tubes until next day morning.

After loading the receiver with 2 liters of water heating and cooling curves with and without insulation box are plotted. Figure 66 shows the comparison of no load heating curves with and without insulation box.

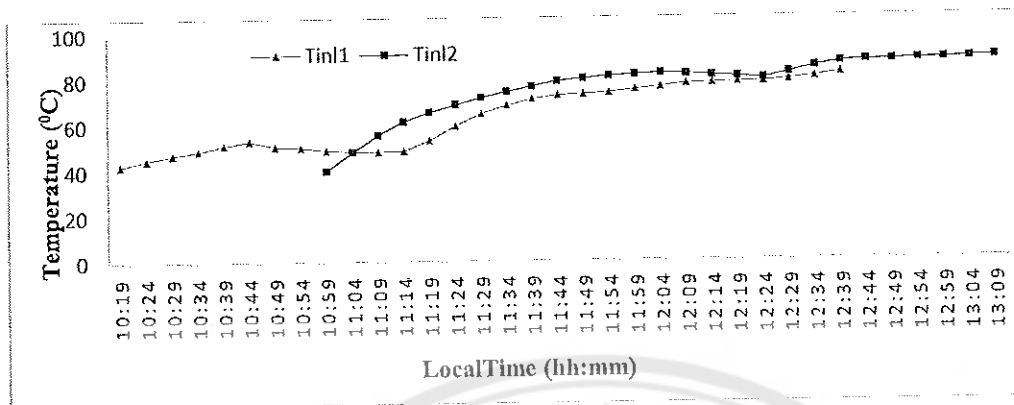


Figure 66 Comparison of second set no load heating curves with and without insulation box

In Figure 66, T_{in1} , T_{in2} are the heating curves for no-load test with and without receiver placed inside the insulation box. Both the curves took almost same time to reach the maximum temperature from the starting time of the experiment. The lag in the second curve is because of the time of starting of the experiment in the day. The Second curve is more than that of the first curve due to the variation in the solar radiation on the two particular days.

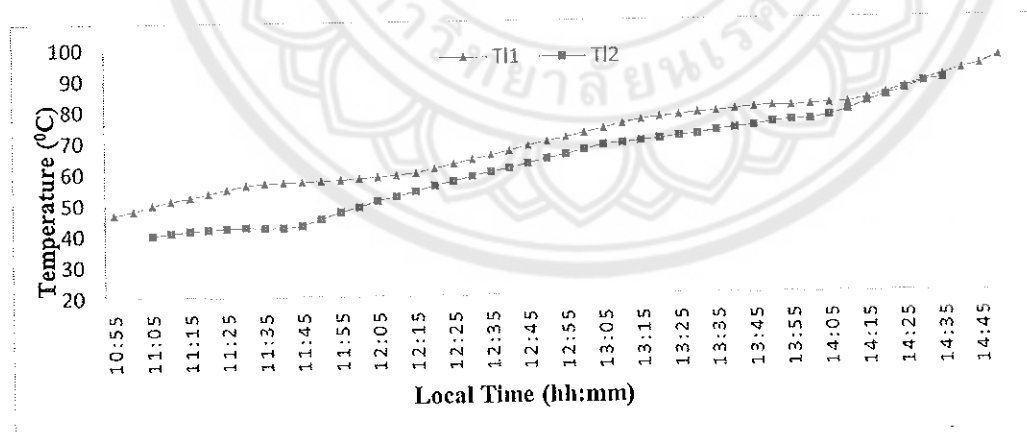


Figure 67 Comparison of second set load heating curves with and without insulation box

Figure 67 shows the comparison of set 2 load heating curves with and without insulation box. From the figure, it is observed that the variation in the solar radiation on the particular days. Compared to Figure 66 curves, Figure 67 heating curves took more time to reach boiling point of the water as the water present inside the cooking layer of the cooking pot.

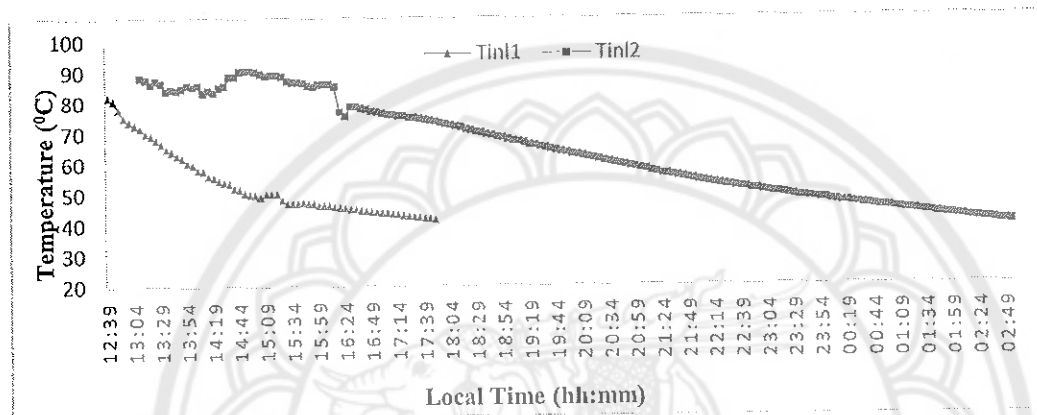


Figure 68 Comparison of second set no load cooling curves with and without insulation box

Figure 68 shows the comparison of second set no load cooling curves with and without insulation box. The no-load cooling curve without insulation box is shorter than that of the no-load cooling curve with insulation box. The heat stored in the PCM and oil is transferred to the cooking layer gradually when the cooking pot is placed inside the insulation box. So that the cooling curve for this case is longer than that of the cooling curve without insulation box.

Figure 69 Comparison second set of load cooling curves with and without insulation box. From the Figure 69, it is observed that the cooling curve of without insulation box is shorter than that of the cooling curve by placing the receiver inside the insulation box. The heat stored in the PCM and oil is transferred to water inside the cooking layer gradually until the next day morning in case of the cooking pot placed inside the insulation box.

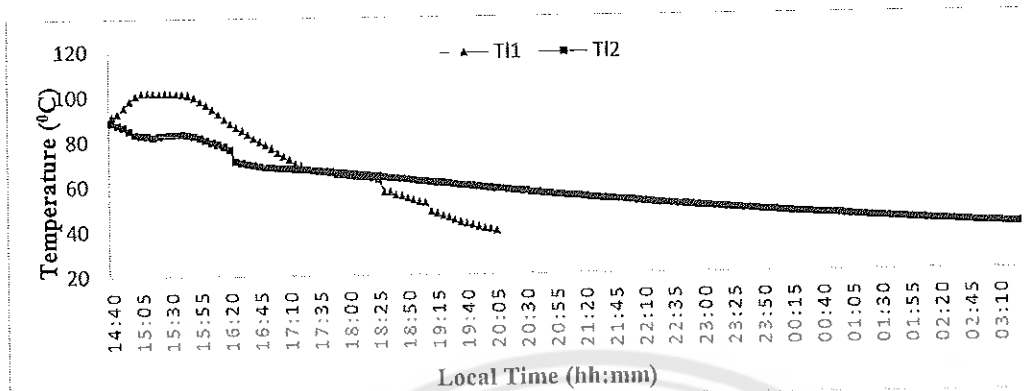


Figure 69 Comparison of second set load cooling curves with and without insulation box

The heating and cooling curves of the no-load and load tests for the third set data of the experiment without and with placing the receiver inside the insulation box respectively are mentioned in appendix D. The reasons for the variations in each plot of the data are likewise that of the reasons for the variations in the corresponding figures in second set data of the experiment. Cooling curves are important while using the storage system and the cooling curves should be long enough to hold the sufficient heat for the boiling purpose. From set 2 and set 3 cooling curves it was observed that the time taken for the temperature to reach minimum value inside the cooking layer of the receiver is more in case of the receiver with PCM in PCM tubes and heat transfer oil in HTF layer and the receiver is placed inside the insulation box.

Figure 70 and 71 show the continuous no load and load temperature profiles of the solar cooking system. From the Figures, it is observed that the temperature profile inside the cooking stuff layer is the same as after the charging process of the PCM irrespective of the solar radiation intensity. In no load case, temperature profile of cooling stuff layer is not similar for all the days. Whereas in load case, the temperature profile similar in all the days after charging period of the PCM. The variation in the intensity of solar radiation couldn't effect the temperature needed to cook food after charging period of PCM.

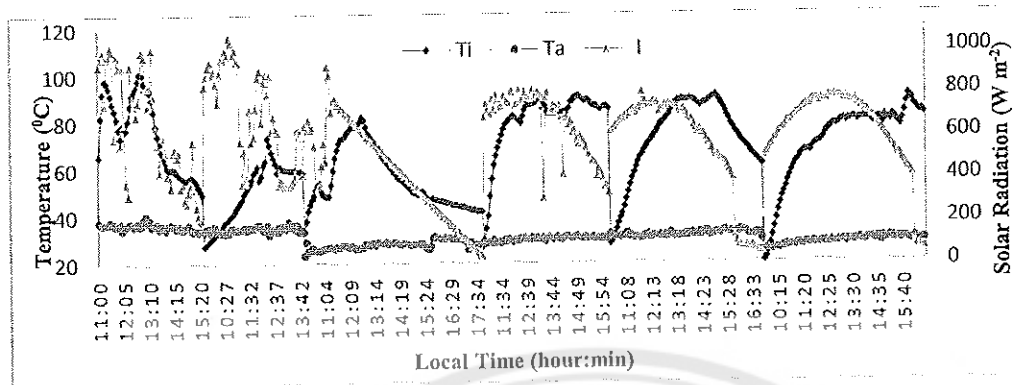


Figure 70 Temperature profile of continuous no load test

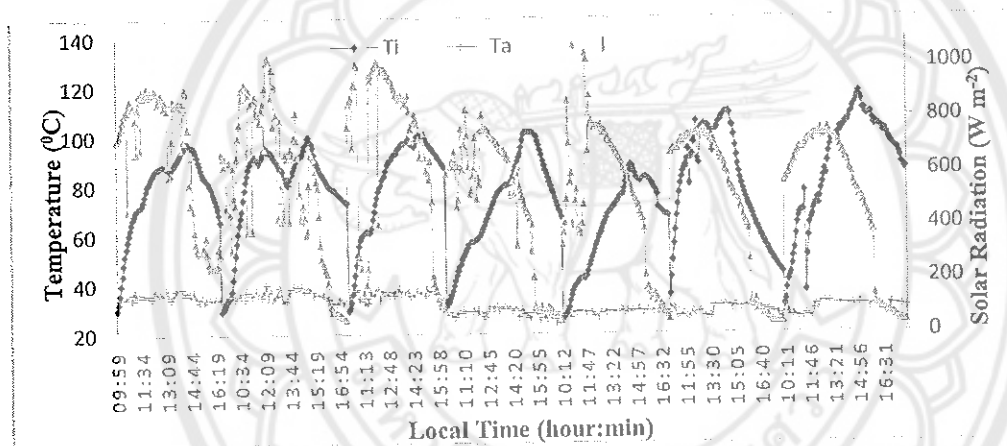


Figure 71 Temperature profile of continuous load test

The effect of wind speed on the experiment is neglected because the wind speed in the area where the experiment is conducted is less than 1 m/s. The variation in wind speed for no-load and load tests is shown in appendix G. The solar cooker parameters mentioned in chapter 3 are calculated based on the experimental data and the results are mentioned in Table 11.

An example calculation for load test with receiver placing inside the insulation box from the second set data is as follows,

Mass of inside cooking pot, $M_w = 2$ kg

Specific heat capacity of water, $C_w = 4.190$ kJ/kg $^{\circ}\text{C}$

Mass of heat transfer oil, $M_{oil} = 0.885$ kg

Specific heat capacity oil, $C_{oil}=1.875 \text{ kJ/kg } ^\circ\text{C}$

Mass of PCM, $M_{PCM}=2 \text{ kg}$

Specific heat capacity of PCM, $C_{PCM}=1.810 \text{ kJ/kg } ^\circ\text{C}$

Mass of empty receiver pot, $M_{pot}=10 \text{ kg}$

Specific heat capacity of pot, $C_{pot}=10 \text{ kJ/kg } ^\circ\text{C}$

Heating time constant, $\tau=12,600 \text{ sec}$

Cooling time constant, $\tau_0=45,600 \text{ sec}$

Final temperature of water, $T_{wf}=88.30 \text{ } ^\circ\text{C}$

Initial temperature of water, $T_{wi}=26 \text{ } ^\circ\text{C}$

Average ambient temperature, $T_{a, avg}=28.3 \text{ } ^\circ\text{C}$

Ambient temperature corresponding to final water temperature, $T_{wa}=29.20 \text{ } ^\circ\text{C}$

Average solar irradiation, $\bar{I}=500.42 \text{ W/m}^2$

Solar irradiation corresponding to final water temperature, $I=543.02 \text{ W/m}^2$

Concentration ratio, $C=5.97$

Area of the receiver or cooking pot, $A_r=0.3 \text{ m}^2$

Combined heat capacity $(MC)_r$ of the receiver was calculated by substituting the above parameters in equation (25).

Combined heat capacity, $(MC)_r=18684 \text{ kJ}^\circ\text{C}$

Heat removal factor $F'U_L$ was calculated by substituting $(MC)_r$, τ_0 and A_r values in equation (26).

Heat removal factor, $F'U_L=18684/(45,600 \times 0.3)$
 $=1.36 \text{ W/m}^2^\circ\text{C}$

Optical efficiency factor $F'\eta_o$ was calculated by substituting $F'U_L$, C and other parameter values in equation (27).

Optical efficiency factor, $F'\eta_o=0.089$

By substituting M_w , C_w , T_{wf} , T_{wa} and τ in equation (28), the cooking power of the PCM solar cooker was calculated.

Cooking power $P=39.3 \text{ W}$

Standardized cooking power (P_s) was calculated from equation (29).

$P_s=50.66 \text{ W}$

Overall heat loss coefficient (U_L) was calculated from the plot between standardized cooking power and $(T_w - T_a)$ which is mentioned in appendix D.

Slope of the plot between (P_s) and $(T_w - T_a) = 1.972$.

The overall heat loss coefficient is calculated by dividing slope with A_r .

$$U_L = 1.972/0.3 = 6.57 \text{ W/m}^2\text{°C}$$

The optical efficiency of the solar concentrator is obtained by substituting U_L value in $F'\eta_o$ value.

$$F'U_L = 1.36$$

$$F' = 1.36/6.57$$

$$F' = 0.207$$

Optical efficiency factor, $F'\eta_o = 0.089$

$$\eta_o = 0.089/0.207$$

$$\eta_o = 43\%$$

Similarly, all the parameters for the remaining data sets were also calculated in the same sequence as above calculation and the values are listed in Table 11.

Table 11 Parameters of solar cooking system

Load characteristics	Set	(MC) _r (J/K)	T _i (sec)	T _{o1} (sec)	F'U _L (W/m ²)	F'η _o	P (W)	P _s (W)
Water in all layers	1	28907.16	6750	8100	11.89	0.513	75.35	68.86
Load		18684	4500	25800	2.413	0.22	118.43	106.74
No load	2	10304	8400	18600	1.84	0.0512	-	-
No load storage		10304	7800	49500	0.69	0.062	-	-
Load		18684	14100	19500	3.19	0.07	69.02	43.6
Load storage		18684	12600	45600	1.36	0.089	50.66	39.3
No load	3	12114	9300	18900	2.136	0.065	--	-
No load storage		12114	8400	48900	0.825	0.0838	-	-
Load		20494	3600	11400	5.99	0.42	210.76	183.1
Load storage		20494	6000	63300	1.079	0.27	165.10	119.9

The energy required to boil the water and the energy required to evaporate the water are mentioned in appendix D. From the calculated parameter values it was

observed that the power obtained by the developed solar cooker is sufficient to boil the water after the charging period of the PCM.

Complete energy and efficiency analysis of the system

The amount of thermal energy, Q stored in cooking stuff layer, HTF layer and PCM layer are calculated and the corresponding efficiencies are also calculated from the above mentioned formulae in section 3.4.2. The amount of thermal energy, Q stored in each layer is shown in Figure 72. The Q stored in the water is greater than the other two layers because of the heat transfer from the PCM and HTF layers to the cooking layer. Thermal energy in PCM and HTF layers helps to hold sustain the temperature inside the cooking layer so, the amount of Q absorbed by the water is more as shown in Figure 72.

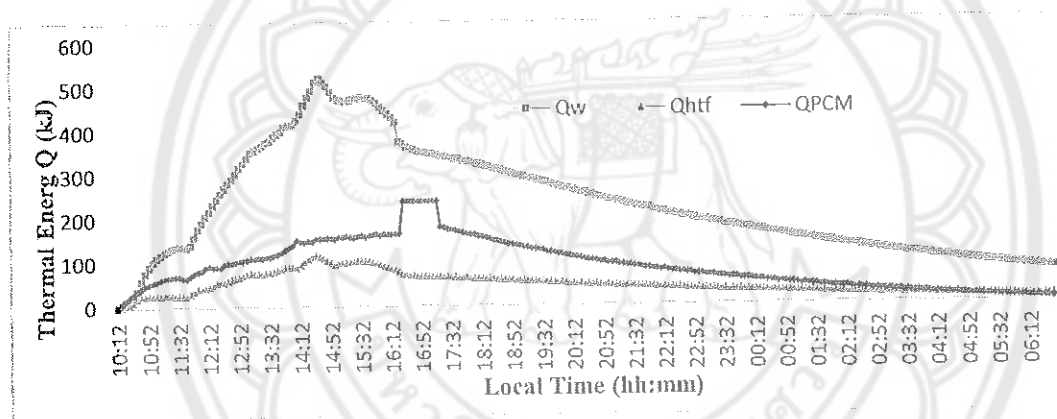


Figure 72 Thermal energy of the receiver in different layers

The amount of thermal energy Q stored in the receiver or cooking pot by adding corresponding materials in the layers of the receiver is shown Figure 73. In figure 73, $Q_{total, 1}$ is the thermal energy of the receiver only water which is filled in cooking stuff layer. $Q_{total, 2}$ is the thermal energy of the receiver with HTF oil and water in corresponding layers. $Q_{total, 3}$ is the thermal energy of the receiver with PCM, heat transfer oil and water in respective layers of the receiver.

From Figure 73, it is observed that, addition of heat transfer oil increases the thermal energy of the receiver which in turn increases the thermal energy transferred to the cooking stuff layer. By incorporating PCM inside the PCM tubes of the developed solar cooker, Q of the receiver is further increased compared to the Q increment after

adding heat transfer oil. The reason for this further increment is the three step energy storage of PCM material. $Q_{PCM\text{sensible},1}$, Q_{latent} and $Q_{PCM\text{sensible},2}$ are the three steps of energy storage for PCM whereas for water and heat transfer oil, the Q is stored only in the form of sensible heat.

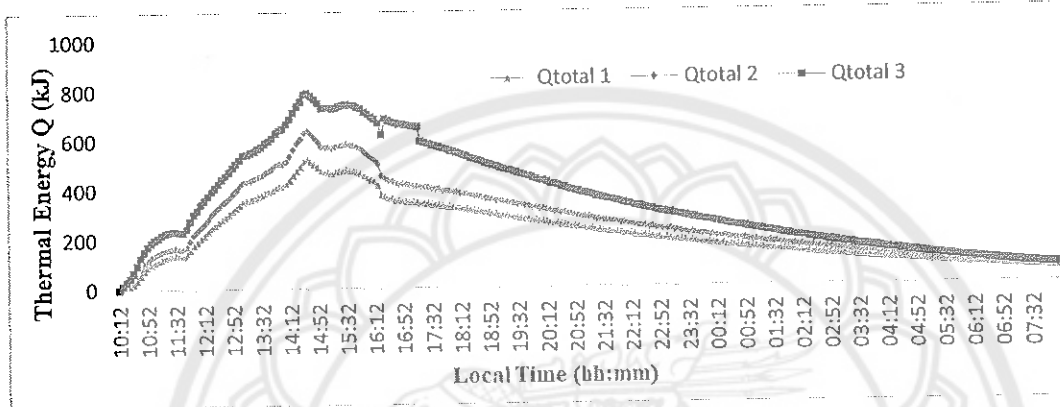


Figure 73 Total amount of heat stored in the receiver

The efficiencies of the PCM solar cooker corresponding to the thermal energy Q mentioned in Figure 73 are shown in Figure 74. Efficiency₁, efficiency₂ and efficiency₃ are the efficiencies of the system with water, water and heat transfer oil, water, heat transfer oil and PCM inside the cooking pot layers respectively. Because of the 3 steps heat storage, the efficiency of the system with PCM is more than that of the other two cases. During off sunshine hours, the receiver is placed inside the insulation box, so all the efficiencies are calculated for sunshine hours of the throughout the experiment period. The average efficiencies for the corresponding cases are 22%, 28% and 40% respectively.

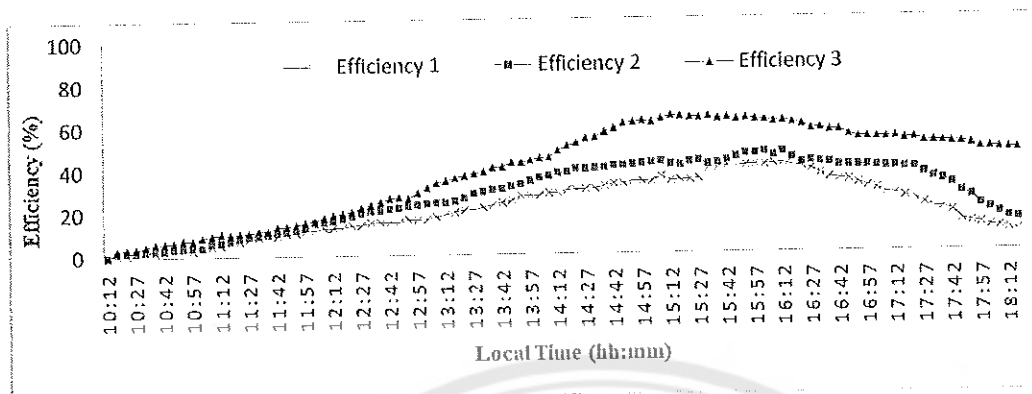


Figure 74 Efficiencies of the system in different cases

Real time applications analysis

The developed solar cooking system is tested for real time cooking applications like boiling and frying with different food materials. The temperature and time profile of green bean and red bean cooking in day 1 boiling application of the developed PCM solar cooker is shown in Figure 75.

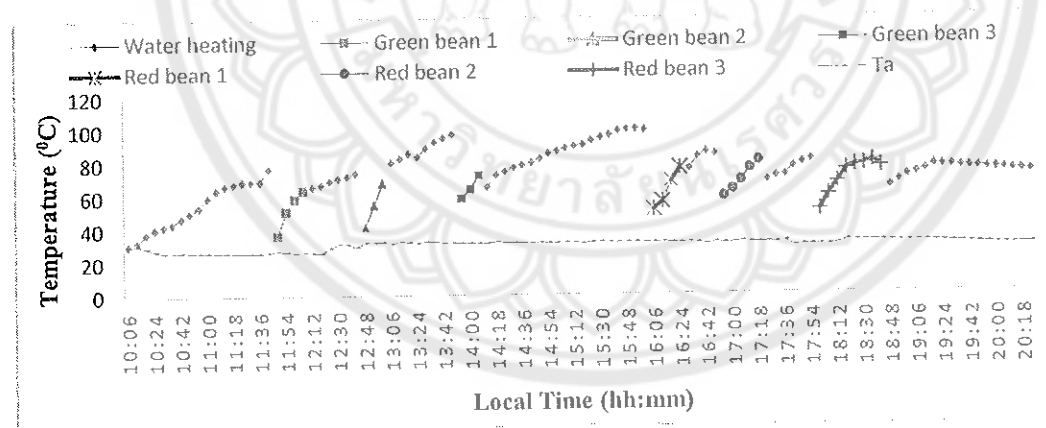


Figure 75 Temperature profile for day 1 boiling

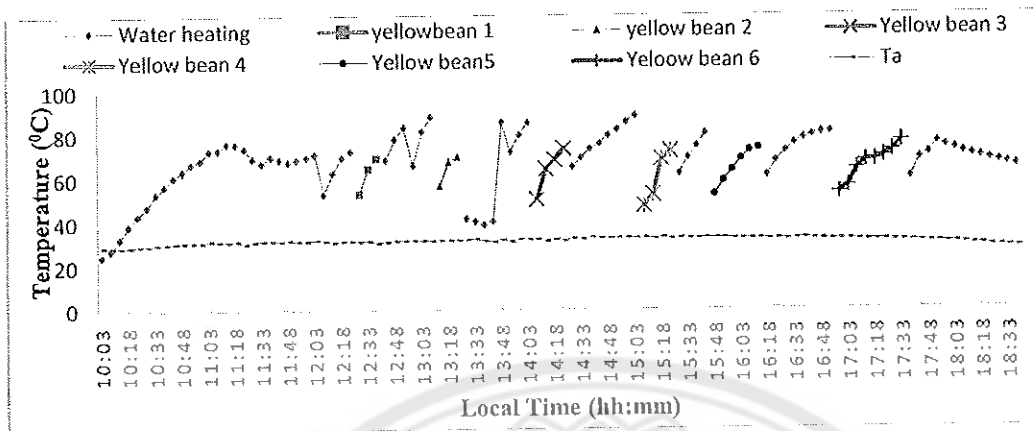


Figure 76 Temperature profile for day 2 boiling

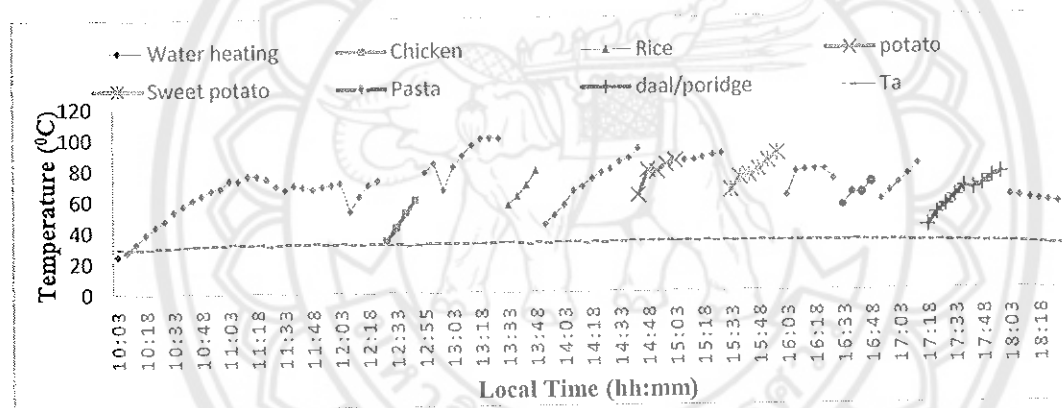


Figure 77 Temperature profile for day 3 boiling

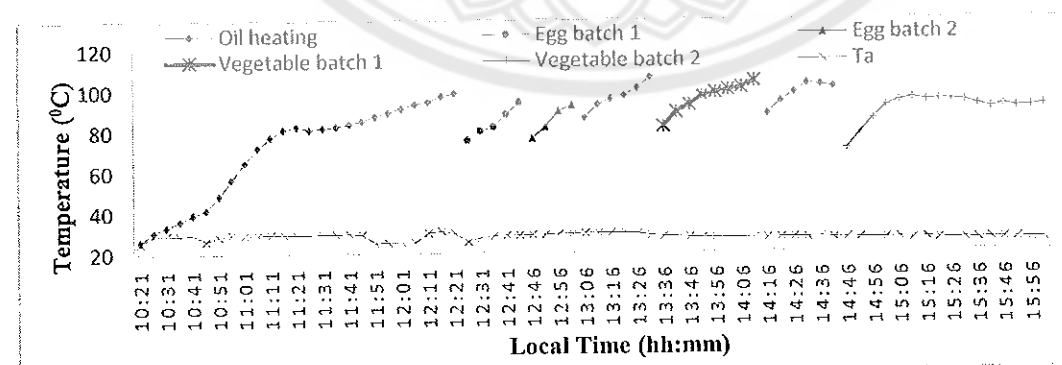


Figure 78 Temperature profile for frying

Figure 75 illustrates the cooking time of green bean and red bean for different cooking batches in throughout the experiment period. In boiling applications, water is heated in the receiver before adding the beans for cooking experiment. After water reaches near boiling temperature, beans are added. So that the cooking time of beans is reduced. From time profile of Figure 75, it was noticed that, six batches of beans are cooked throughout the day. Among the six cooking batches, three batches of green bean were cooked in outdoor and three batches of red bean are cooked indoors after placing the receiver in insulation box.

The second day boiling application was performed by cooking six batches of mung split bean throughout the experiment period. The temperature and time profile of second day boiling experiment is shown in Figure 76. From the time profile, it is shown that three batches of mung bean were cooked during sunshine hours and the other three batches were cooked during off sunshine hours. The off sunshine cooking or indoor cooking was performed by placing the cooking pot inside the insulation box.

From Figures 75 and 76, it was observed that the same type of food can be cooked upto three batches outdoor and three batches can be cooked indoor with the available thermal energy stored in the PCM. A total of six batches of the same type of food can be cooked in a day by this PCM solar cooker.

The different food materials were cooked in different batches for the third day boiling experiment. The temperature and time profile for third day boiling experiment are showed in Figure 77. This experiment was performed three consecutive days to notice the average time taken for the cooking process of different food materials. Except daal or porridge all the other food materials in Figure 77 were cooked during sunshine hours and daal is cooked inside during off sunshine hours. Total five batches of different food materials were cooked in outdoor conditions and one batch of food can be cooked inside in the evening hours. The specific heat capacities of the food materials were different for every batch of the food because of this reason, the number of batches cooked during the day was varied compared to the same type of food cooked in different batches. The remaining two-day temperature and time profiles of the different food materials cooked in the same day are mentioned in appendix E.

After boiling experiment, frying of egg and vegetables was also performed to know the deep frying time of the food with the developed PCM solar cooker. The

temperature and time profile of frying experiment was shown in Figure 78. While performing frying experiment, oil is heated initially before adding each batch of food to the cooking pot. After oil reaches 85°C to 95°C , the food materials are added for deep frying. With the available heat stored in the PCM, it was observed that only four batches were fried effectively in this PCM solar cooker.

From all real time application experimental Figures 75, 76, 77 and 78 it was observed that, the temperature of water and oil were reduced after immediately adding the food material to the cooking pot. The temperature drop is due to the addition of food materials which were at room temperature. After adding the food materials to the cooking pot, the temperature rising was considered for the proper food cooking. Depending upon the rise in temperature of the food, the cooking quality was observed at regular time intervals.

The cooking time of particular food and the amount of thermal energy and power required to cook food for all the different days of real time applications are mentioned in Table 12, 13 and 14.

The specific heat capacity of the different food materials cooked in this PCM solar cooker is mentioned in Table 19 in appendix E.

For all real time cooking application experiments on the developed PCM solar cooker the following control parameters are considered.

1. Quantity of food material about 0.2 kg
2. Temperature rise in the food material, sec
3. Cooking time, sec
4. Thermal energy (Q), kJ
5. Power (P), mW

The thermal energy, Q used during outdoor cooking is from the direct solar irradiation and the Q used during indoor cooking is from the energy stored in the PCM during sunshine hours. The amount of Q and P used to cook the food materials depends on the temperature rise, cooking time of food and the specific heat capacity of the particular food material.

Table 12 Different parameters to cook same food material in a day

Food material	Cooking mode	Day/ batch	Time (Sec)	ΔT ($^{\circ}C$)	Q (kJ)	P (mW)
Green bean	outdoor	1/1	4500	27.00	17.60	3.91
	outdoor	1/2	3000	26.30	17.14	5.71
	outdoor	1/3	3000	23.90	15.58	5.19
Red bean	indoor	1/4	4500	25.00	10.65	1.77
	indoor	1/5	6000	21.50	9.15	2.03
	indoor	1/6	10500	25.90	11.03	1.05
Mung split bean	outdoor	2/1	3000	16.30	6.84	2.28
	outdoor	2/2	3000	13.50	5.67	1.89
	outdoor	2/3	4500	23.20	9.70	2.16
Mung split bean	indoor	2/4	4500	25.10	10.54	2.34
	indoor	2/5	7500	21.10	8.86	1.18
	indoor	2/6	10500	23.40	9.80	1.06

From Table 12 it was calculated that, the average time taken to cook Green bean and mung split bean in outdoor conditions is 3500 seconds. For Red bean and Mung split bean the average time taken to cook indoor conditions is 7000 seconds and 7500 seconds respectively. The thermal energy required to cook green bean, red bean, mung bean is 16.7 kJ, 10.27 kJ and 8.56 kJ respectively. The total amount of outdoor Q_o produced for the first and second days during sunshine hours is about 50.32 kJ and 22.21 kJ respectively. The total amount of indoor Q_i produced for the first and second days during off sunshine hours is about 30.83 kJ and 29.2 kJ respectively.

In Table 13, the cooking time of different food materials in different batches and the energy used to cook that food materials were mentioned. The total Q utilized to cook different food materials for first, second and third days of the experiments including both indoor and outdoor conditions is 148.45 kJ, 150.89 kJ and 149.788 kJ respectively. The amount of energy required to cook the food materials in Table 13 is varied from material to material due to the variation in specific heat capacity of the food materials and the cooking time of that food material. The average total amount Q utilized to cook different food materials in different batches throughout a day is about 150 kJ.

Table 13 Different parameters for cooking different food material in a day

Food	Day 1				Day 2				Day 3			
	Time (sec)	ΔT ($^{\circ}C$)	Q (kJ)	P (mW)	Time (sec)	ΔT ($^{\circ}C$)	Q (kJ)	P (mW)	Time (sec)	ΔT ($^{\circ}C$)	Q (kJ)	P (mW)
Chicken	4500	28.5	18.3	4.06	4500	26.3	16.9	3.76	4500	27	17.38	3.86
Rice	4500	23.2	9.95	2.21	4500	22	9.44	3.77	6000	22.3	9.57	1.59
Potato	4500	21.7	14.88	3.30	6000	22.2	15.2	2.53	4500	23.3	15.98	3.55
Sweet Potato	6000	25.2	15.82	2.63	7500	23.4	14.6	1.95	7500	24.2	15.19	2.02
Pasta	3000	15.1	5.4	1.81	4500	14.7	5.2	1.17	3000	14.3	5.148	1.71
Daal/ Porridge	12000	31.8	84.1	7.01	12000	33.8	89.43	7.45	10500	32.7	86.52	8.24

Table 14 Different parameters for frying application

Food material	Batch	Time (Sec)	ΔT ($^{\circ}C$)	TE (kJ)	P (mW)
Egg	1	6000	18.5	11.76	1.96
Egg	2	4500	16.3	10.36	2.3
Vegetables	3	10500	22	49.36	4.7
Vegetables	4	21000	20.8	46.67	2.22

It was observed that, the average Q required to fry egg is about 17.40 kJ and to fry vegetables is about 48 kJ. In general, deep frying application needs high temperature for short time interval. So, the time taken to fry vegetables is more in this experiment because of the uniform rise in temperature and Q in the PCM cooker.

Some of the food materials cooked in the developed PCM solar cooker are shown in Figure 79.

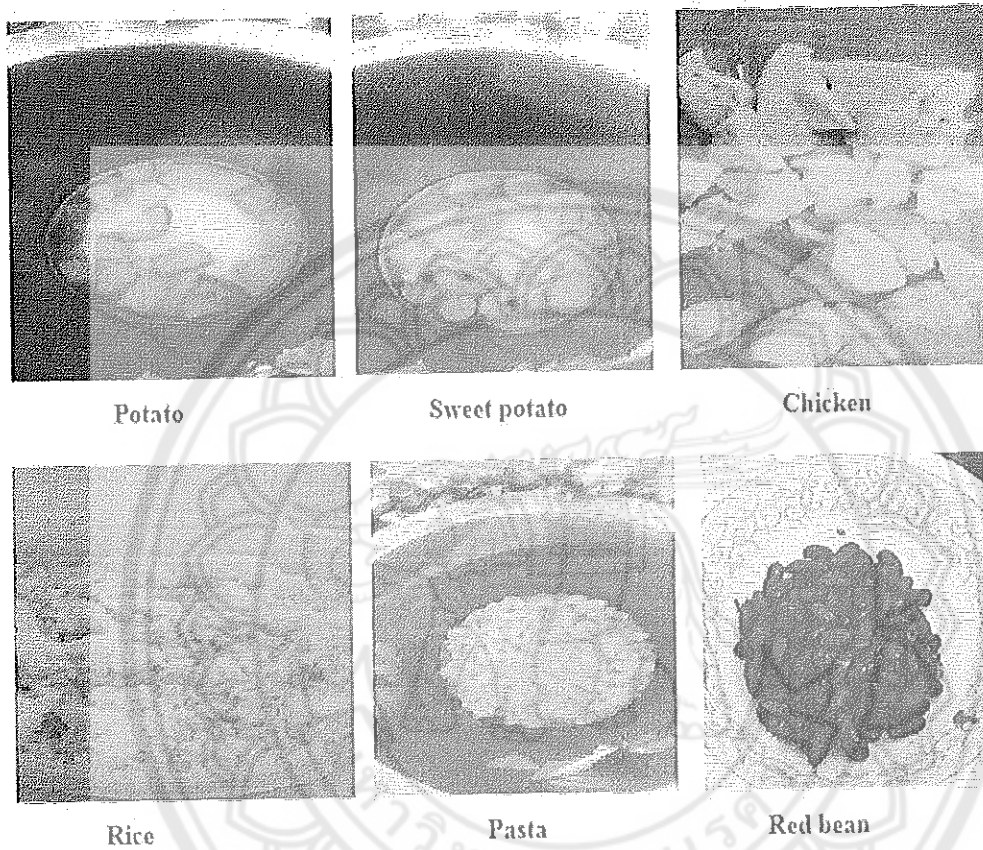


Figure 79 Some of the cooked food materials in PCM solar cooker

Thermal image Analysis

The solar cooking system is captured in different periods of the day with the help of Fluke thermal camera. The temperature profile of the receiver with the help of thermal camera is helpful to see the temperature variations directly and to know the intensity of the temperature instantly for the safety operation of the cooking system. The maximum, minimum, average and centre point temperatures of the captured image are shown on the thermal image figures.

The distance between the thermal camera and the cooking pot and the complete system was about 0.5 m to 1.0 m.

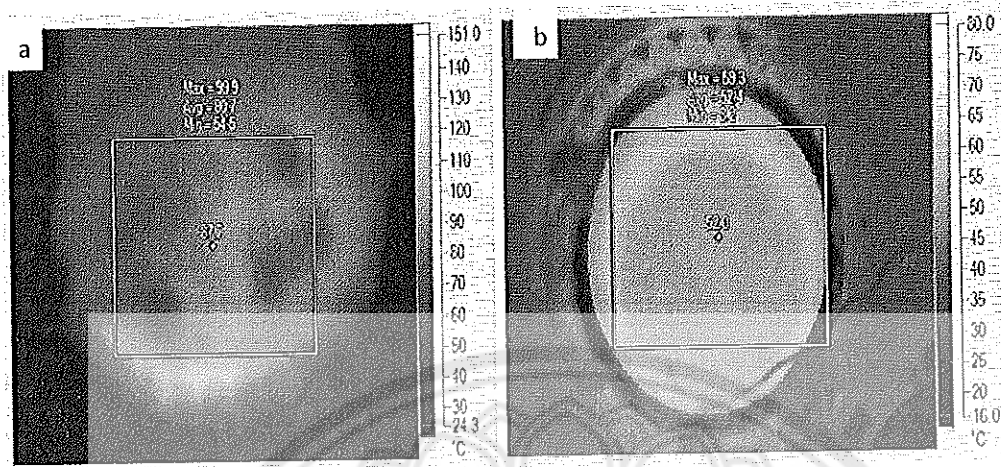


Figure 80 Thermal image of the receiver in the morning (a) bottom view
(b) top view

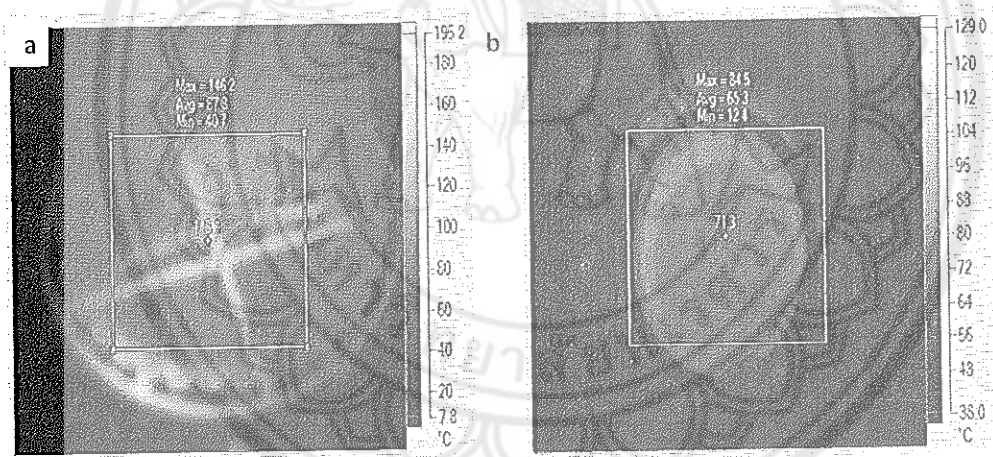


Figure 81 Thermal image of the receiver in the afternoon (a) bottom view
(b) top view

Thermal image of the bottom and top view of the receiver in the morning time is shown in Figure 80. It illustrates the intensity of the temperature in different layers of the receiver. The bottom view temperature intensity is more than the top view figure intensity because of the bottom centered focus of the solar irradiation from the solar concentrator. As Figure 80 is captured in the morning, the average temperatures at bottom and top views were 80.7 °C and 52.4 °C respectively.

Thermal images of the bottom and top views of the receiver in the afternoon are shown in Figure 81. It was observed that the maximum temperature at the bottom of the receiver is 146.2°C because of the increase in solar irradiation during afternoon. The maximum temperature from the top view was 84.5°C as shown in Figure 81. The temperature of the receiver was increased from morning to afternoon and that increment was observed with these thermal images instantly throughout the day.

The bottom and top views of the receiver in evening time are shown in Figure 82. It was monitored that the intensity of the temperature at the bottom and top views were reduced compared to the afternoon thermal images in Figure 82. But, due to the heat storage in PCM tubes, the temperature intensity of evening thermal images was still maintained at 95.6°C and 72.1°C as shown in Figure 82 bottom and top view images respectively.

The temperature intensity pattern of the full system in morning and evening was shown in Figure 83. It was shown that the receiver pot has the high temperature intensity pattern compared to the concentrator and the surroundings of the system. The temperature absorbing and holding capability of the receiver in the morning and evening was clearly illustrated with strong temperature pattern at the receiver pot position.

After the sun shine hours experiment period, the receiver was placed inside the insulation box. Thermal image of the receiver inside the insulation box is shown in Figure 84. (a). This figure illustrates the storage capability of the receiver by observing the temperature pattern inside the insulation box. The maximum temperature of the receiver in Figure 84. (a) is 78.4°C . The safety personnel operation of the complete system is shown in Figure 84. (b). It was observed that the system is safe to operate in outdoor conditions due to the negligible effect of temperature on the person even while the temperature of receiver is at 161.5°C .

The 3D thermal images of the receiver and complete system are shown in appendix G.

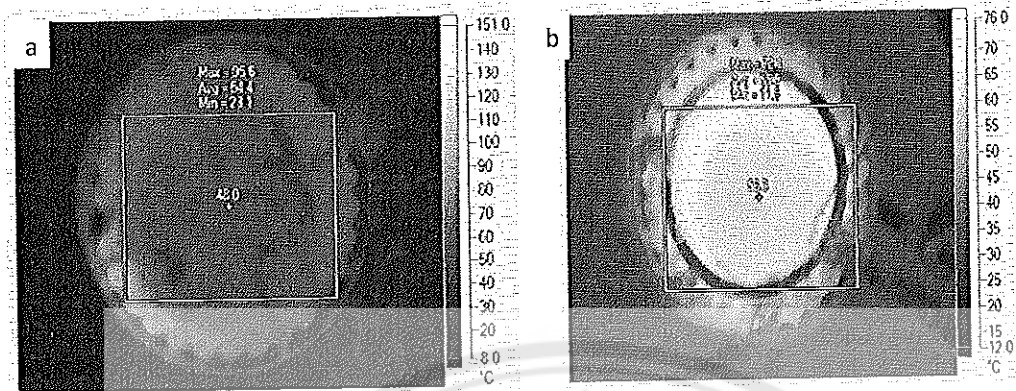


Figure 82 Thermal image of the receiver in the evening (a) bottom view
(b) top view

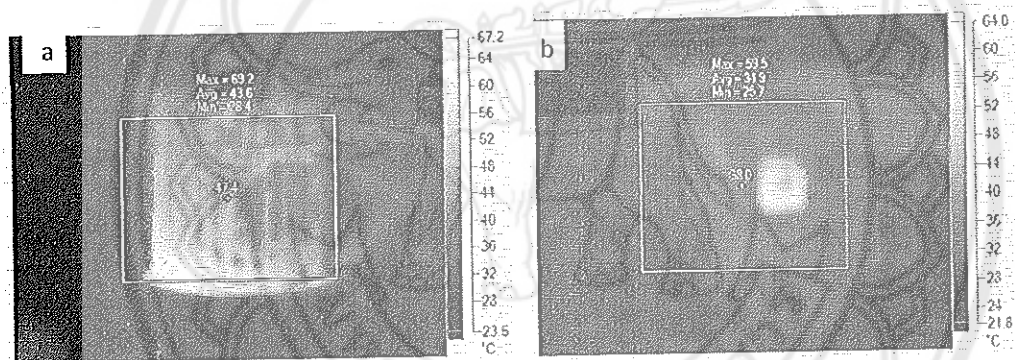


Figure 83 Thermal image of (a) receiver inside insulation box (b) total system

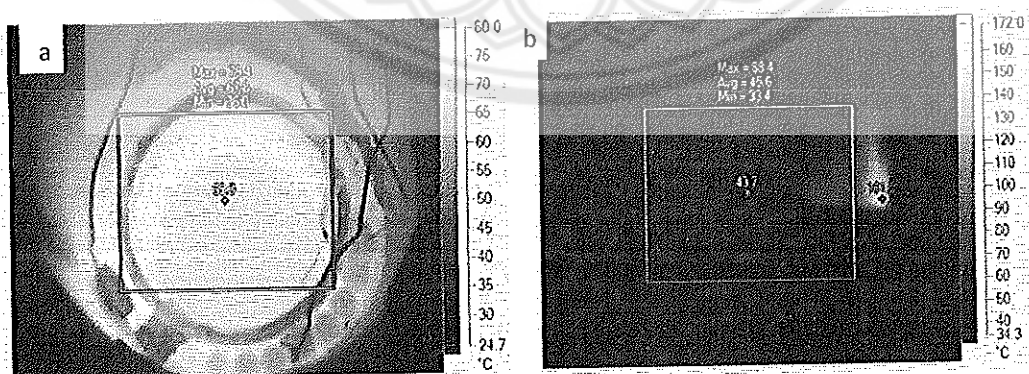


Figure 84 Thermal image of (a) receiver inside insulation box
(b) safety operation

Economic and emission analysis

Economic analysis of the developed system is calculated by some assumptions in the usage of the solar cooker. Solar cooker is used 20 days in a month where 6 useful sunshine hours per day can be used to cook food. The price of different components used in the project were mentioned in Table 15. The calculation of economic analysis was performed as follows by considering the assumption mentioned in Chapter III.

Table 15 Price details of different components

Component	Material	Cost (\$)
Glass/Mirror film	Refleech tech 3M mirror	84.78
Mechanical structure	Aluminum	63.30
Receiver stand	Aluminum	63.30
Receiver pot	Stainless steel	189.93
PCM	Mg(NO ₃) ₂ ·6H ₂ O	101.30
HTF	Palm oil	1.58
Total		501.84

Economic analysis calculation:

Capitall cost of the system, $C_T = 501.84$ \$

Capitall cost of the system for life time includes the intial capitall cost and the PCM cost for the remaining years.

Complete Capitall cost of the system throughout the life time of the project is denoted as C_T .

$$C_T = 501.84 + (9 \times 101.30)$$

$$C_T = 1413.54 \text{ \$}$$

Mass of LPG used per month, $M = 20$ kg

Price of LPG in Thailand = $0.71 \text{ \$ / kg} = 0.71 \times 20 = 14.2 \text{ \$ / 20 kg}$

Price of LPG in India, $P_m = 0.79 \text{ \$ / kg} = 0.79 \times 20 = 15.8 \text{ \$ / 20 kg}$

Project life time, $N = 10$ years

Discount rate per year, $d = 5\%$

Maintenance and repair cost, $\alpha = 10\%$

To calculate Capital Recovery Factor CRF, the values of d , N were substituted in equation (55).

Capital recovery factor, $CRF = 5$

After calculating CRF, Net Present Value NPV of the system was calculated by substituting CRF and C_T values in equation (54).

Net Present Value, $NPV = 282.36 \$$

The developed solar cooker can be used in nine months per year because three months in the year was considered as monsoon season. In monsoon season the solar irradiation is less compared to the other seasons. In a month, it was assumed that solar cooker can be used for 20 days and the useful sunshine hours per day are considered as 6 hours/day.

Total number of hours in month $= 30 \times 24 = 720$ hours

Total number of hours the solar cooker can be used $= 20 \times 6 = 120$ hours.

The fraction of solar cooker can be used per month, $P_r = 720 / 120 = 0.16$

The price of LPG saved in a month, $P_m = 0.16 \times 20 \times 14.2 = 45.44 \$$ in Thailand

The price of LPG saved in an year, $P_y = 45.44 \times 9 = 408.96 \$$ in Thailand

The price of LPG saved in a day, $P_d = 45.44 / 20 = 2.27 \$$ in Thailand

The different statistical values for economic analysis for India are shown in Table 16.

Number of meals can be cooked using solar cooker were calculated by using equation (56).

Number of meals cooked in year, $n_m = 501.84(10 + 5) / 2.52$

$n_m = 3316$ in Thailand

Payback Period of developed PCM solar cooker was calculated by substituting C_i and P_y values in equation (59).

Payback Period, $PP = 501.84 / 408.96$

$PP = 1.22$ years in Thailand

Table 16 Economic analysis parameters

Country	Price of LPG (\$/kg)	C ₀ (\$)	P _y (\$)	CRF	n _m	PP (Years)
Thailand	0.71	501.84	408.96	5	3316	1.22
India	0.79	501.84	455.04	5	2987	1.10

The reduced amount of CO₂ emission is calculated using the expression mentioned in chapter 3. One kg of LPG after complete combustion produces 3.02 kg of CO₂. By using the developed solar cooker 0.16 % in the month instead of LPG as cooking fuel. The reduced amount of CO₂ mission per year by using the developed PCM solar cooker is about 725 kg weight equivalent of CO₂.

CHAPTER V

CONCLUSION AND RECOMMENDATION

The present dissertation development of $\text{Mg}(\text{NO}_3)_2 \cdot 6\text{H}_2\text{O}$ phase change material based solar thermal energy storage system for community solar cooking application was designed and developed. The performance analysis of the system is also conducted to obtain the experimental results of the system which are mentioned in Chapter 4. The important conclusions of the dissertation are mentioned as follows

Conclusion

1. The design of solar cooking system with solar concentrator and receiver or cooking pot. A parabolic antenna dish of 1.49 m diameter and 0.26 m height and 0.52 m of focal length was developed as a solar concentrator by fixing the pieces high reflective mirror on the surface. A hollow concentric cylindrical shape stainless steel receiver is designed for the cooking purpose and which is placed at the focal point of the concentrator. 28 stainless steel cylindrical tubes are welded on the surface of the receiver to fill $\text{Mg}(\text{NO}_3)_2 \cdot 6\text{H}_2\text{O}$ inside the tubes to use as the storage system.

2. $\text{Mg}(\text{NO}_3)_2 \cdot 6\text{H}_2\text{O}$ is selected as PCM for this dissertation from different criteria of the selection of PCM. 1000 thermal cycles were performed to analyze the performance of $\text{Mg}(\text{NO}_3)_2 \cdot 6\text{H}_2\text{O}$. In 1000 thermal cycles the weight and time taken for solidification are more in solidification cycle than that of melting cycle. After 1000 thermal cycles, from the DSC analysis, variations in melting point temperature and latent heat of fusion are analyzed. The $\text{Mg}(\text{NO}_3)_2 \cdot 6\text{H}_2\text{O}$ sample has 78.71 % of latent heat of fusion from the initial sample after 1000 thermal cycles. From the corrosion analysis of $\text{Mg}(\text{NO}_3)_2 \cdot 6\text{H}_2\text{O}$ on container material and SEM analysis it was concluded that the stainless steel has the less corrosive effect due to $\text{Mg}(\text{NO}_3)_2 \cdot 6\text{H}_2\text{O}$ and that material is selected to design the PCM tubes and receiver of the solar cooking system.

3. From the results of performance analysis, the parabolic solar cooker parameters heat loss factor $F'U_L$, optical efficiency factor $F'\eta_0$, cooking power P and the standard cooking power P_s were calculated for three sets of collected data. 0.513 and

0.22 are the optical efficiency factors of the solar cooker with all the layers the receiver is filled with water and receiver layers are filled with the corresponding materials respectively. 210.76 W, 165.10 W are the cooking powers of the solar cooker with load conditions without and with receiver is placed in the insulation box respectively. The optical efficiency factor of the solar cooker with PCM receiver is 2 times more than that receiver without PCM.

4. From the heat transfer analysis and thermal energy calculations of the receiver with corresponding materials inside the layers of the receiver are performed. From the analysis it can be concluded that, the three stage heat storage capacity of the selected PCM for this proposed solar cooking system helps to sustain the more amount of heat inside the cooking stuff layer. The efficiency of the solar cooker is more in the case of PCM incorporation which is about 40%.

5. From the results of economic analysis of the solar cooker compared with LPG cooking system. The saved money per month by using the developed solar cooker over LPG cooking system is 455.04 \$, 408.96 \$ in India and Thailand respectively. The payback period of the solar cooking system is 1.10 years and 1.22 years in India and Thailand respectively. From the emission analysis it was concluded that The reduced amount of CO₂ emission per year by using the developed PCM solar cooker is about 725 kg.

From the above mentioned conclusions different parameters, it can be concluded that the designed $\text{Mg}(\text{NO}_3)_2 \cdot 6\text{H}_2\text{O}$ phase change material based solar thermal energy storage system is a promising solution for cooking applications in rural areas of developing countries to reduce carbon foot prints and improves the socio- economic situations of rural communities.

Recommendations

1. Since the developed solar cooking system is designed for the rural communities based on their economic conditions, manual tracking is incorporated in the cooking system. The same solar cooking system can also be used in industrial purposes by scaling up both storage and solar cooking system with automatic tracking system.

2. A common PCM tube to which connects all the PCM tubes in the design of receiver to get more uniform melting of the PCM throughout the sunshine hours is recommended while scaling up the system for industrial purposes.





REFERENCES

REFERENCES

1. Olivier Lavagne, Adrian. International Energy Agency, IRENA. Renewable Energy Capacity Statistics 2015. UAE. 2015; 44(2): 978-92.
2. Venkataraman C, Sagar AD, Habib G, Lam N, Smith KR. The Indian National Initiative for Advanced Biomass Cookstoves: The benefits of clean combustion. Energy for Sustainable Development. 2010;14(2):63-72.
3. Das S.K. Energy Sources of Indian Households for Cooking and Lighting. New Delhi: National Sample Survey Office, Ministry of Statistics and Programme Implementation, Government of India; 2012 Sep. Report No.: 542 (66/1.0/4).
4. International Energy Agency. Energy for cooking in developing countries. In: World Energy Outlook 2006. Paris: n.p. 2006. p. 419-445.
5. World Health Organization [Internet]. Geneva: The Association; c2018. Available from: <http://www.who.int/news-room/fact-sheets/detail/household-air-pollution-and-health>
6. Garg HP, Prakash J. Solar energy : fundamentals and applications. New Delhi: Tata McGraw-Hill; 2000.
7. Tiwari G, Suneja s. Solar Thermal Engineering Systems. New Delhi: Narosa Publishing House; 1997.
8. Boonsu R. Performance of thermal energy prototype[dissertation]. Phitsanulok: Naresuan University; 2015.
9. Lucas B, Hyman PE, Leed AP. Sustainable thermal storage systems planning, design, and operations. 1st ed. New York: McGraw - Hill; 2011.
10. Kant K, Shukla A, Sharma A, Kumar A, Jain A. Thermal energy storage based solar drying systems: A review. Innovative Food Science & Emerging Technologies. 2016;34:86-99.
11. Dinçer I, Rosen M. Thermal energy storage : systems and applications. 2nd ed. Chichester: Wiley; 2011.
12. Cabeza, Harald. solid liquid phase change materials. In: Dieter M, Franz M, editors. Heat and cold storage with PCM: An up to date introduction into basics and applications. Berlin: Springer; 2008.

13. Raam Dheep G, Sreekumar A. Influence of nanomaterials on properties of latent heat solar thermal energy storage materials – A review. *Energy Conversion and Management*. 2014;83:133-48.
14. Silva T, Vicente R, Rodrigues F. Literature review on the use of phase change materials in glazing and shading solutions. *Renewable and Sustainable Energy Reviews*. 2016;53:515-35.
15. Sharon H, Reddy KS. A review of solar energy driven desalination technologies. *Renewable and Sustainable Energy Reviews*. 2015;41:1080-118.
16. Seppala A. Load research and load estimation in electricity distribution [dissertation]. Espoo, Finland: Helsinki University of Technology; 1996.
17. Barlev D, Vidu R, Stroeve P. Innovation in concentrated solar power. *Solar Energy Materials and Solar Cells*. 2011;95(10):2703-25.
18. Agency IE. Technology road map of concentrating solar power. 2010; p. 49.
19. Kenisarin M, Mahkamov K. Solar energy storage using phase change materials. *Renewable and Sustainable Energy Reviews*. 2007;11(9):1913-65.
20. Lecuona A, Nogueira J-I, Ventas R, Rodríguez-Hidalgo M-d-C, Legrand M. Solar cooker of the portable parabolic type incorporating heat storage based on PCM. *Applied Energy*. 2013;111:1136-46.
21. Muthusivagami RM, Velraj R, Sethumadhavan R. Solar cookers with and without thermal storage—A review. *Renewable and Sustainable Energy Reviews*. 2010;14(2):691-701.
22. John G, König-Haagen A, King'onde CK, Brüggemann D, Nkhonjera L. Galactitol as phase change material for latent heat storage of solar cookers: Investigating thermal behavior in bulk cycling. *Solar Energy*. 2015;119:415-21.
23. Sharma RK, Ganesan P, Tyagi VV, Metselaar HSC, Sandaran SC. Developments in organic solid–liquid phase change materials and their applications in thermal energy storage. *Energy Conversion and Management*. 2015;95:193-228.
24. Sharma SD, Buddhi D, Sawhney RL, Sharma A. Design, development and performance evaluation of a latent heat storage unit for evening cooking in a solar cooker. *Energy Conversion and Management*. 2000;41(14):1497-508.

25. Buddhi D, Sharma SD, Sharma A. Thermal performance evaluation of a latent heat storage unit for late evening cooking in a solar cooker having three reflectors. *Energy Conversion and Management*. 2003;44(6):809-17.
26. Sharma SD, Iwata T, Kitano H, Sagara K. Thermal performance of a solar cooker based on an evacuated tube solar collector with a PCM storage unit. *Solar Energy*. 2005;78(3):416-26.
27. El-Sebaï AA, Al-Heniti S, Al-Agel F, Al-Ghamdi AA, Al-Marzouki F. One thousand thermal cycles of magnesium chloride hexahydrate as a promising PCM for indoor solar cooking. *Energy Conversion and Management*. 2011;52(4):1771-7.
28. Tyagi VV, Buddhi D. Thermal cycle testing of calcium chloride hexahydrate as a possible PCM for latent heat storage. *Solar Energy Materials and Solar Cells*. 2008;92(8):891-9.
29. Sharma A, Sharma SD, Buddhi D. Accelerated thermal cycle test of acetamide, stearic acid and paraffin wax for solar thermal latent heat storage applications. *Energy Conversion and Management*. 2002;43(14):1923-30.
30. Otte PP. A (new) cultural turn toward solar cooking—Evidence from six case studies across India and Burkina Faso. *Energy Research & Social Science*. 2014;2:49-58.
31. Dheep G.R, Sreekumar A. Phase Change Materials—A Sustainable Way of Solar Thermal Energy Storage. In: Sharma A, Kar S. editors. *Energy sustainability Through Green Energy*. New Delhi: Springer; 2015. p. 217-244.
32. Merlin K, Delaunay D, Soto J, Traonvouez L. Heat transfer enhancement in latent heat thermal storage systems: Comparative study of different solutions and thermal contact investigation between the exchanger and the PCM. *Applied Energy*. 2016;166:107-16.
33. Kumar S, Kandpal TC, Mullick SC. Experimental test procedures for determination of the optical efficiency factor of a paraboloid concentrator solar cooker. *Renewable Energy*. 1996;7(2):145-51.
34. Sivasamy L, Muthusamy E. Experimental studies on solar parabolic dish cooker with porous medium. *Applied Solar Energy*. 2012 Nov 16; 48(3):169-174.
35. Aidan J. Performance Evaluation of a Parabolic Solar Dish Cooker in Yola, Nigeria. *IOSR Journal of Applied Physics*. 2014; 6(5):46-50 .

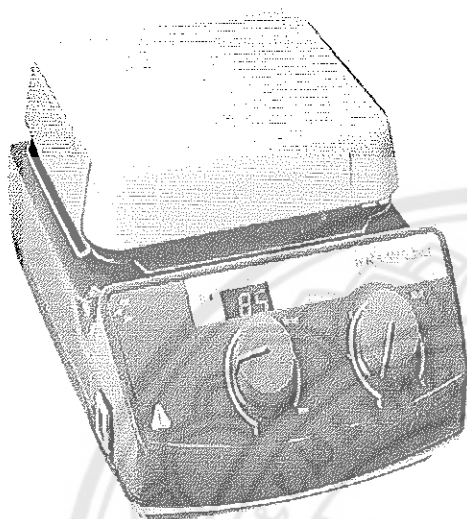
36. Kuravi S, Trahan J, Goswami DY, Rahman MM, Stefanakos EK. Thermal energy storage technologies and systems for concentrating solar power plants. *Progress in Energy and Combustion Science*. 2013;39(4):285-319.
37. Ferrer G, Solé A, Barreneche C, Martorell I, Cabeza LF. Review on the methodology used in thermal stability characterization of phase change materials. *Renewable and Sustainable Energy Reviews*. 2015;50:665-85.
38. METTLER TOLEDO. Interpreting DSC curves, Information for users of METTLER TOLEDO thermal analysis systems. UserCom. 2000; 11(1): 1-27.
39. Duffie JA, Beckman WA. *Solar Engineering of Thermal Processes*. 4th ed. USA: Wiley; 2006.
40. Kalogirou SA. *Solar Energy Engineering: Processes and Systems*. 2nd ed. USA: Elsevier Academic Press; 2013.
41. Stine WB, Geyer M, editors. *Power from the sun.net* [Internet]. Wiley; 2001. Available from: <http://www.powerfromthesun.net/Book/chapter08/chapter08.html>
42. Kedar SA, Sonawale P, Valve P, Khujat P, Talekar P. Thermal Analysis of Parabolic Solar Cooker with Back Reflection. *Materials Today: Proceedings*. 2017;4(8):8035-9.
43. Harmim A, Merzouk M, Boukar M, Amar M. Mathematical modeling of a box-type solar cooker employing an asymmetric compound parabolic concentrator. *Solar Energy*. 2012;86(6):1673-82.
44. Hafez AZ, Soliman A, El-Metwally KA, Ismail IM. Solar parabolic dish Stirling engine system design, simulation, and thermal analysis. *Energy Conversion and Management*. 2016;126:60-75.
45. J A. Performance evaluation of a parabolic solar dish cooker in yola, Nigeria. *IOSR Journal of Applied Physics*. 2014;6(5):46-50.
46. Mawire A, McPherson M, van den Heetkamp RRJ. Simulated energy and exergy analyses of the charging of an oil-pebble bed thermal energy storage system for a solar cooker. *Solar Energy Materials and Solar Cells*. 2008;92(12):1668-76.
47. Panwar NL, Kothari S, Kaushik SC. Techno-economic evaluation of masonry type animal feed solar cooker in rural areas of an Indian state Rajasthan. *Energy Policy*. 2013;52:583-6.

48. Chauhan A, Saini RP. Techno-economic feasibility study on Integrated Renewable Energy System for an isolated community of India. *Renewable and Sustainable Energy Reviews*. 2016;59:388-405.
49. Herez A, Ramadan M, Khaled M. Review on solar cooker systems: Economic and environmental study for different Lebanese scenarios. *Renewable and Sustainable Energy Reviews*. 2018;81:421-32.
50. Thai PBS. LPG price goes up Tuesday by 0.67 baht/kg [press release]. Bangkok. 2017 Feb 06; Business. A:1 (col. 2). Available from: <http://englishnews.thaipbs.or.th/lpg-price-goes-tuesday-0-67-bahtkg>
51. NDTV. Latest LPG Cylinder Price: Subsidised, Non-Subsidised Rates In Top Cities [Press release]. New Delhi, India. 2018 Jan 02; A:1 (col. 1). Available from: <https://www.ndtv.com/business/latest-lpg-cylinder-price-subsidised-non-subsidised-rates-in-top-cities-1794399>

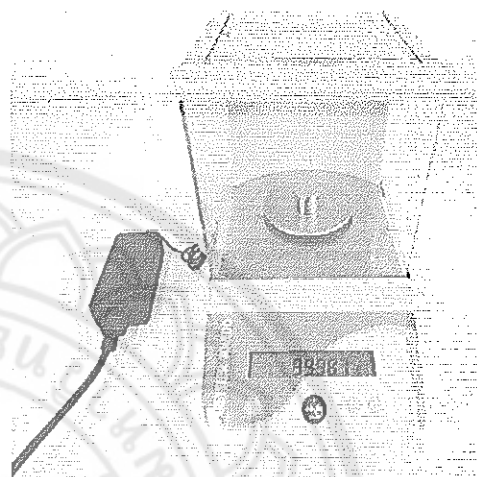
APPENDIX



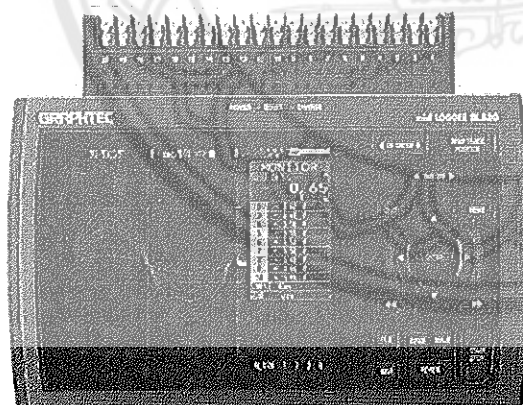
APPENDIX A INSTRUMENTS



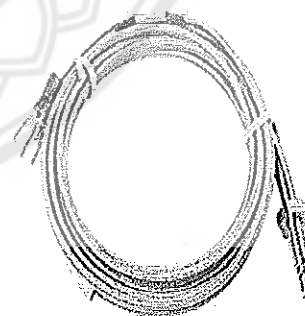
Hot plate (50 °C to 500 °C ,230 V, 1000 W)
(METTLER TOLEDO)



Sensitive balance
(0 g to 310 g with 0.001 g increment)

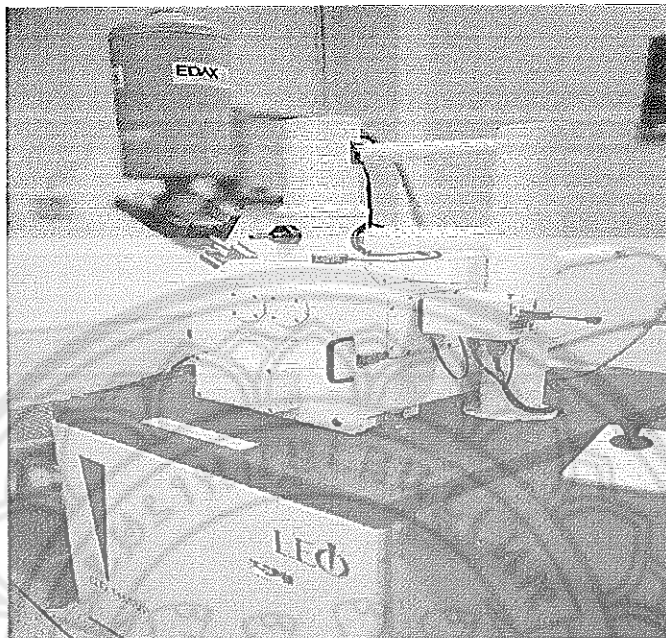


Data recorder (GRAPHTEC midi LOGGER,
GL 820-UM-851)



Thermocouple type K
(-270°C to 1260 °C)

Figure 85 Instruments

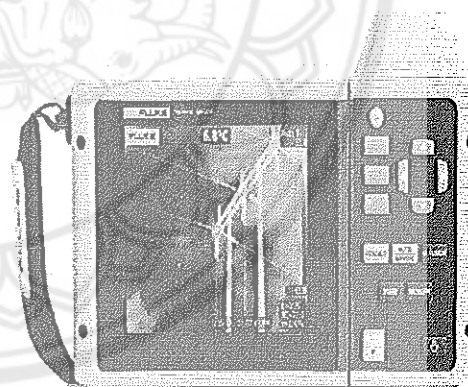


Scanning Electron Microscope (LEO, 1455 VP, England, 20 kV)



Differential Scanning Calorimeter

(METTLER TOLEDO DSC 1,
Switzerland, -150 °C to 700 °C, 400 W)



Thermal imager

(Fluke TiX560 9Hz, -20 °C to 1200 °C)

Figure 86 Instruments

APPENDIX B SURFACE AREA CALCULATIONS FOR THE RECEIVER OR COOKING POT

The receiver or the cooking pot in this solar cooker is made up of stainless steel and in the shape of hollow concentric cylinder.

Total surface area of the receiver = lateral area + base area

$$= 2\pi rh + 2\pi r^2$$

Lateral area of cooking stuff layer with radius 9 cm and height 25 cm = $2*\pi*9*25$
= 1413.71 cm²

Lateral area of HTF layer with radius 10 cm and height 25 cm = $2*\pi*10*25$
= 1570.79 cm²

If third layer which is PCM layer also designed as a concentric layer as HTF layer with radius 12.5 cm and height 23 cm = $2*\pi*12.5*23$
= 1806.41 cm²

Instead of a single concentric layer, a small cylindrical tube of radius 1.25 cm with a height of 23 cm is placed on the HTF layer.

Lateral area of the PCM tube = $2*\pi*1.25*23$
= 180.641 cm²

The individual PCM tube is welded on the surface of two layer cooking pot, but half of the lateral area is in direct contact with the Two layer concentric cooking pot. 28 PCM tubes are welded on the surface of HTF layer.

So, the total lateral area of the all PCM tubes = $(180.641*28)/2$
= 2528.96 cm²

Increase in surface area of PCM tubes instead of single concentric PCM layer is the difference of lateral area of 28 PCM tube and the lateral area of single concentric PCM tube = $2528.96 - 1806.41$
= 722.55 cm²

Therefore, 722.55 cm² of surface area is increased with the design of individual PCM tubes.

APPENDIX C COMPLETE EXPERIMENTAL PROCEDURE OF LOAD TEST FOR THE PCM SOLAR COOKER

Purpose: To determine the performance parameters of the PCM solar cooker for the load test.

Required equipment: PCM solar cooker, thermocouples, data recorder, measuring beaker, aluminum tape, insulation box.

Test procedure:

1. The receiver or the cooking pot PCM tubes are filled with $\text{Mg}(\text{NO}_3)_2 \cdot 6\text{H}_2\text{O}$ as PCM and palm oil as heat transfer fluid in PCM tubes and HTF layer respectively.
2. Place the receiver or the cooking pot in the receiver stand and place both solar concentrator and the receiver stand in outdoors.
3. Measure the two liters of water with measuring beaker and place inside the cooking stuff layer.
4. Place the thermocouples inside the cooking stuff layer, HTF layer, PCM tubes, bottom of the cooking pot, on the surface of the solar concentrator and in the surrounding environment to measure ambient temperature with the help of aluminum tape.
5. Place the thermocouples in PCM tubes uniformly in the 28 PCM tubes. Each thermocouple is placed for every 4 PCM tubes. Total 7 thermocouples are used to measure the PCM temperature in PCM tubes.
6. All the thermocouples are connected to data recorder to record the temperature in all the places where the thermocouples are placed.
7. After arranging all the thermocouples, adjust the focus for the cooking pot by adjusting the solar concentrator according to the position of the sun.
8. Switch on the data recorder and adjust the channels or ports in the data recorder. After that press "START" in data recorder to record the temperature in the memory of the data recorder.
9. For every 5 minutes temperature is recorded and for every 20 minutes of regular interval the solar cooking system is tracked manually according to the position of the sun.

10. After sunshine hours, the receiver or cooking pot is removed from the stand and placed inside the insulation box. Again record the temperature of the PCM tubes, HTF layer, water inside the cooking pot till next day morning.

11. All the temperature readings are tabulated and the performance parameters are calculated with the help of related mathematical expressions.

Mathematical expressions:

$$1. \text{ Combined heat capacity } (MC)_r = (MC)_{l1} + (MC)_{l2} + (MC)_{l3} + (MC)_{pot}$$

$$2. \text{ Heat loss factor } F'U_L = \frac{(MC)_r}{\tau_0 A_r}$$

$$3. \text{ Optical efficiency factor } F'\eta_0 = \frac{F'U_L}{C} \left[\frac{\left(\frac{T_{wf} - T_a}{I} \right) - \left(\frac{T_{wi} - T_a}{I} \right) e^{\frac{-\tau}{\tau_0}}}{1 - e^{\frac{-\tau}{\tau_0}}} \right]$$

$$4. \text{ Cooking power } P = M_w C_w \frac{(T_{wf} - T_{wa})}{\tau}$$

$$5. \text{ Standardized cooking power } P_s = M_w C_w \frac{(T_{wf} - T_{wa}) \times 700}{\tau I}$$

Graphs:

1. Temperature profile of all the layers, focal point, ambient, surface of the solar concentrator throughout the day with solar radiation.
2. Temperature profile of PCM tubes throughout the day.
3. Heating and cooling curves

The sample temperature data required for the above two graphs is shown in Table 17 and Table 18. The related graphs and statistical values of performance parameters are shown in Table 12.

Table 17 Temperature profile of the receiver

Local time (hh:mm)	T _i (°C)	T _{bir} (°C)	T _{PCM} (°C)	T _r (°C)	T _p (°C)	T _a (°C)	T _l (°C)	I (W/m ²)
10:12	26	27.4	28.7	29.7	30.8	25.7	29	329.73
10:17	26.7	28.8	30.6	31.1	31.9	26.9	29.8	375.90
10:22	27.4	30.1	32.4	31.6	32.8	27	30.5	411.62
10:27	27.9	31.9	33.8	37.5	33.8	26.6	31.7	498.13
10:32	29	35	35	42.4	35.4	27.1	33	862.62
10:37	30.5	40.3	36.5	51.3	38.5	27.4	35.8	706.40
10:42	33.1	43	38	47.9	37.3	26.2	38.5	561.07
10:47	35.2	42.7	39.5	48.5	35.9	28.6	40	596.40
10:52	36.9	43.7	40.6	47.6	35.6	28.5	41	411.94
10:57	38.4	43.4	41.4	44.2	34.2	28	41.4	399.46
11:02	39.3	43.9	42.2	44.4	34.7	28.3	41.8	491.19
11:07	40.1	43.7	43.1	44.8	35.2	28.5	42.1	531.49
11:12	40.8	44.5	43.7	44.8	36.2	29	42.6	394.14
11:17	41.5	44.6	44.1	43.2	34.9	28.7	42.4	371.47
11:22	41.9	44.2	44.5	42.3	34.2	28.8	42	379.93
11:27	42.2	43.8	44.6	41.5	33.6	28.7	41.7	407.69
11:32	42.5	43.7	44.3	40.6	33.1	28.8	41.1	478.14
11:37	42.3	43.3	44.2	40.9	33.5	28.3	40.8	479.34
11:42	42.3	43.4	44	42	34.5	27.8	41.2	1040.31
11:47	42.9	46.1	45.7	79.4	36.9	28.5	42.3	1020.07
11:52	45.1	49.4	47.7	72.7	37.8	28.3	44.9	678.56
11:57	47.3	52.3	49.1	65	37.1	28.3	46.3	883.52
12:02	48.8	53.2	49.5	66.4	35.5	28.7	46.3	779.91
12:07	50.7	54.5	50.3	67.8	35.5	28.2	46.9	790.03
12:12	52.1	56	51	65.9	34.8	26.9	47.5	779.28
12:17	53.8	57.8	52.2	73.3	37	27.8	49.2	763.86
12:22	55.5	60.6	53.2	74.2	37.2	27	49.9	765.91
12:27	56.9	62	53.2	72.1	37.2	27.5	49.7	771.01
12:32	58.4	61.8	54.5	76.6	39.1	26.3	51.7	767.76
12:37	59.7	64.1	54.8	79.4	39.8	28.5	53.2	771.31
12:42	60.9	65.8	55.7	83.5	39.2	28.4	54.6	773.64
12:47	62.3	67.2	56.4	90.8	39.5	27.9	55.8	758.48
12:52	63.9	68.6	57.1	84.6	39.1	27.9	56.8	746.02

Table 18 Temperature profile of PCM tubes

Local time hh:mm	T _a (°C)	T _{p1} (°C)	T _{p5} (°C)	T _{p9} (°C)	T _{p13} (°C)	T _{p17} (°C)	T _{p21} (°C)	T _{p25} (°C)	T _{p28} (°C)	I (W/m ²)
10:12	25.7	28.7	29.8	30.7	30.3	28.7	27.2	29.5	31.9	329.73
10:17	26.9	29.3	31.8	33.2	32.4	30.6	28.6	31.3	33.8	375.90
10:22	27	30.2	33.1	35.9	34.8	32.4	30	32.4	35.5	411.62
10:27	26.6	31	34.5	38.2	36.9	33.8	31.5	34	36.9	498.13
10:32	27.1	32.1	36.3	40.4	38.6	35	32.9	35.7	39.1	862.62
10:37	27.4	33.6	37.8	42.6	40.6	36.5	35	39.1	42	706.40
10:42	26.2	35.5	39.8	44.8	42.3	38	37.1	41.6	41.8	561.07
10:47	28.6	36.2	40.3	46.1	44	39.5	38.3	42.4	41.1	596.40
10:52	28.5	36.8	40.9	46.8	45	40.6	39.4	43.1	41.4	411.94
10:57	28	37.5	41.6	47.2	45.9	41.4	40.3	42.9	40.9	399.46
11:02	28.3	38	42.2	48	46.8	42.2	40.9	43.2	41.4	491.19
11:07	28.5	38.3	42.6	48.8	47.8	43.1	41.7	43.7	42	531.49
11:12	29	38.8	43.5	49.7	48.6	43.7	42.3	44.1	43.8	394.14
11:17	28.7	39.1	43.5	50	49.2	44.1	42.9	44.2	43.4	371.47
11:22	28.8	39.4	43.7	50	49.5	44.5	42.9	43.8	42.6	379.93
11:27	28.7	39.6	43.4	49.8	49.7	44.6	43.3	43.6	42.3	407.69
11:32	28.8	39.8	43.2	49.2	49.4	44.3	43.4	43.2	41.6	478.14
11:37	28.3	39.8	43	48.5	48.9	44.2	43.1	42.9	42	479.34
11:42	27.8	39.9	45.2	47.6	48.6	44	43.4	43.5	40.8	1040.31
11:47	28.5	40.3	48.6	48.8	50.1	45.7	44.4	44.4	44.1	1020.07
11:52	28.3	41.8	51.2	51.4	51.8	47.7	46	46.8	48.4	678.56
11:57	28.3	43.4	50.4	52.8	52.7	49.1	47.7	48.1	48.1	883.52
12:02	28.7	44.8	51.7	52.3	53.7	49.5	48.4	48.3	46.8	779.91
12:07	28.2	46.3	52.5	52.5	55.1	50.3	49.9	49.1	48.2	790.03
12:12	26.9	47.9	52.8	52.4	55.7	51	51.1	49.9	47.8	779.28
12:17	27.8	49.1	51.8	51.8	55.5	52.2	52.2	50.7	48.7	763.86
12:22	27	50.1	51.4	51.1	55.4	53.2	53.1	51.4	47.1	765.91
12:27	27.5	51.2	51.8	51.1	55.5	53.2	53.7	51.4	48	771.01
12:32	26.3	52.3	52	52	57.2	54.5	54.4	52.2	51.9	767.76
12:37	28.5	53.5	52.9	52.7	57.8	54.8	54.7	52.8	51.3	771.31
12:42	28.4	54.6	53	52.5	58.1	55.7	55.4	54	51.3	773.64
12:47	27.9	55.7	53.1	52.5	58.4	56.4	55.8	54.7	52.6	758.48
12:52	27.9	56.7	52.8	52.7	58.9	57.1	56.2	55.7	52	746.02

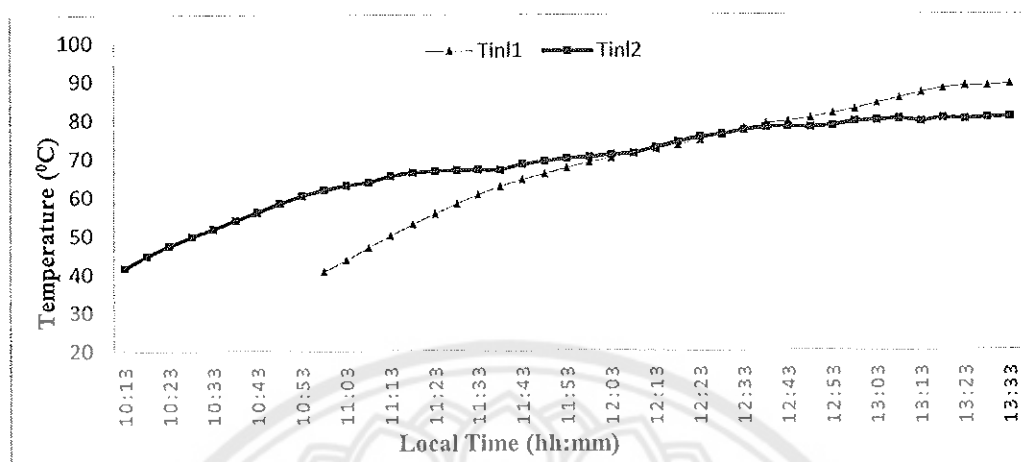


Figure 87 Comparison of set 3 no load heating curves with and without insulation box

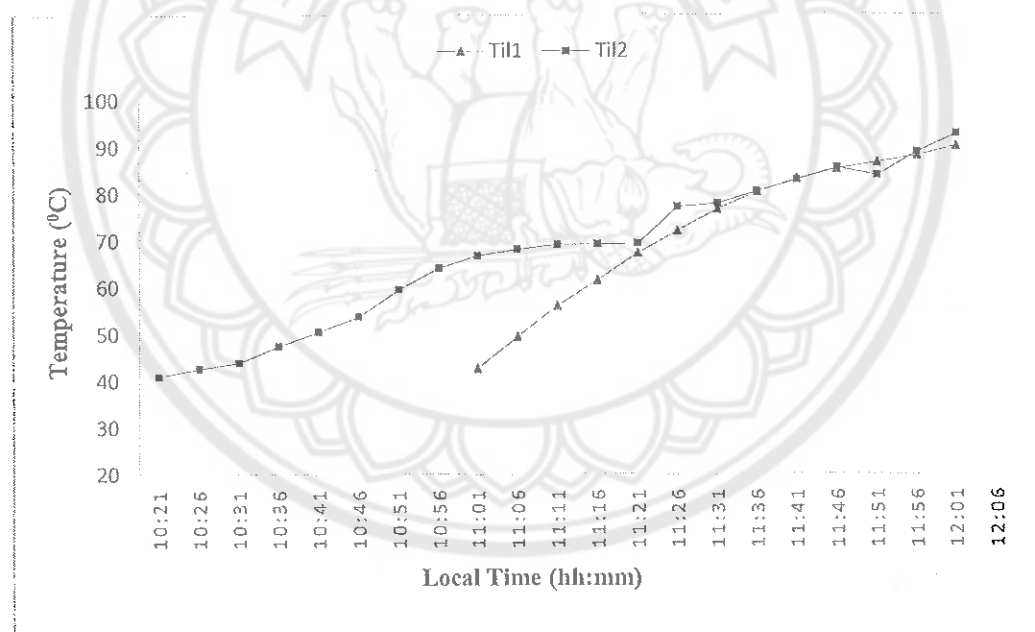


Figure 88 Comparison of set 3 load heating curves with and without insulation box

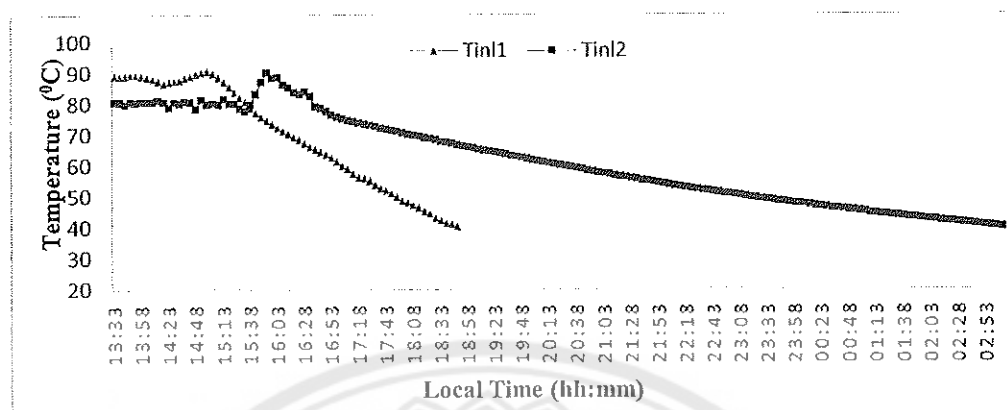


Figure 89 Comparison of set 3 no load cooling curves with and without insulation

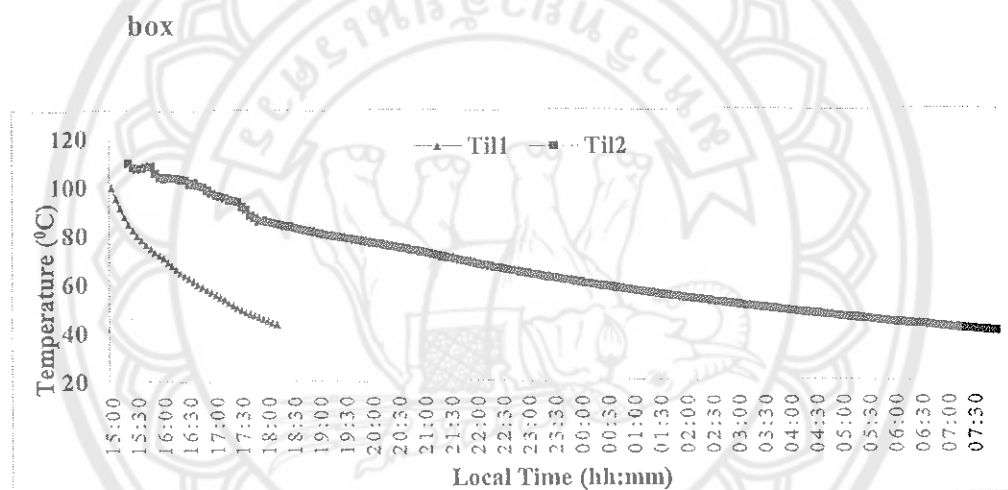


Figure 90 Comparison of set 3 load cooling curves with and without insulation

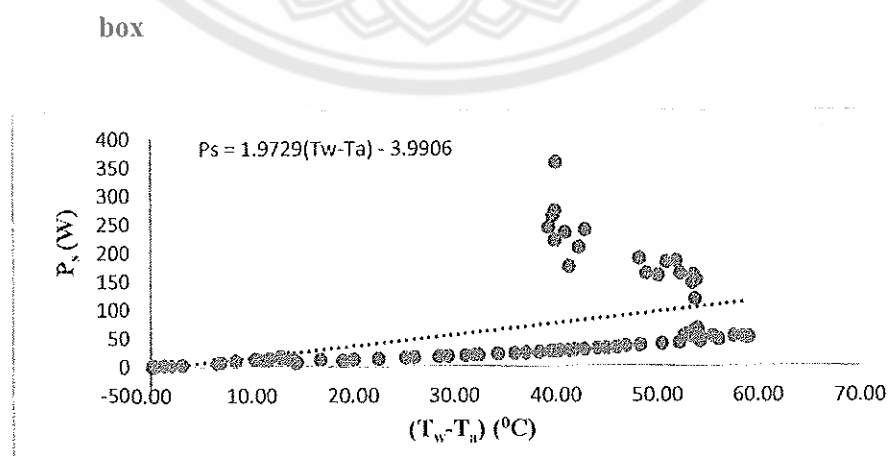


Figure 91 Slope curve for U_L calculation

APPENDIX D GENERAL ENERGY CALCULATIONS

Specific heat of water = 4.186 kJ/kg °C

Specific heat of ice = 2.06 kJ/kg °C

Specific heat of steam = 2.1 kJ/kg °C

Latent heat of fusion for ice = 334 kJ/kg

Latent heat of evaporation of water = 2256 kJ/kg

Energy required to raise the temperature of 1 litre of water from 24 °C to 100 °C

means to boil the water $Q = mC_p\Delta T$

$$= 1 * 4.186 * (100 - 24) = 318.136 \text{ kJ} = 0.088 \text{ kWh}$$

Energy required to evaporate one litre of water completely $Q_e = m * L = 1 * 2256$

$$= 2256 \text{ kJ} = 0.625 \text{ kWh}$$

These basic energy calculations for water boiling and evaporation are useful to compare the cooking power of the proposed PCM solar cooker.

APPENDIX E REAL TIME COOKING APPLICATION GRAPHS

Table 19 Specific heat capacity of different food materials

S.No	Food material	Specific heat capacity kJ/kg °C
1	Green bean	3.26
2	Red bean	2.13
3	Mung split bean	2.1
4	Chicken	3.22
5	Rice	2.146
6	Potato	3.43
7	Sweet Potato	3.14
8	Pasta	1.8
9	Daal/poridge	13.23
10	Egg	3.18
11	Vegetables	11.22

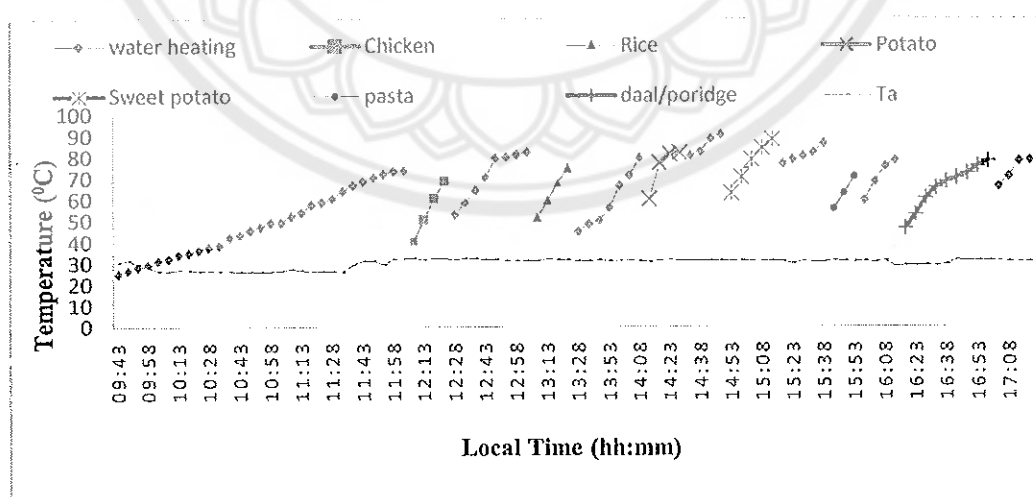


Figure 92 Temperature profile of day 4 boiling

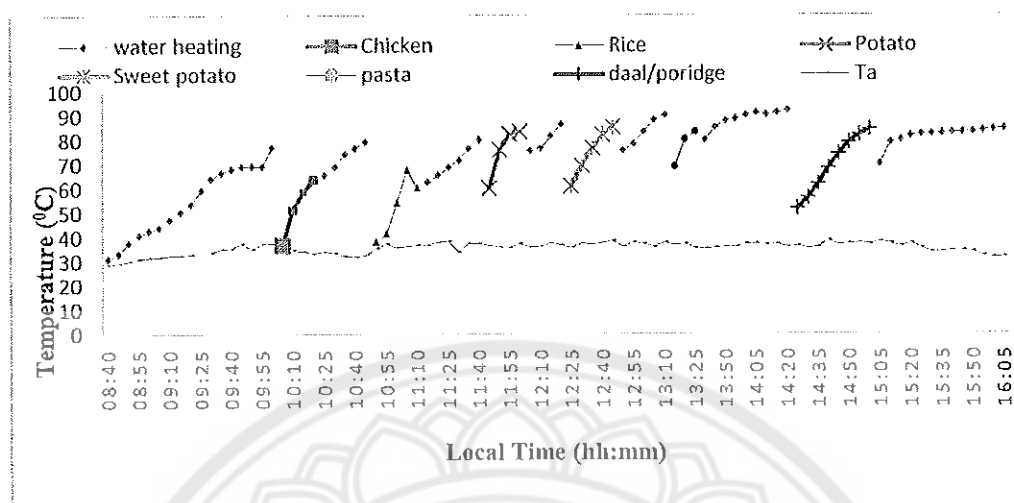


Figure 93 Temperature profile of day 5 boiling

APPENDIX F 3D GRAPHS FOR THERMAL IMAGES

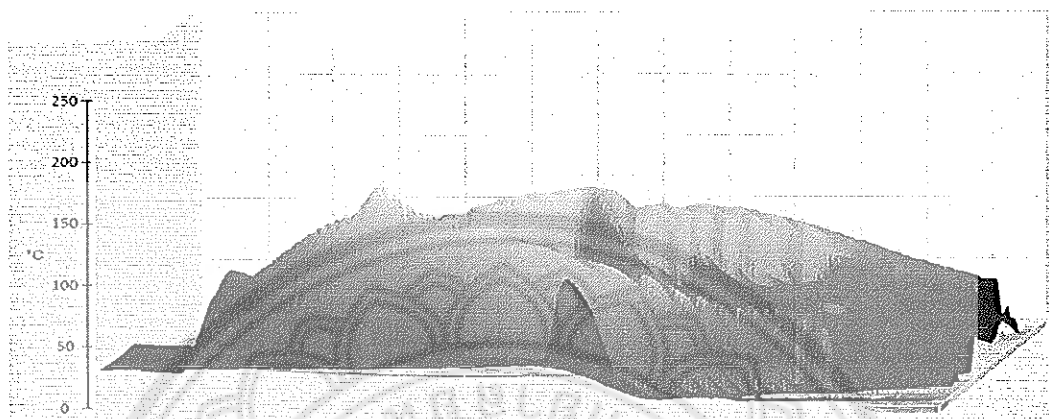


Figure 94 3D thermal image of the receiver bottom view



Figure 95 3D thermal image of the receiver top view

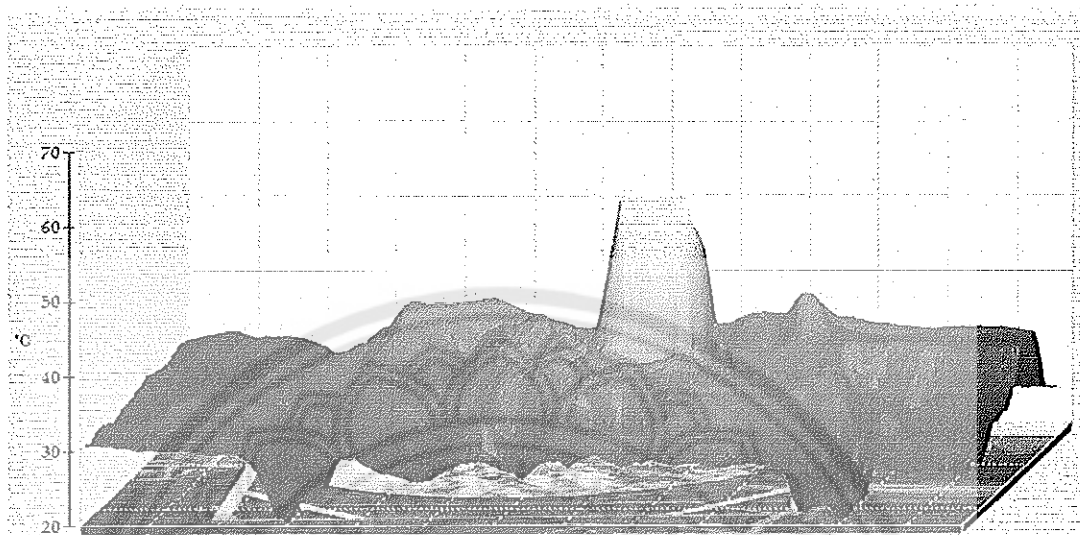


Figure 96 3D thermal image of the complete system

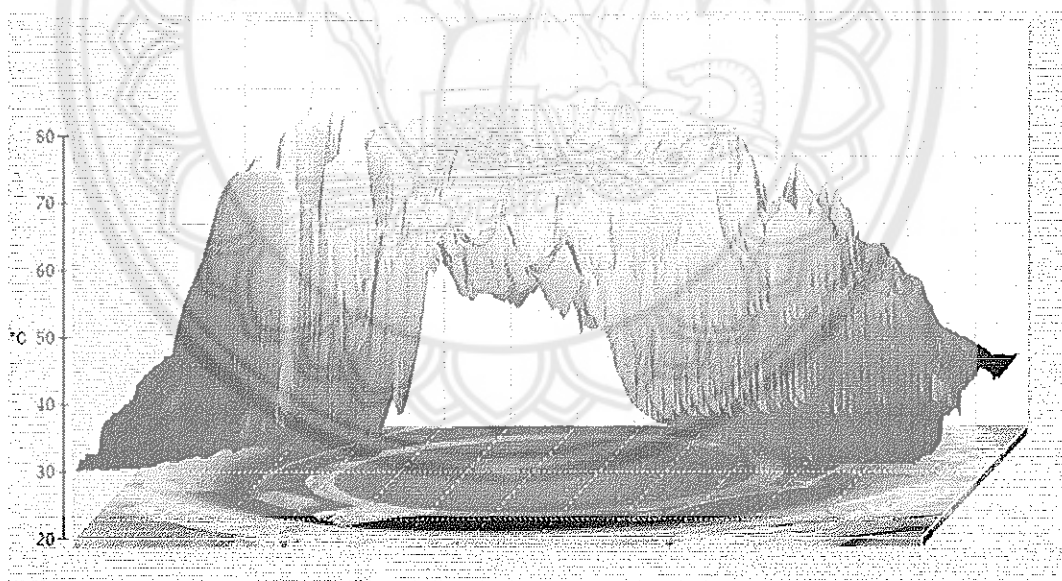


Figure 97 3D thermal image of the receiver inside the insulation box

APPENDIX G THE VARIATION IN WIND SPEED FOR NO LOAD AND LOAD TESTS

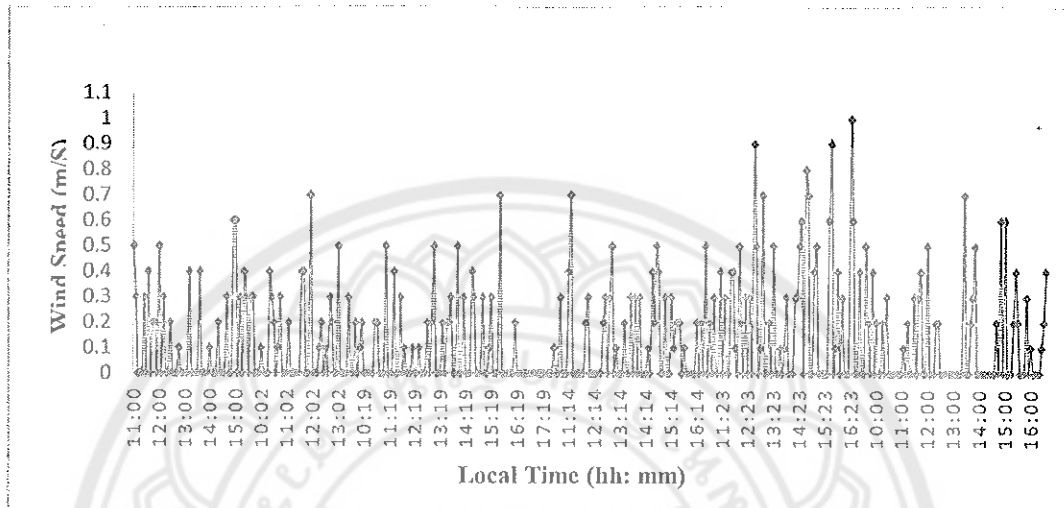


Figure 98 Variation in wind speed for continuous no-load test

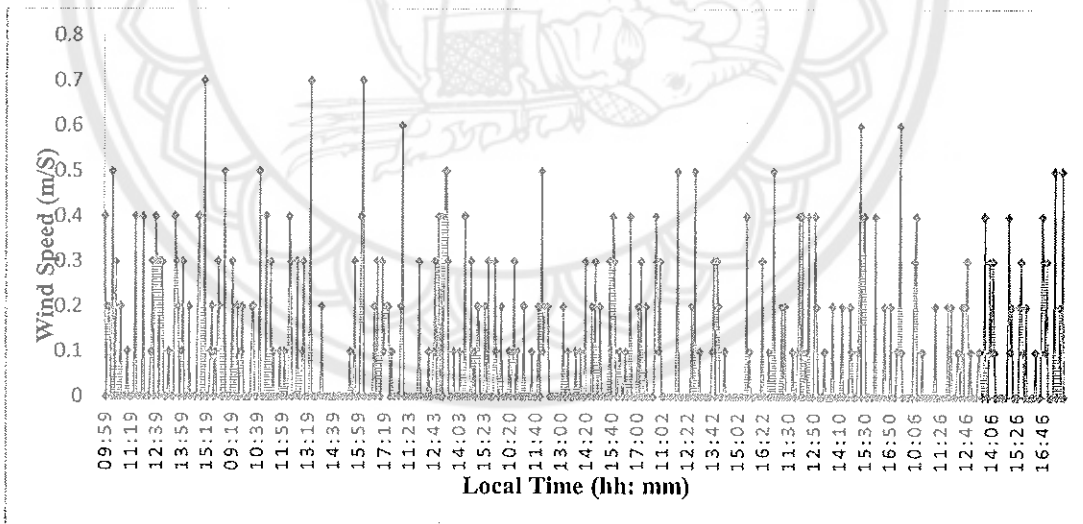


Figure 99 Variation in wind speed for continuous load test

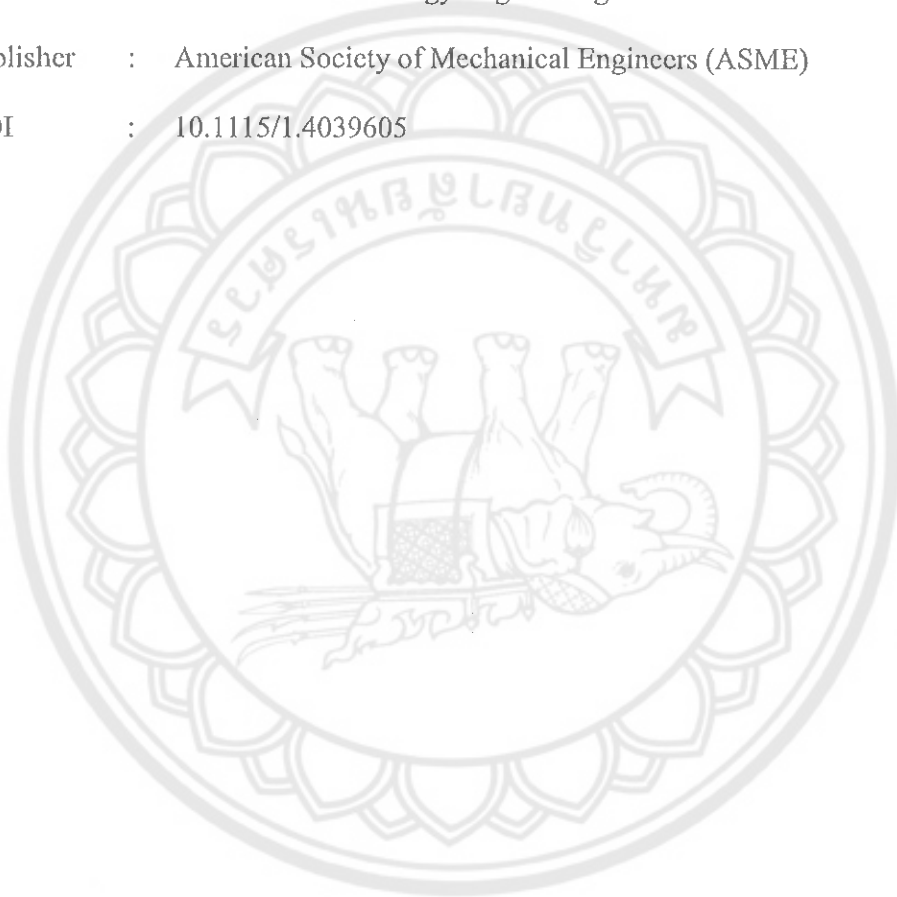
APPENDIX H PAPER PUBLICATIONS

Paper Title : Design of Phase Change Material Based Domestic Solar Cooking System for Both Indoor and Outdoor Cooking Applications

Journal Name: Journal of Solar Energy Engineering

Publisher : American Society of Mechanical Engineers (ASME)

DOI : 10.1115/1.4039605



Design of Phase Change Material Based Domestic Solar Cooking System for Both Indoor and Outdoor Cooking Applications

S. M. Santhi Rekha¹

Thermal Energy Research Unit,
School of Renewable Energy Technology,
Naresuan University,
Phitsanulok 65000, Thailand
e-mail: rekha.anu.eee@gmail.com

Sukruedee Sukchai

Thermal Energy Research Unit,
School of Renewable Energy Technology,
Naresuan University,
Phitsanulok 65000, Thailand
e-mail: sukruedee@hotmail.com

This paper mainly focuses on the design of solar concentric parabolic cooker with proper arrangement of phase change material (PCM) heat storage system. The receiver is a hollow concentric cylinder with inner and outer radii being 0.09 m and 0.1 m, respectively. The thickness or the gap between the two layers of the receiver is 0.01 m and is filled with heat transfer oil. The outer layer of the receiver is surrounded by the vertical cylindrical PCM tubes of diameter 0.025 m. The three modes of heat transfer, radiation, convection, and conduction, are explained and analyzed by heat transfer network. The schematic view of the receiver is shown with the help of SKETCHUP software. The performance parameters, heat loss factor, optical efficiency factor, cooking power of the solar cooker, were calculated with and without PCM in the receiver. 7.74 W m^{-2} and 2.46 W m^{-2} are the heat loss factors, and 0.098 and 0.22 are the optical efficiency factors of the solar cooker without and with PCM presented in the receiver. The optical efficiency factor of the solar cooker with PCM receiver is two times more than that receiver without PCM. The cooking power of the solar cooker with PCM receiver is 125.3 W which is 65.6 W more than that of the cooking power without PCM receiver. From these results, it can be concluded that the design of PCM solar cooking system can expand the applicability of solar cookers as a compatible cooking solution for cooking applications instead of using fossil fuel based cooking systems. [DOI: 10.1115/1.4039605]

Keywords: phase change material, heat storage medium, heat transfer, optical efficiency factor

1 Introduction

In most of the developing countries, the major share of domestic sector energy has been consuming for different daily need functions like water heating, lighting, and cooking applications throughout the year. This domestic sector energy sharing is different for urban and rural areas in developing countries [1]. The footprints of carbon and greenhouse gases by the use of these resources lead to create health, environmental, and other socio-economic problems especially in the rural areas throughout the world [2]. These issues are leading to think about the alternative renewable ways of energy consumption for this application. In recent years, solar cooking got the importance to avoid all the issues raised with the use of fossil fuels. The effective usage of solar cookers needs a proper and efficient design of cooking system with heat storage technology to avoid the problems like direct sun cooking, off sunshine cooking, danger of getting burnt, and other socio-economic challenges [3]. Solar thermal energy can be stored during sunshine hours through different techniques and which can be used during off sunshine hours effectively for different applications.

Kenisarin and Mahkamov performed the studies of different phase change materials (PCMs) which are useful for active and passive solar space heating and cooling and solar cooking applications [4]. Latent heat storage type concentrating solar cooker using a PCM A-164 was developed by Muthusivagami. The PCM

is filled in 1 m long and 22 mm diameter tubes functioned as heat exchanger to store the heat during sunshine hours and the heat stored in the PCM can be retrieved during the off sunshine hours. Cooking surface flat hot plate is similar to that of electric cooking and the oil flows under the hot plate to keep the temperature around 140–150 °C. The PCM used in this system is economically not viable, but with change of PCM the system is effective for residential cooking purposes [5]. Lecuona from Madrid presented about the portable parabolic type solar cooker along with the heat storage facility using phase change materials. The developed utensil was a two conventional coaxial cylindrical cooking pots. The pot contains an inner layer which is small and the outer layer which is larger compared to the inner layer. The hollow space between the two layers of the pot was filled with paraffin and erythritol. A numerical model was developed to study the transient behavior of the system with the climatic conditions of Madrid. The utensil can be moved inside the home 2 h earlier in winter than summer to retain the heat effective for future usage. Paraffin at 100 °C is effectively working than that of erythritol but it is effective for fast cooking indoor applications [6]. The thermal performance of acetamide latent heat storage unit for evening cooking was compared with the standard solar cooker. From the experiment, it was concluded that the developed unit is capable for cooking purpose in the evening time and the PCM did not affect the cooking process in the afternoon [7].

The thermal behavior of the PCM on bulk cycling was presented by John et al. [8]. Galactitol was used as PCM for solar cooking. Three bulk samples of the material which are having different upper cycle temperatures compared to each other were taken and melted and frozen repetitively. The properties of the materials like specific heat, temperature, and phase change

¹Corresponding author.

Contributed by the Solar Energy Division of ASME for publication in the JOURNAL OF SOLAR ENERGY ENGINEERING: INCLUDING WIND ENERGY AND BUILDING ENERGY CONSERVATION. Manuscript received July 13, 2017; final manuscript received March 9, 2018; published online April 9, 2018. Assoc. Editor: Gerardo Diaz.

enthalpies were measured with the help of differential scanning calorimetry, and thermal diffusivity was measured by flash diffusivity instrument. The lowest upper cycle temperature is 200°C and with the possibility of 90 thermal cycles for the solar cooking at temperatures greater than 150°C. It was concluded that galactitol as PCM with thermal cycling at least once in a day can afford of life span less than 100 days for cooking purpose. So, galactitol was unstable and short life span PCM for medium temperature range solar cooking applications.

Different experimental test procedures of paraboloid concentrator solar cooker to determine the optical efficiency factor were presented by Kumar et al. [9]. The heat loss factor ($F'U_L$) and the optical efficiency factor ($F'\eta_o$) were calculated with three different experimental procedures. The first process uses sensible water heating curve of the water in the cooking pot placed at the focus of the paraboloid. The second process uses the steady flow of water through the focal zone of the cooker and the third process is the combination of the above two processes. 0.335, 0.273, and 0.347 are the optical efficiency factors of the paraboloid solar cooker from the first, second, and third test procedures, respectively. From this study, they concluded that the first and second procedures are good, whereas the first procedure is recommended for the accurate determination of optical efficiency factor.

The heat transfer enhancement in latent heat thermal energy storage with conductive structures like finned exchangers, graphite powder, and expanded natural graphite (ENG) matrix was performed by Merlin et al. [10]. The practical setup consists of heat exchanger tube and the outer annular of the heat exchanger filled with PCM. The overall heat transfer coefficient is measured for each configuration. The study concludes that the PCM embedded in ENG matrix is the best storage configuration for industrial purposes with the overall heat transfer coefficient around 3000 W m⁻² K⁻¹. Thermal conductivity of the ENG/PCM composite is 100 times more than that of PCM alone.

The heat transfer enhancement of solar parabolic cooker by a porous medium was designed and analyzed by Lokeswaran and Eswaremoorthy [11]. Waste metal chips made of copper of size 1.5 cm length and 0.5–1 cm thickness are used as porous medium. This porous medium was placed in a cylindrical container of height 8 cm and diameter is equal to the cooking utensil. That container is filled with porous medium up to 5 cm and is placed below the cooking utensil. Stagnation temperature test, water heating and cooling tests were performed with this parabolic cooker. The stagnation temperature was 80°C more than that of the utensil without porous medium. The minimum heat loss factor with and without porous medium was 20 W m⁻² and 14 W m⁻², respectively. The optical efficiency factor increases up to a maximum value of 61 with porous medium.

A parabolic dish solar cooker of 1.25 m diameter and height 0.23 m with a cylindrical receiver of diameter 0.215 m and height 0.15 m was designed and analyzed for the climatic conditions in Yola, Nigeria by Aidan [12]. 0.4 kg mass of cooking pot containing 0.37 kg of water placed at the focal point and the temperature of water is recorded for every 5 min time interval. ($F'U_L$), ($F'\eta_o$), combined heat capacity, and cooking power were calculated. For a combined heat capacity of 1914.3 J K⁻¹, the optical efficiency factor, heat loss factor, and the cooking power are 0.0198, 4.404 W m⁻², and 96.53 W, respectively.

This paper mainly focuses on the design of solar cooker with proper arrangement of PCM heat storage system. This particular design of receiver with PCM tubes provides better combined heat capacity, heat loss factor, optical efficiency factor, and cooking power compared to that of a plain receiver with PCM storage facility. The required Mathematical calculations, modes of heat transfers involved in the proposed design and the schematic views of the solar cooking pot are presented in this paper.

2 Design of Solar Cooking System

The solar cooking system presented in this paper consists of a solar concentrator and a receiver or cooking pot. A parabolic dish

is designed as a solar concentrator and the receiver is placed at the focal point of the parabolic dish. The constructional details of these parts are mentioned in detail in Secs. 2.1 and 2.2.

2.1 Mathematical Calculations. A parabolic antenna dish with a diameter of 1.495 m and a depth or height of 0.268 m is considered to design the solar concentrator. The surface of the parabolic dish is covered by a number of high reflective solar parabolic mirrors of size 2.5 cm². Different parameters of the parabolic dish like focal length, rim angle, acceptance angle, concentration ratio, arc length, surface and aperture areas, and the focus area of the receiver pot were calculated with the following sequence of expressions [3,13–15].

The focal length f of solar concentrator is the distance from the vertex to the focus point F . It is calculated using the below equation:

$$f = \frac{D^2}{16h} \quad (1)$$

After finding the value of focal length, rim angle of the parabolic solar concentrator is found using the below equation:

$$\phi = 2 \tan^{-1} \left[\frac{D}{4f} \right] \quad (2)$$

Half acceptance angle of the parabolic concentrator is the half of the angular limit to which the incident ray may deviate from the normal to the aperture plane and still reach the absorber or receiver, which is calculated using the below equation:

$$\theta_A = \frac{90 - \phi}{2} \quad (3)$$

Concentration ratio is an important factor for the parabolic concentrators which is expressed as a function of rim angle and is also expressed as the ratio of aperture area of the solar concentrator to the surface area of the receiver. Concentration ratio is calculated using the below equation:

$$C = \frac{1}{\sin^2 \varpi} \quad \text{or} \quad C = A_a/A_r \quad (4)$$

The maximum radius of the parabolic concentrator is calculated using Eq. (5). It is a function of focal length and rim angle

$$P = \frac{2f}{1 + \cos \phi} \quad (5)$$

Surface area of the parabolic concentrator is the outer area of the parabolic concentrator and is calculated using the below equation:

$$A_s = \frac{8\pi f^2}{3} \left\{ \left[\left(\frac{D}{4f} \right)^2 + 1 \right]^{\frac{3}{2}} - 1 \right\} \quad (6)$$

Aperture area of the solar concentrator is the area where the solar radiation incident on the parabolic concentrator. It is calculated using Eq. (7) and is a sin function of maximum radius and rim angle of the concentrator

$$A_a = \frac{\pi}{4} (2P \sin \phi)^2 \quad (7)$$

The diameter of the focal point of the concentrator is calculated using the below equation:

$$D_{fo} = 2P \sin \theta_A \quad (8)$$

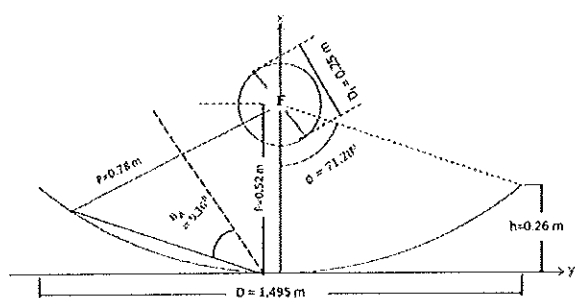


Fig. 1 Geometrical representation of design parameters

After finding the diameter of the focal point, area of the focal point is calculated by Eq. (9). These both parameters are useful to calculate and design the receiver or cooking pot

$$A_f = \frac{\pi}{4} (D_{fo})^2 \quad (9)$$

Figure 1 shows the geometrical representation of the abovementioned parameters.

2.2 Receiver or Cooking Pot Design. The receiver or cooking pot of the solar cooker is made up of stainless steel which is in the shape of hollow concentric cylinder with outer and inner radii being 10 cm and 9 cm, respectively.

The gap or thickness between the layers of the receiver is 1 cm and the height of the receiver is 25 cm. This gap between the layers is filled by heat transfer oil. A cylindrical tube of diameter 2.5 cm and height of 23 cm is used as PCM tube and is filled with selected PCM. A number of such tubes are placed on the surface of the outer layer of the receiver. The PCM is filled in the tubes up to a height of 20 cm.

Area of the receiver or cooking pot is calculated using the below expression:

$$A_r = 2\pi r_p (r_p + h_p) \quad (10)$$

The schematic view of the cooking pot or receiver is shown in Fig. 2. The 25 PCM tubes on the surface of the cooking pot will increase the surface area of the contact of the PCM material with the heat transfer fluid layer. Instead of a single concentric layer, this individual tube design will help to increase the heat storage capacity and to avoid the problems of food contamination because of the PCM material. The side and top views of the designed cooking pot are shown in Fig. 3.

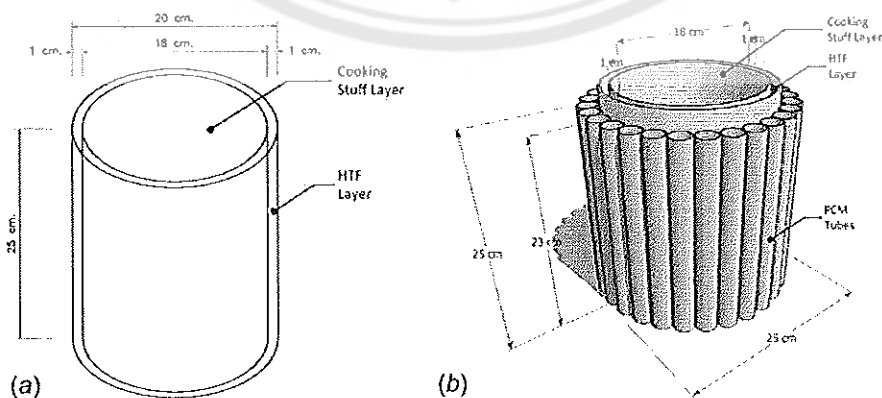


Fig. 2 Schematic view of (a) cooking pot layers and (b) cooking pot with PCM tubes

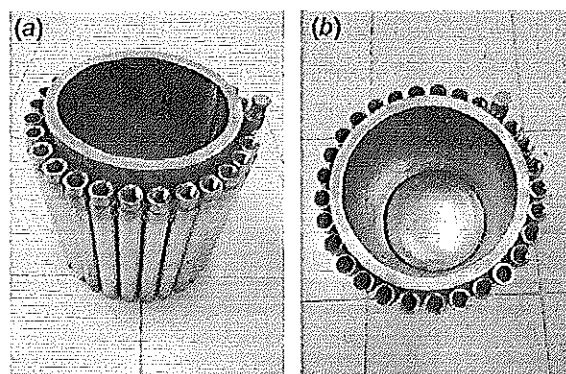


Fig. 3 Design of the receiver: (a) front view and (b) top view

The receiver pot is not in contact with the solar concentrator directly. The solar concentrator is constructed with the dragging wheels. The solar concentrator and the receiver are constructed in a way that it is possible to track the system manually by adjusting the screws. The manual tracking for the solar cooker is designed in the vertical holder of the receiver or cooking pot. It is possible to track the cooking pot in both vertical and horizontal directions. The solar concentrator can also be tracked with the help of rotatable frame which is attached back side of the concentrator.

3 Methodology

3.1 Selection of Phase Change Material. If the material changes its phase at a certain temperature while heating the substance, then the heat is stored in the phase change material. This type of heat storage is called latent heat storage. The materials which are used as the storage medium for the latent heat storage technology are called as PCMs. The PCMs are classified mainly into three categories which are organic, inorganic, and eutectic PCMs [16]. The phase change materials are selected based on the melting point of the materials and the type of application for which the storage system will be incorporated. Different criteria like thermodynamic, kinetic, chemical, technical, and economic are to be checked for the selection of PCM [17].

Thermodynamic criteria:

- Phase change material should have the melting point in desired operating range around 90–110 °C.
- High latent heat of fusion per unit mass in the range of 150–200 J g⁻¹.
- High density in the range of 1.5–1.7 g cm⁻³ so that volume of the material is reduced.

Table 1 Applications of different PCMs based on required melting temperature

Required PCM melting temp ($^{\circ}\text{C}$)	PCM can be used	Heat of fusion (J g^{-1})	Melting point temp of PCM ($^{\circ}\text{C}$)	Application of PCM
Room temperature	$\text{CaCl}_2 \cdot 6\text{H}_2\text{O}$	170	27	Diurnal storage for building structure
20–35	$\text{CaCl}_2 \cdot 6\text{H}_2\text{O}$	170	27	Building heating using heat pumps
25–30	$\text{CaCl}_2 \cdot 6\text{H}_2\text{O}$	170	27	Solar hot air systems
40–60	$\text{Mg}(\text{NO}_3)_2 \cdot 6\text{H}_2\text{O}$ $\text{MgCl}_2 \cdot 6\text{H}_2\text{O}$	163	Around 58	Day and night solar hot air heating systems
		169		
55–70	$\text{Mg}(\text{NO}_3)_2 \cdot 6\text{H}_2\text{O}$ $\text{MgCl}_2 \cdot 6\text{H}_2\text{O}$	163	Around 58	Domestic solar hot water system
		169		
60–95	$\text{Mg}(\text{NO}_3)_2 \cdot 6\text{H}_2\text{O}$	163	89	Solar hot water base board systems
100–175	$\text{Mg}(\text{NO}_3)_2 \cdot 6\text{H}_2\text{O}$	163	117	Concentrated solar systems

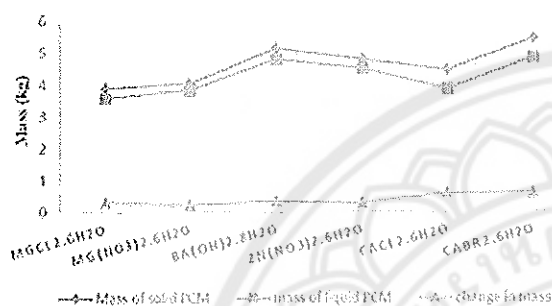


Fig. 4 Variation in mass of different PCMs

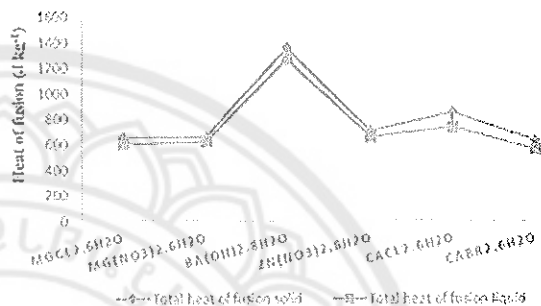


Fig. 5 Variation in heat of fusion for different PCMs

- High thermal conductivity in between $0.5 \text{ W m}^{-1} \text{ }^{\circ}\text{C}^{-1}$ and $0.7 \text{ W m}^{-1} \text{ }^{\circ}\text{C}^{-1}$.
- High specific heat in the range of $1.8\text{--}2.5 \text{ J g}^{-1} \text{ }^{\circ}\text{C}^{-1}$.
- Small volume changes during phase transition.

Kinetic criteria:

- The PCM should have very low super cooling phenomenon during freezing cycle.

Chemical criteria:

- Chemical stability.
- Noncorrosive to the storage tank material.
- Nontoxic, nonflammable, and nonexplosive.

Technical and economic criteria:

- Applicability.
- Compactness and effectiveness.
- Reliability and viability.
- Commercial availability.
- Economically viable.

For different required melting temperatures of PCMs, the corresponding applications of those PCMs are mentioned in Table 1.

As the inorganic salt hydrate PCMs having different densities in solid and liquid states, the mass of the PCM material is varied from material to material. As the combined heat capacity of the solar cooker is the function of mass of the material, the variation in the mass and heat of fusion of different PCMs is shown in Figs. 4 and 5 [17].

3.2 Heat Transfer Network. In the solar cookers with heat storage technology, the heat from the solar collector to the receiver or cooking pot is transferred in the form of three modes, namely, radiation, convection, and conduction [18].

In most of the solar cookers, radiation and convection are the two modes of heat transfers involved to transfer heat. But, in this solar cooker with PCM as storage, conductive mode of heat transfer also involves while storing and transferring heat from the solar

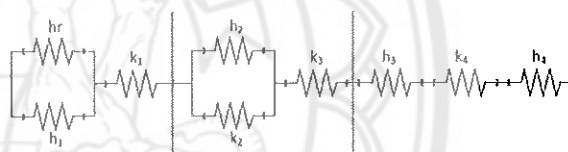


Fig. 6 Heat transfer network of PCM solar cooker

collector to the cooking stuff inside the receiver which is explained with the help of heat transfer network. The heat transfer network is the combination of different thermal resistances which represents the conductive, convective and radiative heat transfer modes involved in the system. The complete heat transfer network for PCM solar cooker is shown in Fig. 6.

The solar energy reflected from the solar collector is transferred to the receiver at the focal point of the parabolic collector by radiative and convective heat transfer modes. The radiative and convective heat transfer resistances are represented as h_r and h_1 in the heat transfer network. As the outermost part of the receiver is covered with PCM tubes, the mode of heat transfer involved between the outer wall of the PCM and surroundings is conduction and is denoted by k_1 . The heat is transferred to the entire PCM inside the tube by convection and from the last layer of the PCM to PCM wall heat is transferred by conduction which are represented by h_2 and k_2 respectively. The heat is transferred from the wall of PCM tube to outer layer of the receiver by conduction and is represented as k_3 . The heat from the outer layer of the receiver is transferred by convection to the entire oil which presents in the gap between the layers of the receiver pot which is denoted by h_3 . The heat is transferred from the oil to the inner layer of the receiver by conduction and is represented as k_4 and that heat is transferred to the cooking material inside the pot by convection which is represented as h_4 in the heat transfer network. These are the complete modes of heat transfer and are explained at each stage with the help of heat transfer network.

Table 2 Performance parameters of solar cooker

Parameter (units)	Step 1		Step 2	
$(MC)_r$ ($J K^{-1}$)	$(MC)_{w_r}$	8380	$(MC)_{w_r}$	8380
	$(MC)_{htw}$	5028	$(MC)_{htf}$	1659.3
	$(MC)_{PCMw}$	10,475	$(MC)_{PCM}$	3620
	$(MC)_{pot}$	5024.16	$(MC)_{p-1}$	5024.16
	$(MC)_{r1}$	18,432.16	$(MC)_{r2}$	18,683.46
$F'U_L$ ($W m^{-2}$)	7.74		2.46	
$F'\eta_o$	0.098		0.22	
P (W)	59.7		125.3	
P_r (W)	54.57		121.05	

3.3 Solar Cooker Parameters. The efficient solar concentrator cooker should provide sufficient amount of energy for cooking processes. The performance of this solar cooker is analyzed by calculating some major parameters like combined heat capacity $((MC)_r)$, heat loss factor $(F'U_L)$, optical efficiency factor $(F'\eta_o)$, cooking power (P) , and standard cooking power (P_s) . A salt hydrate within the abovementioned ranges of thermodynamic properties was used as PCM. Palm oil is taken as heat transfer fluid and the cooking stuff is considered as water.

The combined heat capacity of the receiver is the combination of individual heat capacities of the materials presented in each layer of the receiver and the heat capacity of the stainless steel receiver. The combined heat capacity is calculated from the below equation:

$$(MC)_r = (MC)_{l_1} + (MC)_{l_2} + (MC)_{l_3} + (MC)_{pot} \quad (11)$$

where l_1 , l_2 , and l_3 represent the layers of the receiver.

Heat loss factor is the ratio of combined heat capacity of the receiver to the surface area and the time taken for cooking. It is expressed as in the below equation:

$$F'U_L = \frac{(MC)_r}{\tau_0 A_r} \quad (12)$$

where τ_0 is the time constant determined from the temperature difference that falls to $1/e$ of its initial value [12].

The theoretical maximum limit of the overall efficiency of a concentrator solar cooker is defined as the optical efficiency factor $F'\eta_o$ [9]. It is expressed in the below equation:

$$F'\eta_o = \frac{F'U_L}{C} \left[\frac{\left(\frac{T_{wf} - T_a}{I} \right) - \left(\frac{T_{wi} - T_a}{I} \right) e^{-\frac{1}{\tau_0}}}{1 - e^{-\frac{1}{\tau_0}}} \right] \quad (13)$$

where τ is the time required for the water temperature to increase from initial to final temperature.

The rate of useful energy available during heating period of the concentrator solar cooker is known as the cooking power P [12]. It is expressed in the below equation:

$$P = M_w C_w \frac{(T_{wf} - T_{wa})}{\tau} \quad (14)$$

The corrected cooking power P at each interval to a standard irradiance of $700 W m^{-2}$ defines the standardized cooking power P_r of the solar concentrating cooker [12]. It is mentioned in the below equation:



Fig. 7 The complete design of PCM solar cooker

$$P_r = M_w C_w \frac{(T_{wf} - T_{wa}) \times 700}{\tau I} \quad (15)$$

3.4 Experimental Procedure. The experiment is performed in two steps by keeping the 10 kg mass of receiver or cooking pot at the focus of the parabolic dish. Water heating test and cooling test were performed in both the steps of the experiment. In the first step, the receiver is filled with 2 l of water inside the pot and both heat transfer layer and PCM tubes are also filled with water. Temperature of the water in all the layers of receiver is recorded for every 5 min time interval. After water inside the receiver reaches final temperature, the receiver is covered from the solar radiation for the cooling test. The temperature of the water inside the receiver is recorded again from the final value till it reaches $60^\circ C$. The time constants τ are calculated for the temperature rise from $60^\circ C$ to boiling point and τ_0 is calculated from fall of temperature till the water temperature reaches to $60^\circ C$ from the boiling point of water.

In the second step, the PCM tubes of the receiver are filled with PCM material. Heat transfer layer is filled with palm oil and 2 l of water is filled in the cooking layer of the receiver. The temperature in all layers of the receiver was recorded for every 5 min. After water reaches boiling point, the receiver is covered from the solar radiation and cooling test was performed. Temperature of the water is recorded for every 5 min till the water reaches from boiling temperature to $40^\circ C$. Again, the time constants were calculated by following the same procedures as mentioned in the first step.

Table 3 Parameters of solar concentrator and receiver

Parameter (units)	f (m)	ϕ ($^\circ$)	θ_A ($^\circ$)	C	P (m)	A_s (m^2)	A_a (m^2)	D_{to} (m)	A_f (m^2)	A_r (m^2)	N
Value	0.52	71.28	9.36	5.97	0.789	1.9647	1.7554	0.256	0.05173	0.294	25

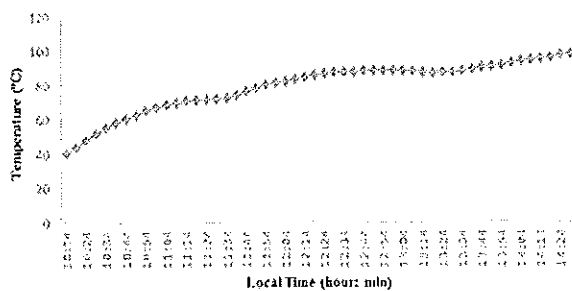


Fig. 8 Heating curve of receiver in the first step

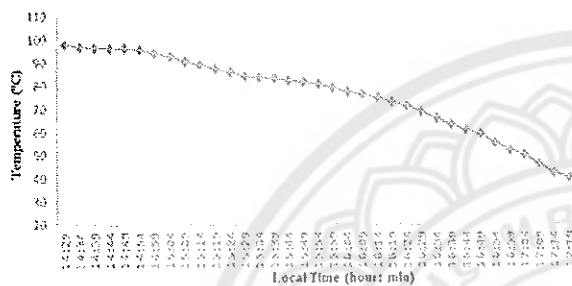


Fig. 9 Cooling curve of receiver in the first step

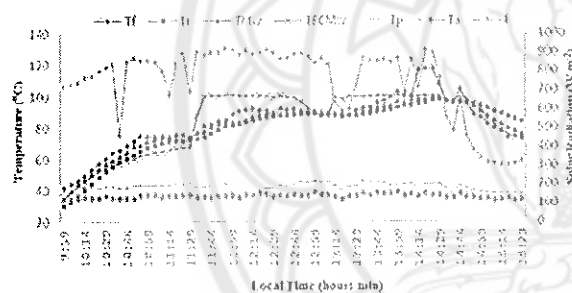


Fig. 10 Temperature profiles of receiver in the first step

All the parameters mentioned in Sec. 3.3 were calculated and mentioned in Table 2.

4 Results and Discussion

The experiment and the design of the system are being performed in School of Renewable Energy Technology (SERT), Naresuan University, Thailand in the month of September, 2017. Different types of analyses are performed on this design and the results are presented in this section. From the abovementioned mathematical expressions of parabolic dish and receiver, the values of all the parameters are mentioned in Table 3. The complete design of the solar cooker with PCM is shown in Fig. 7. From Figs. 4 and 5 analysis, it is observed that the mass and heat of fusion of PCMs in solid state are more than that of mass of PCMs in liquid state. From Fig. 4, $\text{CaBr}_2 \cdot 6\text{H}_2\text{O}$ has the maximum mass requirement among the all inorganic salt hydrate PCMs in both solid and liquid states as 5.41 kg and 4.82 kg, respectively.

$\text{MgCl}_2 \cdot 6\text{H}_2\text{O}$ has the minimum mass requirement in both solid and liquid states as 3.87 kg and 3.57 kg, respectively. From Fig. 5, it is observed that $\text{CaBr}_2 \cdot 6\text{H}_2\text{O}$ has the minimum heat of fusion in

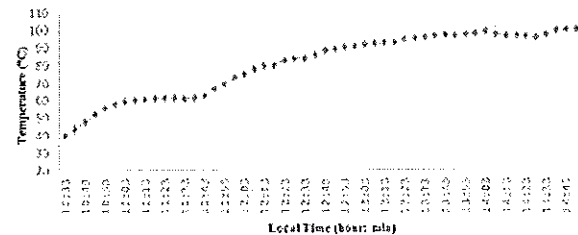


Fig. 11 Heating curve of receiver in the second step

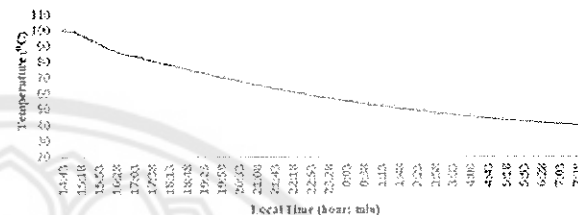


Fig. 12 Cooling curve of receiver in the second step

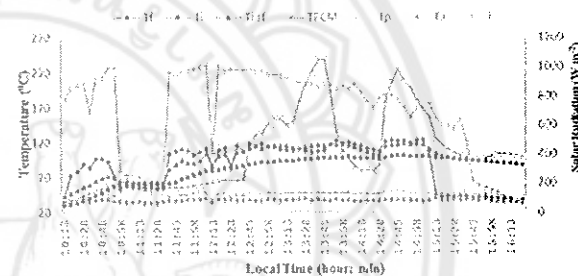


Fig. 13 Temperature profiles of receiver in the second step

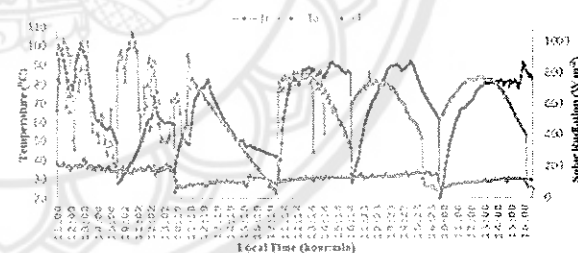


Fig. 14 A 6 day temperature profile of the receiver cooking layer in the first step

both solid and liquid states as 625.25 J kg^{-1} and 557.43 J kg^{-1} , respectively. $\text{Ba}(\text{OH})_2 \cdot 6\text{H}_2\text{O}$ has the maximum heat of fusion in both solid and liquid states as $1357.06 \text{ J kg}^{-1}$ and $1269.87 \text{ J kg}^{-1}$, respectively.

From the first step of the experiment, heating curve, cooling curve, and the temperature profiles of water in all layers of the receiver for the corresponding local time are shown in Figs. 8–10, respectively. From Fig. 8, it is observed that water temperature raises from 60°C to 97.7°C in almost 6750 s which is considered as τ_1 . From Fig. 9, it is observed that the water temperature falls from 97.7°C to 60°C in 8100 s which is considered as τ_{01} .

Figure 10 shows the temperature profile of water in the three layers of the receiver. T_f represents the temperature at the bottom of the receiver, T_i represents the water temperature inside the

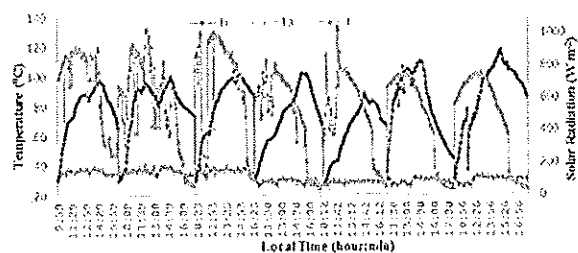


Fig. 15 A 7day temperature profile of the receiver cooking layer in the second step

cooking layer, T_{hw} represents the temperature of water inside the heat transfer layer, T_{PCMw} represents the temperature of water inside the PCM tubes, T_p is the temperature on the surface of parabolic dish, and T_a is ambient temperature. Solar radiation of the corresponding day is also shown in Fig. 10. The average solar radiation is 673.30 W m^{-2} .

Figure 11 shows the heating curve of the water inside the receiver in the second step of the experiment. Time constant τ_2 of the heating process to raise the water temperature from 60°C to 100.2°C is 4500 s. Figure 12 shows the cooling curve of the water inside the receiver in second step. In 25,800 s, the temperature of water inside the receiver falls to 60°C from 100.2°C , which is considered as time constant τ_{02} . It is observed that the time taken for the cooling test is three times greater than that of time taken for the cooling test in step 1. This increase in the time inside is due to the presence of the heat transfer oil and the PCM in the PCM tubes.

Figure 13 shows the temperature profile of different layers of the receiver and parabolic dish. T_f and T_i are the temperatures of the bottom of the receiver and temperature of water in cooking layer of the receiver, respectively. T_{htf} is the temperature of heat transfer fluid and T_{PCM} is the temperature of the PCM inside the PCM tubes. The PCM reaches a maximum temperature of 238°C in the afternoon and the corresponding solar radiation is 886.551 W m^{-2} . The average solar radiation on that day is 693.53 W m^{-2} .

Figure 14 represents the temperature profile of the receiver cooking layer for 6 days in different months for the first step of the experiment. The corresponding solar radiation and the ambient temperature of the particular days are also mentioned in Fig. 14. From that figure, the effect of ambient temperature and solar radiation on the temperature of the cooking layer of the receiver is observed. As the PCM tubes are filled with water in the first step instead of PCM, the temperature profile of the cooking layer is different for 6 days.

Figure 15 represents the temperature profile of the receiver cooking layer for 7 days in different months for the second step of the experiment. In this case, the PCM tubes are filled with the PCM. The temperature profile of the cooking layer is almost similar in all the 7 days. The heat stored in the PCM helps to maintain the constant temperature profile inside the cooking layer irrespective of the variation in the solar radiation and the ambient temperature. The variation in the ambient temperature and the solar radiation of the particular days is also shown in Fig. 15.

The combined heat capacity of the solar cooker for the first step is obtained from Eq. (11). In step 1, all the layers of the receiver are filled with water. The corresponding combined heat capacity equation for the first step is shown in Eq. (16) and the corresponding values are listed in Table 2

$$(MC)_{r1} = (MC)_w + (MC)_{htw} + (MC)_{PCMw} + (MC)_{pot} \quad (16)$$

Similarly, in the second step, the water in the heat transfer layer and PCM tubes was replaced with palm oil and PCM. The corresponding combined heat capacity equation is shown in Eq. (17) and the values are listed in Table 2

$$(MC)_{r2} = (MC)_w + (MC)_{htf} + (MC)_{PCM} + (MC)_{pot} \quad (17)$$

where $(MC)_{r1}$ and $(MC)_{r2}$ are the combined heat capacities of the receiver in step 1 and step 2, respectively.

The heat loss factor $F'U_L$, optical efficiency factor $F'\eta_o$, cooking power P , and the standard cooking power P_s were calculated for both steps and the values are listed in Table 2. From Table 2, it is observed that the above mentioned four parameters were improved for step 2 compared to that of step 1 due to the presence of PCM inside the PCM tubes.

As compared to the performance results of the considered reference parabolic cooker designed by Aidan [19] with the present solar cooker performance results, the heat loss factor in step 1 is 1.75 times more than that of the reference cooker, and in step 2, it is 1.79 times less than that of reference cooker. The heat storage in PCM helps to improve the heat loss factor compared to step 1 and the reference cooker. The time constants τ_{01} and τ_{02} are 2.57 and eight times more than that of the reference cooker, respectively. The other parameters like optical efficiency factor and cooking power in step 2 are more than that of the reference cooker parameters. The proposed design of solar cooker with PCM storage is able to achieve good results in terms of its performance parameters. However, the tracking efficiency and the combined heat capacity of the cooking pot are the limitations to achieve even better performance results of the solar cooker presented in this paper.

5 Conclusion

The PCM-based domestic solar cooker for both indoor and outdoor applications was designed and analyzed. 25 PCM tubes are placed on the surface of receiver which is placed at the focus of the parabolic dish. Different solar parabolic dish parameters and the receiver or cooking pot parameters are obtained from the mathematical calculations. The performance of the different PCMs requirements regarding the mass, heat of fusion, and the combined heat capacities are analyzed. The selection of proper PCM for a particular temperature requirement may help to increase the combined heat capacity of the receiver. The heat loss factor of solar cooker with and without PCM is 7.74 W m^{-2} and 2.46 W m^{-2} , respectively. 0.098 and 0.22 are the optical efficiency factors of the solar cooker without and with PCM presented in the receiver of the solar cooker. The optical efficiency factor of the solar cooker with PCM receiver is two times more than that receiver without PCM. The cooking power of the solar cooker with PCM receiver is 125.3 W which is 65.6 W more than that of the cooking power without PCM in the receiver. From the results, it can be concluded that the overall performance of this proposed solar cooker is satisfactory with PCM receiver. After sunshine hours, the retained heat in the PCM is useful for indoor cooking by keeping the receiver pot inside the insulating box. So, this proposed design of solar cooker with PCM storage can be a promising solution for fossil fuel based cooking methods to reduce carbon foot prints and improves the socio-economic situations of rural communities.

The proposed work will be continued for the other different cooking tasks like frying and boiling of different materials in outdoors as well as indoors. The economic analysis of this PCM solar cooker can also be compared with the traditional ways of cooking in the future.

Acknowledgment

The authors would like to express sincere thanks to School of Renewable Energy Technology (SERT), Naresuan University, Thailand for the facilities and the constant support throughout the work.

Nomenclature

A_a = aperture area of the dish (m^2)
 A_f = focal point area (m^2)

- A_r = area of the receiver (m^2)
 A_d = surface area of the dish (m^2)
 C = concentration ratio
 C_p = specific heat of the material ($\text{J kg}^{-1} \text{K}^{-1}$)
 D = diameter of parabolic dish (m)
 D_{fo} = focal point diameter (m)
 f = focal length of parabolic dish (m)
 h = height of parabolic dish (m)
 h_r = height of the receiver (m)
 I = instantaneous solar radiation (W m^{-2})
 \bar{I} = average solar radiation (W m^{-2})
 M = mass of the material (kg)
 $(MC)_{htf}$ = heat capacity of heat transfer fluid (J K^{-1})
 $(MC)_{htw}$ = heat capacity of water in HTF layer (J K^{-1})
 $(MC)_{PCM}$ = heat capacity of PCM (J K^{-1})
 $(MC)_{PCMw}$ = heat capacity of water in PCM tubes (J K^{-1})
 $(MC)_{pot}$ = heat capacity of stainless steel receiver (J K^{-1})
 $(MC)_r$ = combined heat capacity of the receiver (J K^{-1})
 $(MC)_w$ = heat capacity of water (J K^{-1})
 N = number of PCM tubes
 P = maximum radius of parabolic dish (m)
 r_i = inner radius of hollow cylinder (m)
 r_o = outer radius of hollow cylinder (m)
 T_a = average ambient temperature ($^{\circ}\text{C}$)
 T_{wf} = final temperature of water ($^{\circ}\text{C}$)
 T_{wi} = initial temperature of water ($^{\circ}\text{C}$)
 θ_A = half acceptance angle of parabola (deg)
 τ_{01} = cooling time constant in first step (s)
 τ_{02} = cooling time constant in second step (s)
 τ_1 = heating time constant in first step (s)
 τ_2 = heating time constant in second step (s)
 ϕ = rim angle of parabola (deg)

References

- [1] Daiglou, V., van Ruijven, B. J., and van Vuuren, D. P., 2012, "Model Projections for Household Energy Use in Developing Countries," *Energy*, 37(1), pp. 601–615.
- [2] Abdullahi, K. L., Delgado-Saborit, J. M., and Harrison, R. M., 2013, "Emissions and Indoor Concentrations of Particulate Matter and Its Specific Chemical Components From Cooking: A Review," *Atmos. Environ.*, 71, pp. 260–294.
- [3] Garg, H. P., and Prakash, J., 2000, *Solar Energy: Fundamentals and Applications*, Tata McGraw-Hill Publishing, New Delhi, India.
- [4] Kenisarin, M., and Mahkamov, K., 2007, "Solar Energy Storage Using Phase Change Materials," *Renewable Sustainable Energy Rev.*, 11(9), pp. 1913–1965.
- [5] Muthusivagami, R. M., Velraj, R., and Sethumadhavan, R., 2010, "Solar Cookers With and Without Thermal Storage—A Review," *Renewable Sustainable Energy Rev.*, 14(2), pp. 691–701.
- [6] Lecuona, A., Nogueira, J.-I., Ventas, R., Rodríguez-Hidalgo, M.-d.-C., and Legrand, M., 2013, "Solar Cooker of the Portable Parabolic Type Incorporating Heat Storage Based on PCM," *Appl. Energy*, 111, pp. 1136–1146.
- [7] Sharma, S. D., Buddhi, D., Sawhney, R. L., and Sharma, A., 2000, "Design, Development and Performance Evaluation of a Latent Heat Storage Unit for Evening Cooking in a Solar Cooker," *Energy Convers. Manage.*, 41(14), pp. 1497–1508.
- [8] John, G., König-Haagen, A., King'ondo, C. K., Brüggemann, D., and Nkhonjera, L., 2015, "Galactitol as Phase Change Material for Latent Heat Storage of Solar Cookers: Investigating Thermal Behavior in Bulk Cycling," *Sol. Energy*, 119, pp. 415–421.
- [9] Kumar, S., Kandpal, T. C., and Mullick, S. C., 1996, "Experimental Test Procedures for Determination of the Optical Efficiency Factor of a Paraboloid Concentrator Solar Cooker," *Renewable Energy*, 7(2), pp. 145–151.
- [10] Merlin, K., Delaunay, D., Soto, J., and Traonvouez, L., 2016, "Heat Transfer Enhancement in Latent Heat Thermal Storage Systems: Comparative Study of Different Solutions and Thermal Contact Investigation Between the Exchanger and the PCM," *Appl. Energy*, 166, pp. 107–116.
- [11] Lokeswaran, S., and Eswaramoorthy, M., 2012, "Experimental Studies on Solar Parabolic Dish Cooker With Porous Medium," *Appl. Sol. Energy*, 48(3), pp. 169–174.
- [12] Aidan, J., 2014, "Performance Evaluation of a Parabolic Solar Dish Cooker in Yola, Nigeria," *IOSR J. Appl. Phys.*, 6, pp. 46–50.
- [13] Duffie, J. A., and Beckman, W. A., 2006, *Solar Engineering of Thermal Processes*, Wiley, Chichester, UK.
- [14] Kalogirou, S. A., 2013, *Solar Energy Engineering: Processes and Systems*, Academic Press, Boston, MA.
- [15] Barlev, D., Vidu, R., and Stroeve, P., 2011, "Innovation in Concentrated Solar Power," *Sol. Energy Mater. Sol. Cells*, 95(10), pp. 2703–2725.
- [16] Raam Dheep, G., and Sreekumar, A., 2014, "Influence of Nanomaterials on Properties of Latent Heat Solar Thermal Energy Storage Materials—A Review," *Energy Convers. Manage.*, 83, pp. 133–148.
- [17] Dincer, I., and Rosen, M., 2011, *Thermal Energy Storage: Systems and Applications*, 2nd ed., Wiley, Chichester, UK.
- [18] Tiwari, G., and Suneja, S., 1997, *Solar Thermal Engineering Systems*, Narosa Publishing House, New Delhi, India.
- [19] Aidan, J., 2014, "Performance Evaluation of a Parabolic Solar Dish Cooker in Yola, Nigeria," *IOSR J. Appl. Phys.*, 6, pp. 46–50.